


1-1-2017

Brain Connectivity After Concussion

Armin Iraji
Wayne State University,

Follow this and additional works at: http://digitalcommons.wayne.edu/oa_dissertations

 Part of the [Biomedical Engineering and Bioengineering Commons](#), and the [Neurosciences Commons](#)

Recommended Citation

Iraji, Armin, "Brain Connectivity After Concussion" (2017). *Wayne State University Dissertations*. 1711.
http://digitalcommons.wayne.edu/oa_dissertations/1711

This Open Access Dissertation is brought to you for free and open access by DigitalCommons@WayneState. It has been accepted for inclusion in Wayne State University Dissertations by an authorized administrator of DigitalCommons@WayneState.

BRAIN CONNECTIVITY AFTER CONCUSSION

by

ARMIN IRAJI

DISSERTATION

Submitted to the Graduate School

of Wayne State University,

Detroit, Michigan

in partial fulfillment of the requirements

for the degree of

DOCTOR OF PHILOSOPHY

2017

MAJOR: BIOMEDICAL ENGINEERING

Approved By:

Advisor

Date

© COPYRIGHT BY

ARMIN IRAJI

2017

All Rights Reserved

DEDICATION

For my mom whose hug I missed and my dad whose smile I missed.

For my sister who always loves me unconditionally.

For my oldest brother who always takes care of family problems.

And to you who are spending your precious time to read this work.

ACKNOWLEDGMENTS

First and foremost, I would like to extend my deepest thanks to my amazing parents for their unconditional love and limitless support. I am also very grateful for having the best and closest friend forever, my sister. You are the best thing that God has sent me, right after I was born. Thanks to all of my family and friends for your encouragement and support.

I would like to express the deepest appreciation to my advisor, Dr. Zhifeng Kou, for his guidance, expertise, and especially his support throughout my Ph.D. studies. Thank you for training me to change from a student to a researcher and for allowing me to evolve into an independent thinker. I am fortunate to have had the opportunity to learn from an exemplary scientist.

I would like to express tremendous gratitude to the members of my committee: Dr. Hamid Soltanian-Zadeh, Dr. Juri G. Gelovani, Dr. Mohammadreza Nasiriavanaki, and Dr. E. Mark Haacke. Your guidance, keen insight, acumen, and encouragement fostered my scientific development, and I am very thankful for everything that you have taught me. I feel so lucky and blessed for having been able to work with you in my time here.

I would like to thank the MR Research Facility group, faculty, post-docs, graduate students and staff for all their help and advice. I would especially like to thank Mrs. Lisa Brownshidle, Dr. Yimin Shen and Mr. Zahid Latif for all their tremendous support and motivation.

I also want to use this opportunity to thank everyone who helped me complete this study. In particular, Dr. Tianming Liu and his group, including Mr. Hanbo Chen and Dr. Jinglei Lv from the University of Georgia who helped and directed me with the DICCCOL analyses and Dr. Woodard and his group, especially Ms. Andria Norman, who immensely guided me with the neurocognitive analyses. I would also like to thank Ms. Adrianna Jordan for proof reading my dissertation.

Finally, I would like to send my special thanks to Ms. Natalie M. Wisemen who is not just a friend or colleague but like a sister. Over the past couple of years, she helped and guided me every day with my research and was always there for me in the best and worst times of my life. Her outstanding skills and progress as a research scientist have allowed me to personally learn a lot from her in our work together. I

appreciate the advice, help, and support she provided. I hope you utilize your talent in the best way. I am blessed for all the moments we shared.

TABLE OF CONTENTS

DEDICATION	ii
ACKNOWLEDGMENTS.....	iii
LIST OF TABLES.....	viii
LIST OF FIGURES.....	ix
LIST OF ABBREVIATIONS AND GLOSSARY OF TERMS	xiv
CHAPTER 1. INTRODUCTION AND BACKGROUND.....	1
1.1. Mild TBI (mTBI) Definition and Causes	1
1.1.1. mTBI Causes.....	2
1.1.2. Definition of mTBI.....	2
1.2. Clinical Imaging mTBI Findings	5
1.3. Brain and Brain Connectivity	7
1.3.1. Brain Connectivity Analysis	8
1.4. Cognitive and Psychiatric Symptoms	11
1.5. Objective and Project Motivation	12
1.6. Current Gaps in the Field.....	14
CHAPTER 2. RESEARCH DESIGN	15
2.1. Project Aims.....	15
2.1.1. Specific Aim 1	15
2.1.2. Specific Aim 2.....	15
2.1.3. Specific Aim 3.....	16
2.2. Participant Population Demographics	16
2.3. Cognitive Assessment	17
2.4. Imaging Protocol.....	18
CHAPTER 3. STRUCTURAL CONNECTIVITY (SC)	19
3.1. Background.....	19

3.2. Previous Findings on TBI.....	20
3.3. Analytical Approach: Dense Individualized Common Connectivity Based Cortical Landmarks (DICCCOLs).....	21
3.4. Data Analysis.....	25
3.4.1. Connectome-scale Assessment of Structural and Functional Connectivity in Mild Traumatic Brain Injury at the Acute Stage - Structural Connectivity Part.....	25
3.4.2. Validation of Results of DICCCOL Framework Analyzed Using Probabilistic Tractography ...	30
3.5. Discussion.....	32
CHAPTER 4. FUNCTIONAL CONNECTIVITY (FC).....	34
4.1. Background.....	34
4.2. Previous Findings on TBI.....	36
4.3. Analytical Approach.....	37
4.3.1. Seed-based Analysis.....	37
4.3.2. Independent Component Analysis	38
4.4. Data Analysis.....	39
4.4.1. Image Preprocessing.....	39
4.4.2. Resting State Functional Connectivity in Mild Traumatic Brain Injury at the Acute Stage: Independent Component and Seed Based Analyses	40
4.4.3. Connectome-scale Assessment of Structural and Functional Connectivity in Mild Traumatic Brain Injury at the Acute Stage - Functional Connectivity Part	49
4.4.4. Compensation Through Functional Hyperconnectivity: A Longitudinal Connectome Assessment of Mild Traumatic Brain Injury	52
4.5. Discussion.....	57
CHAPTER 5. RELATIONSHIP BETWEEN NEUROPSYCHOLOGICAL DATA AND NEUROIMAGING DATA.....	59
5.1. Background.....	59
5.2. Previous Findings	59
5.3. Analytical Approach.....	60
5.3.1. Meta-analysis to Predict Affected Neurocognitive Domain	60
5.3.2. Statistical Inference between Neurocognitive and Neuroimaging Data (Prediction Analysis) .	62
5.4. Data Analysis.....	66

5.4.1. Meta-analysis	66
5.4.2. Statistical Relationship Between Neurocognitive and Neuroimaging Data.....	69
5.5. Discussion.....	71
CHAPTER 6. CONNECTIVITY DOMAIN ANALYSIS	72
6.1. Background.....	72
6.2. Analytical Approach: The Connectivity Domain.....	76
6.2.1. The Connectivity Domain: Analyzing Resting State fMRI Data Using Feature-based Data-driven and Model-based Methods	76
6.3. Discussion.....	83
Chapter 7. CONCLUSION, DISCUSSION, AND FUTURE WORK	85
7.1. Contribution and Conclusions.....	85
7.2. Discussion.....	86
7.3. Future Work	87
APPENDIX: STATISTICAL INFERENCE BETWEEN NEUROCOGNITIVE AND NEUROIMAGING VARIABLES USING COVARIATES	91
REFERENCES.....	98
ABSTRACT	124
AUTOBIOGRAPHICAL STATEMENT	125

LIST OF TABLES

Table 1. Locations of discrepant DICCCOLs and their Brodmann areas and connected major fiber tracts	30
Table 2. Demographic characteristics of mTBI patients with neuroimaging data at the first time point and neurocognitive data at the second time point.	69
Table 3. Covariates Contributions in Neuropsychological Tests (NPTs).	70
Table 4. Summary of regression analysis for memory composite score. Regression analysis was performed between memory composite score and 60 connectomic signatures using several models. Results shows the number of analysis that each covariate show significant contribution using p-value < 0.05.	92
Table 5. Memory composite score. Red represents those DICCCOLs that show significant relationship with both attention/executive function score and memory score. Bold shows the DICCCOLs involved in more than one connectomic signature.	93
Table 6. Summary of regression analysis for the attention/processing speed composite score. Regression analysis was performed between attention/processing speed composite score and 60 connectomic signatures using several models. Results show the number of analysis that each covariate show significant contribution using p-value < 0.05.	94
Table 7. Attention/processing speed composite score results. Red represents those DICCCOLs that show significant relationship with both attention/executive function score and memory score. Blue represents connectomic signature which shows significant correlation after FDR correction. Orange shows cognitive domains involved in both DICCCOLs of a connectomic signature. Bold shows the DICCCOLs involved in more than one connectomic signature.	95
Table 8. Summary of regression analysis for the total composite score. Regression analysis was performed between the total composite score and the 60 connectomic signatures using several models. Results show the number of analyses for which each covariate showed a significant contribution using p-value < 0.05.	96
Table 9. Total composite score. Orange shows cognitive domains involved in both DICCCOLs of a connectomic signature. Bold shows the DICCCOLs involved in more than one connectomic signature. Bold shows the DICCCOLs involved in more than one connectomic signature	97

LIST OF FIGURES

Figure 1. Classification of traumatic brain injury using Mayo Criteria (Sharp and Jenkins, 2015) 4

Figure 2. Pipeline of procedure for identifying the locations of DICCCOLs on the brain of an individual. Figure 2.A: Fiber tracking and tractography of the whole brain was performed via MedINRIA (<http://med.inria.fr/>). Box "a" presents the preprocessing steps (including brain extraction, motion correction, and eddy current correction) and deterministic tractography. A(I) shows diffusion data of an individual brain at b_0 and some different gradient directions, and A(II) shows the result of tractography in 3D space in the sagittal, axial, and coronal views. Figure 2.B: The transformation matrix to transfer coordinates from the subject space to the template space was obtained by registering the brain of an individual subject to the brain template. B(III) shows the schematic of this procedure in which box b represents the transformation matrix. B(IV) and B(V) show the coronal, axial, and sagittal views of individual and template's brains, respectively. Figure 2.C: Transformation and identification of the initial location of DICCCOLs. The transformation matrix (b) is applied to transfer the individual surface and fiber bundles to the template space for prediction. As a result, the initial location of DICCCOLs on the individual's brain is obtained. C(VI) is the surface of an individual in the subject space, and C(VII) is the surface of the same individual, which is transferred to the template space. The initial location of DICCCOLs on an individual's brain was obtained by overlaying the location of DICCCOLs of the template on the transformed surface of the individual. Figure 2.D: The schematic procedure of optimization in which the local neighborhood (6 mm radius) was searched in order to identify the location where the profile of connected fiber has the most similarity with the WM fiber connection profile of the DICCCOL on the template. D(VIII) shows the initial location of a DICCCOL, obtained from the previous step. Using the information of deterministic tractography (A(II)), the connected fibers at this initial location was extracted (D(X)). Next, the similarity between the connected fibers at this location and the connected WM fiber on the template was measured. The same procedure took place for all local neighborhoods, and the location with maximum similarity of the connected WM fibers was identified as the optimized location of the DICCCOL. Box d represents the optimization procedure. D(IX) shows the initial and optimized locations of a DICCCOL in red and green, respectively. D(X) and D(XI) show the connected fibers at the initial and optimized locations of the DICCCOL, respectively. Figure 2.E represents the optimized locations of all DICCCOLs on an individual's brain. E(XII), E(XIII), and E(XIV) show the coronal, sagittal, and axial views in 3D space, respectively. 23

Figure 3. Illustration of trace-map calculation and DICCCOL prediction. (a)-(d): trace-map calculation. (a) The fiber bundle emanating from a selected ROI; (b) visualization of two single streamlines of the fiber bundle and calculation of the connection orientation profiles; (c) projection of directions onto unit spheres; and (d) visualization of distribution of orientation vectors on the sphere (trace-map). 24

Figure 4. Joint visualization of a common DICCCOL (#178, yellow arrows) and the discrepant DICCCOL # 19 (indicated by yellow arrows). (A) and (B) show the connected DTI-derived axonal fibers (colorful lines) connected to the common DICCCOL on the cortical surface for 20 patients and 20 control subjects, respectively. Visual inspection reveals the patterns of fiber bundles are consistent across individuals for both patients and healthy subjects. Figure (C) and (D) respectively show the trace-map distance for 20 patients and 20 healthy controls selected in (A) and (B). As we can see, healthy subjects and patients have similar trace-map distance values for the common DICCCOL # 178. (E) and (F) show the connected DTI-derived axonal fibers (colorful lines) connected to the discrepant DICCCOL # 19 on the cortical surface for the same 20 patients and 20 control subjects as figures (A) and (B), respectively. Several patients have different fiber shapes (red outlines) in these randomly chosen 20 samples, which drive the group difference between patients and controls. At the same time, measuring the trace-map distances for DICCCOL #19 for same subjects shows that patients in general have a higher trace-map distance. Same scale has been used to make it visually easy to compare with the trace-map distance of discrepant DICCCOL. 27

Figure 5. Visualization of location of discrepant DICCCOLs (red sphere) and the rest DICCCOLs (green sphere) on cortical surface. ID numbers are shown for discrepant DICCCOLs. 28

Figure 6. White matter fiber tractography of a randomly chosen control subject (A) and a randomly chosen mTBI patient (B) by using the 41 discrepant DICCCOLs (yellow spheres) as seed points. Despite the negative findings on the mTBI patient's structural MRI, the patient's white matter structure shows significant differences in the 41 discrepant networks in comparison with controls. Of particular note, the difference in the major white matter tracts between controls and patients is not because of the loss of white matter tracts in the patient; instead, it is the injury at these discrepant networks fail the fiber tractography algorithm when using the selected DICCCOL landmark as seed regions. 29

Figure 7. Validation of the DICCCOL prediction of structurally disrupted fibers by evaluating overall FA along affected white matter bundles. The right ILF shows decreased FA values in mTBI patients. 32

Figure 8. Schematic of the BOLD hemodynamic response morphology (Kornak et al., 2011). 34

Figure 9. Functional connectivity analysis using a seed-based approach. The red circle shows an example of the desired region of interest (selected seed). The temporal dependency (for instance, the temporal correlation between the time course of the selected seed and other brain regions (two examples identifies in green) is measured. The output will be a spatial map of the brain in which a higher value represents stronger functional connectivity with the selected seed. 37

Figure 10. Functional connectivity analysis using independent component analysis (ICA). The whole collected fMRI data will be used as the input for ICA analysis, and the output will be a set of independent spatial maps including spatial maps of brain intrinsic connectivity networks (ICNs) and other spatial maps such as noises and artifacts. 39

Figure 11 Cross-validation results of the group independent component analysis on number of associated voxels to the ICNs. The DMN shows a difference between the two groups in (a) the PCC, Brodmann area (BA) 10, BA 11 and (b) precuneus. (c) The basal ganglia network does not show any significant difference. Error bar is one standard deviation. 43

Figure 12. Cross-validation results of the group independent component analysis on voxel dependency to the ICNs. The DMN shows a difference between the two groups in the (a) PCC and (b) precuneus. (c) The basal ganglia network does not show any significant difference. Error bar is one standard deviation. 44

Figure 13. Two-sample t-test using a p-value of 0.001 on the DMN extracted from the cross-validation of group independent component analysis. Results identified a cluster of 50 voxels in the PCC (green arrow) and a cluster of 442 voxels in the precuneus (blue arrow) that have significantly lower voxel dependency to the DMN in patients as compared with healthy control subjects. 44

Figure 14. Two-sample t-test results demonstrate a difference in the DMN between the two groups in individual independent component analysis. Highlighted area shows the cluster is statistically significant ($p < 0.05$), which includes 55 voxel in the PCC. The warm color labels the voxels with reduced DMN dependency in patients compared with healthy controls. 45

Figure 15. Two-sample t-test ($p = 0.01$) for the PCC connectivity map. The cold color labels the region that has more correlation with the posterior cingulate in the patient group than in the controls. The cross bar is located in different positions in the same FC map in images a and b. These regions do not belong to the DMN. 46

Figure 16. Two-sample t-test ($p < 0.05$) of the precuneus functional connectivity map. The between-group comparison using the precuneus as seed revealed differences in the supramarginal gyrus (red arrow) and the junction between BA 8 and the anterior cingulate cortex (BA 32) (green arrow). 46

Figure 17. Two-sample t-test ($p < 0.01$) of thalamus functional connectivity map. The seed is located in the thalamus and the cold color shows the regions that have higher correlation with seed point in the patient group compared with the healthy control group. (a) Shows a statistical difference between two groups at the anterior prefrontal cortex (BA 10) (green arrow) and (b) shows the difference in the supramarginal gyrus (BA 40) (red arrow)..... 47

Figure 18 Two-sample t-test ($p < 0.01$) for the amygdala correlation map. The cold color labels the region (the left parietal superior cortex) that has stronger correlation with the amygdala (red arrow) in the patient group than in controls..... 47

Figure 19. One-sample t-test of the amygdala map ($p < 0.01$). (a) the FC map for the healthy control group and (b) the FC map of the patient group. The higher signal intensity on (a) shows higher intrinsic FC in the amygdala in the healthy group than in patients..... 48

Figure 20. Two-sample t-test ($p < 0.01$) for the hippocampus FC map. The cold color labels the regions with more correlation with the hippocampus in the patient group compared with controls while the warm color labels the region with more correlation in the controls than in the patient group. The FC map was sectioned through (a) the precuneus association cortex (BA 7), red arrow; (b) the inferior frontal gyrus, green arrow; and (c) the fusiform gyrus, purple arrow. 48

Figure 21. FC was measured across the brain using the DICCCOL framework. Figure 21.A, B, and C show the optimized locations of DICCCOLs across the brain in the coronal, sagittal and axial views, respectively. Figure 21.D, E, and F represent the time series allocated to three DICCCOLs obtained from the rsfMRI data of the gray matter of the neighborhood of each DICCCOL. The Pearson correlation was calculated between time series of each DICCCOL pairs in order to obtain the FC of the brain at large scale. Figure 21.G and H show two examples of FC measurement, and Figure 21.I is a symmetric affinity matrix, which represents FC at a connectomic level. 50

Figure 22. T-values from the longitudinal statistical analysis using a mixed design ANOVA and NBS on the 258 FC pairs which are significantly stronger in the patient group. Since the FC matrix is symmetric, only the lower half was used for the statistical analysis..... 54

Figure 23. Eight FC clusters as results of using a multi-view group-wise clustering. Eight functional clusters were identified in different colored bubbles. 55

Figure 24. Categorizing the disturbed functional connectivity, which has been obtained using longitudinal statistical analysis by a mixed design ANOVA and NBS, into eight functional connectivity clusters that have been obtained using the multi-view group-wise clustering method. Results show that some clusters (especially cluster #1) are more involved in FC alteration after mTBI. The color-bar indicates number of involved connectomic signatures. 56

Figure 25. Categorization of affected functional connectivity using the multi-view cluster-wise cluster method. (a)-(c) shows the connectomic signatures involve in the interaction between cluster #1 (C1) and clusters #4 (C4), 5 (C5), and 8 (C8), respectively. These interactions represented in important role of the PCC as the central hub of the brain and its interactions with association brain areas as compensatory affect after brain injury. (d) reveals the interaction between the occipital lobe, cluster #3 (C3), and the frontal lobe, cluster #8 (C8)..... 56

Figure 26. Changes in behavioral domain interactions at the acute state. Negative values indicate decreases in interaction in patient group. Color-bar indicates the percent change..... 67

Figure 27. Functional roles of connectomic signatures. The affected DICCCOLs were divided in 5 categories with 53 sub-categories using meta-analysis. Meta-analysis reveals that the emotion, cognition/attention, and action/execution categories are involved in more connectomic signatures than

others, with 25, 23, and 23 DICCCOLs each, respectively. The vertical axis is number of the affected DICCCOLs associated with each functional role 67

Figure 28. Categorization of altered functional connectivity in mTBI. The color-bar indicates percent change. The results show that the action and cognition networks have been disrupted the most. Further functional analysis using the 53 subcategories shows that interaction between execution (from the action category) and attention (from the cognition category) and between execution (from the action category) and working memory (from the cognition category) have been affected the most (yellow arrow). This is consistent with published literature on attention, working memory and executive function deficit. 68

Figure 29. Schematic of analytical approaches which can be applied on rsfMRI data. The connectivity domain, similar to the time domain, allows us to perform a wide range of data-driven methods. The connectivity domain also supports implementing model-based methods such as first-level generalized linear model (GLM) on rsfMRI data (blue box). While feature-based approaches have been performed as second-level analyses, the connectivity domain provides us the opportunity to perform feature-based techniques at both first and second levels. 76

Figure 30. A schematic of the analysis pipeline. Data was preprocessed, and either kept in the time domain or transformed into the connectivity domain, which involved calculating connectivity weights using seed networks. Similar data-driven approaches were applied in both domains and compared between the two domains. Feasibility of applying model-based methods was evaluated in the connectivity domain. ... 77

Figure 31. Functional connectivity weights calculation. Overlay of 145 ROIs on (a) coronal, (b) sagittal, and (c) axial views of MNI atlas. (d) Color code map of 145 ROIs. (e) Functional connectivity weights of ROIs 50 (right insular cortex), 75 (right subcallosal cortex), 83 (posterior division of parahippocampal gyrus), 101 (left caudate), and 102 (left putamen), respectively; the ROIs are annotated on Figure 31.a and c. For this study Harvard-Oxford cortical and subcortical structural atlases were used. 78

Figure 32. Spatial maps identified for both domains at both time points. The upper portion of the figure reveals nine consistent brain networks found in both domains including the DMN (a), left parietal-frontal (working memory) network (b), right parietal-frontal (working memory) network (c), auditory network (d), frontal DMN (e), motor network (f), primary visual network (g), secondary visual network (h), and subcallosal network (i). An attention network (j) seems consistent between two domains; however, it was not appropriately extracted in the second session for the time domain (j^2). The lower portion shows the spatial maps which were identified in one domain but not the other one, or one time point but not the other 80

Figure 33. Spatial similarity between consistently-identified networks (Figure+++), including the DMN (a), left parietal-frontal (working memory) network (b), right parietal-frontal (working memory) network (c), auditory network (d), frontal DMN (e), motor network (f), primary visual network (g), secondary visual network (h), and subcallosal network (i) in the time (red) and connectivity (blue) domains for test-retest analysis. The spatial similarities between independent components were obtained from the TC-BR analysis using the data of the two parts of the first session. * identifies significantly higher spatial similarities in the connectivity domain as compared to the time domain. 81

Figure 34. The ICNs identified using a GLM method from the independent dataset (i.e. Henry Ford Hospital). The design matrix that was used for this analysis is from the first session of WSU data (a different group of subjects)..... 83

Figure 35. DICCCOLs (yellow spheres) and the connected fiber bundles that are involved in the connectomic signatures 21 (a) and 26 (b). These connectomic signatures show significant correlation with the memory composite score in all the applied models 93

Figure 36. DICCCOLs are shown in yellow sphere. DICCCOLs are involved in the connectomic signatures 36 (a) and 25 (b) which show a significant correlation with the attention/processing speed composite score after FDR correction. The connected fiber bundles have also been shown..... 95

LIST OF ABBREVIATIONS AND GLOSSARY OF TERMS

AAL	Automated Anatomical Labeling
ACC	Anterior Cingulate Cortex
AD	Alzheimer's Disease
ADHD	Attention Deficit Hyperactivity Disorder
AF	Arcuate Fasciculus
BA	Brodmann Areas
BGN	Basal Ganglia Network
BOLD	Blood-Oxygenation-Level Dependent
CC	Corpus Callosum
Cing	Cingulum
DAI	Diffuse Axonal Injury
DICCCOLS	Dense Individualized Common Connectivity based Cortical Landmarks
DLPFC	Dorsolateral Prefrontal Cortex
dHB	Deoxyhemoglobin
DMN	Default Mode Network
dMRI	Diffusion Magnetic Resonance Imaging
EEG	Electroencephalogram
EN	Executive Network
FC	Functional Connectivity
FDR	False Discovery Rate
FEF	Frontal Eye Field

FIC	Fronto-Insular Cortex
FLAIR	Fluid Attenuation Inversion Recovery
fMRI	Functional Magnetic Resonance Imaging
FPN	Frontoparietal Network
FWER	Family-Wise Error Rate
GICA	Group Independent Component Analysis
GLM	General Linear Model
ICA	Independent Component Analysis
ICN	Intrinsic Connectivity Network
IFOF	Inferior Fronto-Occipital Fasciculus
ILF	Inferior Longitudinal Fasciculus
IPL	Inferior Parietal Lobule
IPS	Intraparietal Sulcus
MD	Mean Diffusion
MEG	Magnetoencephalography
MK	Mean Kurtosis
MRI	Magnetic Resonance Imaging
mPFC	Medial Prefrontal Cortex
mTBI	Mild Traumatic Brain Injury
NBS	Network Based Statistic
NEX	Number of Excitations
oHB	Oxyhaemoglobin

PASL	Pulsed Arterial Spin Labeling
PCA	Principle Component Analysis
PCC	Posterior Cingulate Cortex
PET	Positron Emission Tomography
PF	Projection Fibers
PPC	Posterior Parietal Cortex
preSMA	Presupplementary Motor Area
RFIC	Right Fronto-Insular Cortex
ROI	Region Of Interest
rsfMRI	Resting State Functional Magnetic Resonance Imaging
SBA	Seed Based Analysis
SC	Structural Connectivity
SFOF	Superior Frontal Occipital Fasciculus
SLF	Superior Longitudinal Fasciculus
SN	Saliience Network
SVM	Support Vector Machine
SWI	Susceptibility Weighted Imaging
TBI	Traumatic Brain Injury
TE	Echo Time
TPJ	Temporal-Parietal Junction
TR	Repetition Time
UF	Uncinate Fasciculus

VFC	Ventral Frontal Cortex
VLPFC	Ventrolateral Prefrontal Cortex
VMPFC	Ventromedial Prefrontal Cortex
WM	White Matter

CHAPTER 1. INTRODUCTION AND BACKGROUND

1.1. Mild TBI (mTBI) Definition and Causes

Traumatic brain injury (TBI) is a non-degenerative, non-congenital injury that is caused by direct impact or inertial forces (acceleration/deceleration) (Sharp and Jenkins, 2015; Sharp et al., 2014). Trauma of the head is among the most frequent neurological disorders (Vos et al., 2012). However, public awareness about TBI is still limited, and because of that, TBI is referred to as the "silent epidemic" (Faul et al., 2010). TBI, with a rate of approximately 52,000 deaths per year, is a leading cause of death and disability in the United States; people of all ages, races/ethnicities, and incomes are affected (Coronado et al., 2011; Faul et al., 2010; Shenton et al., 2012). Although death rates have decreased thanks to improvements in safety features in motor vehicles, injury detection, and management, a comparison of rates over time reveals an increase in the incidence of TBI-related emergency department (ED) visits and hospitalizations (Coronado et al., 2011). Thus, TBI still remains a significant public health care burden in the US and worldwide (Kay T, 1993; National Institutes of Health, 1999). According to the Centers for Disease Control and Prevention, each year in the United States, almost 1.7 million people sustain traumatic brain injuries. Over the past few years, TBI has also gained national awareness because of injuries resulting from sports and traffic crashes, and because it is the "signature wound" of soldiers in the anti-terrorism wars in Iraq and Afghanistan (Zoroya, 2007). Furthermore, cognitive deficits after TBI are a major cause of daily life disability (CDC, 2003; Ruff, 2005).

More than 75% of TBI cases are classified as mild in severity, often referred to as mild TBI (mTBI) or concussion (Bruns and Jagoda, 2009; Shenton et al., 2012), accounting for over 1 million emergency department (ED) visits annually in the United States (Kay T, 1993). It is also known that a large number of mTBI cases are not treated at hospitals (Cassidy et al., 2004). This clearly underscores the importance of mTBI in public health. Directly and indirectly, mTBI costs the United States more than \$55 billion each year, resulting in a significant economic burden (Bergman and Bay, 2010; Corrigan et al., 2010). Despite these, mTBI has long been considered a non-critical injury. Most mTBI patients usually stay in the ED for only a few hours and then are discharged home without specific follow-up instructions (Iraji et al., 2015). Serious short- and long-term effects have been documented among mTBI patients, and

a significant number of mTBI patients experience acute and protracted neurocognitive symptoms (Ruff, 2005). Additionally, there is broad acceptance that patients with multiple mTBIs can have serious long-term consequences (Guskiewicz et al., 2003). While most mTBI patients recover in the first three months (Kashluba et al., 2004; Sharp and Jenkins, 2015), up to 30% of mTBI patients, known as the “miserable minority,” suffer persistent cognitive and physical symptoms beyond the six months post-injury timeframe, and in some cases, these injuries lead to long-term disability (CDC, 2003; Hou et al., 2012; Ruff, 2005; Sharp and Jenkins, 2015; Stulemeijer et al., 2008). Various factors including previous head injuries, pre-existing psychological problems, older age, and gender can play roles in persistent symptoms (Sharp and Jenkins, 2015). Even a mild injury without such long-term disability can have a substantial impact on quality of life and on society (CDC, 2003; Ruff, 2005).

There are obviously important questions that we need to answer in order to create clear guidelines for the management of mTBI, including uncertainty regarding acute assessment, treatment, and the extent that patients need to receive follow-up care (Sharp and Jenkins, 2015).

1.1.1. mTBI Causes

mTBI can result from several causes such as motor vehicle crashes, bicycle crashes, assault, sport injuries, being struck by a vehicle, and falls. The risk rate of mTBI is almost double in men compared to women (Cassidy et al., 2004). Most of these injuries result from falls and motor vehicle crashes (Bruns and Jagoda, 2009; Cassidy et al., 2004). Falls are responsible for a significant proportion of mTBI at the extremes of age, and motor vehicle collisions are the predominant etiology in adolescent and young adult males (Bruns and Jagoda, 2009).

1.1.2. Definition of mTBI

Definitions of mTBI are not identical but similar enough among scientists (Ruff and Jurica, 1999). According to the American Congress of Rehabilitation Medicine (ACRM) (1993), "A patient with mild traumatic brain injury is a person who has had a traumatically induced physiological disruption of brain function, as manifested by at least one of the following:

1. any period of loss of consciousness;

2. any loss of memory for events immediately before or after the accident;
3. any alteration in mental state at the time of the accident (eg, feeling dazed, disoriented, or confused); and
4. focal neurological deficit(s) that may or may not be transient; but where the severity of the injury does not exceed the following:
 - loss of consciousness of approximately 30 minutes or less;
 - after 30 minutes, an initial Glasgow Coma Scale (GCS) of 13–15; and
 - post-traumatic amnesia (PTA) not greater than 24 hours.

According to the Centers for Disease Control and Prevention (CDC, 2003), "The conceptual definition of mTBI is an injury to the head as a result of blunt trauma or acceleration or deceleration forces that result in one or more of the following conditions:

- Any period of observed or self-reported:
 - Transient confusion, disorientation, or impaired consciousness;
 - Dysfunction of memory around the time of injury;
 - Loss of consciousness lasting less than 30 minutes.
- Observed signs of neurological or neuropsychological dysfunction, such as:
 - Seizures acutely following injury to the head;
 - Among infants and very young children: irritability, lethargy, or vomiting following head injury;
 - Symptoms among older children and adults such as headache, dizziness, irritability, fatigue or poor concentration, when identified soon after injury, can be used to support the diagnosis of mild TBI, but cannot be used to make the diagnosis in the absence of loss of consciousness or altered consciousness. Research may provide additional guidance in this area.

Recently, Sharp and Jenkins took advantage of the Mayo system to classify mTBI patients (Sharp and Jenkins, 2015) (Figure 1). One of the benefits of the Mayo system (Malec et al., 2007) is that it

combines the duration of loss of consciousness, length of post-traumatic amnesia, lowest recorded Glasgow Coma Scale in the first 24 hours, and initial neuroimaging results, and it separates mTBI patients into two groups: probable and possible TBI (Box 1) which together are classically considered as mTBI. For each subject, the Mayo system integrates all available relevant positive indicators which have well-established predictive validity. This increases its ability to better classify mTBI cases in the presence of the heterogeneity in mTBI and decreases the influence of factors unrelated to the severity of mTBI, which could influence the assessment of the well-established indicators when applied individually. While we consider both subgroups as "mTBI", we can use these subgroups classification to classify and evaluate neuroimaging findings.

**B Combined Traumatic Brain Injury
Classification using the Mayo criteria
and separating post-injury symptoms**

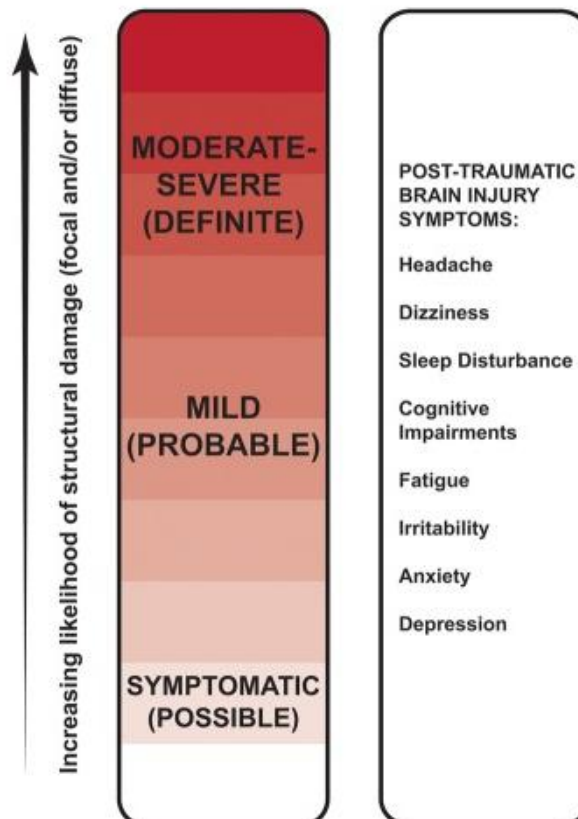


Figure 1. Classification of traumatic brain injury using Mayo Criteria (Sharp and Jenkins, 2015)

Box 1. Mayo Traumatic Brain Injury (TBI) Classification System

- A. Classify as Moderate–Severe (Definite) TBI if one or more of the following criteria apply:
1. Death due to this TBI
 2. Loss of consciousness of 30 min or more
 3. Post-traumatic anterograde amnesia of 24 h or more
 4. Worst Glasgow Coma Scale full score in first 24 h <13 (unless invalidated upon review eg, attributable to intoxication, sedation, systemic shock)
 5. One or more of the following present:
 - Intracerebral hematoma
 - Subdural hematoma
 - Epidural hematoma
 - Cerebral contusion
 - Hemorrhagic contusion
 - Penetrating TBI (dura penetrated)
 - Subarachnoid hemorrhage
 - Brainstem injury
- B. If none of Criteria A apply, classify as Mild (Probable) TBI if one or more of the following criteria apply:
1. Loss of consciousness momentarily to less than 30 min
 2. Post-traumatic anterograde amnesia momentarily to less than 24 h
 3. Depressed, basilar or linear skull fracture (dura intact)
- C. If none of Criteria A or B apply, classify as Symptomatic (Possible) TBI if one or more of the following symptoms are present:
- Blurred vision
 - Confusion (mental state changes)
 - Daze
 - Dizziness
 - Focal neurological symptoms
 - Headache
 - Nausea

1.2. Clinical Imaging mTBI Findings

mTBI remains a difficult diagnosis to confirm. The brain biofluid-based biomarkers do not have enough sensitivity and specificity to accurately diagnose and localize the brain injury (Kou et al., 2012; Kou et al., 2010), and the brain often appears quite normal in conventional clinical imaging modalities, providing false reassurance (Shenton et al., 2012). Specifically, conventional clinical imaging modalities are insensitive to subtle vascular or white matter injuries (Sharp and Jenkins, 2015). While magnetic resonance imaging (MRI), in conventional clinical modes such as T2- and T1-weighted structural, is a premier modality for imaging the brain and surpasses computed tomography (CT) in detecting lesions of the brain (McAllister et al., 2001), it adds only little to clinical diagnoses beyond what is provided by CT

(Eierud et al., 2014; Shenton et al., 2012). As a result, considering the speed and cost, CT is routinely used in the ED despite the health risk from ionizing radiation and ineffectiveness in detection of a wide range of brain alterations after mTBI such as diffuse axonal injuries (DAI) (Eierud et al., 2014; Sharp and Jenkins, 2015; Shenton et al., 2012).

In the ED, the majority of mTBI patients have negative findings on clinical conventional imaging techniques including CT and MRI scans (Belanger et al., 2007; National Academy of Neuropsychology, 2002). However, advanced MRI techniques such as diffusion imaging (Arfanakis K et al., 2002; Benson RR et al., 2007; Conturo et al., 1996; Huisman et al., 2004; Inglese et al., 2005; Kou Z et al., 2007; Mac Donald CL et al., 2007; Mac Donald et al., 2011; Ptak T et al., 2003; Shimony JS et al., 1999), susceptibility weighted imaging (Kou Z, 2010; Paterakis K, 2000; Reichenbach JR, 1997), functional MRI (Iraji et al., 2015; Iraji et al., 2016c; Mayer et al., 2015b; Mayer et al., 2011; Stevens et al., 2012), and many others (Kou et al., 2012; Kou et al., 2010) have significantly improved our ability to investigate the brain from various aspects and show a great potential to detect brain alterations after mTBI (Kou et al., 2012; Kou and Iraji, 2014; Kou et al., 2010). For instance, it has been reported that mTBI patients have microstructural damage, especially in major white matter tracts (Kou and VandeVord, 2014; Kou et al., 2010; Niogi and Mukherjee, 2010; Niogi et al., 2008a). Thus, white matter integrity assessments using diffusion imaging that provides a sensitive marker of white matter injury have become a major part of our focus in TBI studies (Ilvesmaki et al., 2014; Sharp and Jenkins, 2015). For microstructural damage, the most susceptible white matter tracts are long-distance white matter tracts, including the corpus callosum (CC), superior coronal radiata, cingulate bundle, superior and inferior longitudinal fasciculus, and accurate fasciculus (Bonnelle et al., 2011; Kou et al., 2012; Kou and VandeVord, 2014; Kou et al., 2010; Lipton et al., 2012; Narayana et al., 2015; Sharp et al., 2014; Yuh et al., 2014). The damage in these tracts, measured by fractional anisotropy (FA) on diffusion MRI (dMRI), has been reported to be associated with mTBI patients' neurocognitive symptoms or post-concussion syndrome (PCS) scores (Baek et al., 2013; Bazarian et al., 2007; Caeyenberghs et al., 2014; Grossman et al., 2013; Irimia et al., 2012; Jorge et al., 2012; Niogi et al., 2008a; Treble et al., 2013; Wu et al., 2010). Although many studies have reported alterations in white matter integrity after mTBI, the results are inconsistent and diverse so we are still unable to draw conclusions. The inconsistent results could be due to several factors, including

but not limited to various sources of injuries and patient's characteristics, heterogeneous and subject-specific features of mTBI, small sample sizes in previous studies, and differences in the time between injury and scan (Ilvesmaki et al., 2014; Sharp and Jenkins, 2015). In addition, there is still a lack of data to investigate the extent of alteration in the brain's structural connectivity (SC) from a network perspective.

In addition to microstructural damage, alterations in functional activity of the brain also occurs after mTBI, either due to direct damage to the functional networks or the brain's response to the microstructural damage. Therefore, an investigation of the brain's functional activity is also important for a further understanding of brain alterations and for elucidating the neuropathology associated with mTBI. Functional MRI (fMRI) offers great potential for elucidating the neuropathological changes associated with brain diseases (Chen et al., 2012; Irajy et al., 2015; Jafri et al., 2008; Johnson et al., 2012; Kou and Irajy, 2014; Mayer et al., 2011; McAllister et al., 1999; Morgan et al., 2013; Sorg et al., 2007; Tian et al., 2006; Tivarus et al., 2012; Wang et al., 2006; Zhou et al., 2007). For instance, resting state fMRI (rsfMRI) studies show alterations in functional connectivity (FC) of several brain regions and brain networks after brain injury (Irajy et al., 2015; Irajy et al., 2016b; Irajy et al., 2016c; Johnson et al., 2012; Kou and Irajy, 2014; Mayer et al., 2011; Messe et al., 2013; Stevens et al., 2012; Tang et al., 2011; Zhou et al., 2012).

1.3. Brain and Brain Connectivity

The brain is the central processor of all mental and physical activities. The brain consumes more than 20% of total body energy consumption, and 60–80% of the brain's energy usage is related to the intrinsic neuronal activity (Shulman et al., 2004). The brain is a complex nexus, and brain regions are functionally linked with each other to constantly share information and perform various mental activities. Regions of the brain are structurally connected via white matter fibers, directly or indirectly. Due to these direct or indirect structural connections, information is shared and transformed among brain regions, which leads to FC between brain regions despite spatial distance and in the absence of direct structural connection (Allen et al., 2011; Beckmann et al., 2005; Robinson et al., 2009; van den Heuvel et al., 2008b). For instance, considering that a functional brain network reflects a specific pattern of neural communication and interaction between brain regions, there should be a kind of (direct or indirect) structural connectivity (SC) between different regions of a brain network despite the spatial distance

(Bullmore and Sporns, 2009; Damoiseaux and Greicius, 2009; van den Heuvel et al., 2008b). For example, specific white matter tracts have been suggested to structurally interconnect the functionally-linked regions of the default mode network (DMN) (Greicius et al., 2009; van den Heuvel et al., 2008b).

Scientists have been investigating brain function and pathology for specific brain regions for a long period of time, but there is currently a growing interest in studying brain connectivity at a large scale to characterize alterations in the brain after disorders (Fornito and Bullmore, 2015), and findings demonstrate the important role of large-scale neural system connections in many brain disorders (Fornito and Bullmore, 2015; Iraj et al., 2016b; Iraj et al., 2016c; Sharp et al., 2014; Skudlarski et al., 2010; van den Heuvel et al., 2013; Zhang et al., 2011; Zhu et al., 2014a). One category of large-scale connectivity analyses is connectome approaches.

Connectome is a general term and is defined as the comprehensive map of connection patterns of the human brain. The connectome can be studied in several spatio-temporal scales such as a micro-level spatial scale or a macro-level spatial scale (Fornito and Bullmore, 2015; Sporns et al., 2005). Advanced MRI modalities provide us the opportunity to investigate the brain connectome at a macro-level. Investigating the brain connectome at a macro-level scale and combining SC and FC will provide a better understanding of how brain function is related to with structural substrate and the effects of different behaviors and disorders on the brain (Sporns et al., 2005; Toga et al., 2012). Large-scale connectivity analysis can also be modeled in the form of networks (sets of highly connected neural elements) and their interactions (Bullmore and Sporns, 2009; Sharp et al., 2014; Sporns, 2014). Network-based (also known as circuit-based) analysis is another large-scale approach and a promising tool to study brain disorder (Fornito and Bullmore, 2015) and was suggested as being useful for individual measures for clinical usages (Sharp et al., 2014).

1.3.1. Brain Connectivity Analysis

Performing large-scale connectivity analysis with MRI involves several steps (Fornito and Bullmore, 2015; Sporns, 2014): 1) identifying connectivity nodes; 2) defining connectivity indices; 3) calculating brain connectivity; and 4) statistical analysis.

1) Identifying Connectivity Nodes

The first step is to identify a set of similar regions of interest (ROIs) among subjects, which are often called nodes (Fornito and Bullmore, 2015; Sporns, 2014). Identifying connectivity nodes is challenging because there is no accurate way to identify any feature or boundary which truly allows distinction of different brain areas and systems (Fornito and Bullmore, 2015; Sporns, 2014; Wig et al., 2011). Therefore, various methods which use different structural or functional features of the brain have been used to identify nodes (Sporns, 2014; Wig et al., 2011). Researchers have used *a priori* anatomical templates (Desikan et al., 2006; Tzourio et al., 1997); data-driven approaches such as using fMRI information from the blood oxygen level dependent (BOLD) signal (Blumensath et al., 2013; Cohen et al., 2008; Nelson et al., 2010) and random parcellations of varying resolution (Fornito et al., 2010); the SC profiles (Zhu et al., 2013); using other features of the brain cortex such as myelin content (Glasser and Van Essen, 2011); and histological data (Eickhoff et al., 2005). There are also some approaches that fine-tune and adjust connectivity nodes using one or more modalities to study another modality (Cloutman and Lambon Ralph, 2012; Zhu et al., 2014b). A majority of this type of approaches use functional information from fMRI to select or modify connectivity nodes for structural connectivity analysis and tractography. Using functional information in the connectivity node selection step is suggested to be more reliable than using atlases, such as the Brodmann or AAL atlases (Zhu et al., 2014b). The second common category of these approaches utilizes white matter structures to choose or tailor the connectivity nodes for functional connectivity analyses. We can use SC information for cortical parcellation and investigate FC among the parcels (Cloutman and Lambon Ralph, 2012; Honey et al., 2009) or utilize the structural profile to select and predict the corresponding functions of the connectivity node across subjects (Zhu et al., 2013). However, there is no perfect approach, and each approach has its own strengths and limitations; therefore, selection of an approach should be based on the question that a researcher is interested in addressing (Fornito and Bullmore, 2015). For instance, if we are interested to combined several modalities like combining the SC and FC and analyzing them simultaneously, it would be a helpful if the connectivity node selection method is applicable and meaningful across modalities (Sporns, 2014). If the connectivity nodes selection method uses structural information which is not aligned with FC profiles or

uses the FC information which is not aligned with SC profiles, then analyses in either case could lead to inconsistent results across studies (Sporns, 2014).

2) Defining Connectivity Indices

A connectivity index is a measure that represents the strength of a type of brain connectivity. There are several types of brain connectivity, including structural, functional, effective, and dynamic connectivity (Fornito and Bullmore, 2015). All of these connectivity concepts are working together as a whole to facilitate brain activities. In noninvasive studies of brain connectivity, scientists measure different properties which are directly or indirectly related to a specific connectivity. These properties are associated with either brain physical structure or brain physiological activity and are used in order to estimate the connectivity. The BOLD signal, cerebral blood flow (CBF), or diffusion of water molecules are some examples of these properties (Buckner and Vincent, 2007; Johansen-Berg and Behrens, 2013; Logothetis and Wandell, 2004; Rao et al., 2007; Sporns et al., 2005; Wang et al., 2003; Wang et al., 2015).

The next step after choosing properties of interest is to use a connectivity index to calculate and quantify the selected brain connectivity. A wide range of measurements has been used for this purpose with each representing a specific feature of brain connectivity. Some examples of connectivity indices are FA and fiber density for SC (Aron et al., 2007; Bonnelle et al., 2012; Honey et al., 2009; Uddin et al., 2011); and correlation, synchronization likelihood, mutual information, partial correlations, coherence, and Bayes net methods for FC (Fornito and Bullmore, 2015; Smith et al., 2011; Sporns, 2014; Wang et al., 2015).

3) Calculating Brain Connectivity

Similar to previous steps, there is wide range of ways to render and exhibit brain connectivity. The first group of analysis focuses on mapping brain connectivity in specific brain systems known as network-based analysis or circuit-based analysis (Fornito and Bullmore, 2015). A network is defined as a brain system that includes a set of brain regions which are significantly interconnected with each other in a distinguishable way (Meda et al., 2009; Menon and Uddin, 2010; Sporns, 2013). Independent component analysis is an example of a technique in this group of analyses that can be used to investigate

the brain's FC. Network-based approaches are powerful tools for investigating the structural and functional integrity of specific neural systems (Fornito and Bullmore, 2010, 2015; Zhang and Raichle, 2010). These analyses are especially useful and demonstrate significant sensitivity when there is a prior hypothesis or knowledge involving the influence of a brain disorder on a specific brain function or network, for instance, when specific neurocognitive symptoms exist or interactions between some cognitive functions is altered (Beckmann and Smith, 2004; Calhoun et al., 2001; Fornito and Bullmore, 2010, 2015). The second group of analyses is connectome-wide analysis, which is more useful for exploratory investigations. Connectome-wide analyses produce comprehensive connectivity maps between all connectivity nodes and are usually represented in a style known as a connectivity matrix (Fornito and Bullmore, 2015). The connectivity matrix can also be rendered as a graph, and a wide range of graphic analysis can be performed on it. For instance, we can perform topological analyses and evaluate how connections are arranged with respect to each other (Fornito and Bullmore, 2015).

4) Statistical Connectivity Analysis

After defining and calculating brain connectivity, the next step would be performing statistical analysis. Several methods exist, and a researcher should select an approach based on the question and the parameters selected in the previous steps. For instance, a statistical comparison can be applied on each connection independently and isolated from other connections, or it can be applied by considering connections as a part of a larger structure. Zalesky et al. developed the network-based statistic (NBS) method which considers all connections as part of a larger complex. NBS utilizes the benefit of graph features to improve statistical power and provide the ability to reject the null hypothesis at the network level (Zalesky et al., 2010).

1.4. Cognitive and Psychiatric Symptoms

Despite negative findings on clinical imaging for the majority of mTBI patients, including computed tomography (CT) and conventional magnetic resonance imaging (MRI), such as at T1, T2*, and fluid attenuation inversion recovery (FLAIR) sequences, (Belanger et al., 2007; National Academy of Neuropsychology, 2002), many mTBI patients suffer from long term cognitive and emotional symptoms. A multi-center study with a large dataset reported that up to 22% of mTBI patients have impaired functional

status at 12 months (McMahon et al., 2014). Grossman and his colleagues reported 25%, 30%, and 30% impairment after mTBI in executive function, memory and learning, and information processing, respectively (Grossman et al., 2013). Our own investigations also show alterations in the interaction between regions associated with "execution" and "attention", and "execution" and "working memory" after mTBI. Interestingly, all of these cognitive domains are high-level cognitive functions. High-level cognitive functions process information that they acquire from several anatomically distinct brain regions (Sharp et al., 2014), which makes the study of brain function using large-scale approaches an appropriate choice to analyze high-level cognitive functions. Several brain regions are involved in executive functions and working memory, including the posterior cingulate cortex (PCC), medial frontal cortex, the dorsolateral prefrontal cortex and parietal cortex, and the anterior insula (Barbey et al., 2015; Bonnelle et al., 2012; Hillary et al., 2014; Sharp et al., 2014).

1.5. Objective and Project Motivation

In this section, we first explain some concepts about mTBI and brain connectivity which help us to identify gaps in our understanding and to choose appropriate analytical techniques with which to address them.

I) Physiogenic vs. Psychogenic Classification of mTBI: mTBI cannot be merely categorized as a physiogenic or psychogenic disorder. The physiogenic view does not consider the co-morbidities. There are several emotional and mental disturbances such as PTSD, depression, and fear, which can be present after mTBI. They can cause significant alterations in brain connectivity, especially from a functional point of view. On the other hand, the psychogenic view does not carefully consider brain connectivity alterations such as microstructural damage, which cannot be identified using conventional clinical imaging (Shenton et al., 2012).

II) Direct and Indirect Effects: Alteration in one connection can directly or indirectly alter other brain connections. The brain is a complex hyper-connected nexus, and any alteration in a brain connection due to brain injury causes a domino effect that affects other structural or functional connections of the brain. In this situation, the outcome mechanism of the brain after injury is not limited to the location and the origin of the injury. Several studies have demonstrated that damage in one brain

region or connection can lead to disturbances in other brain regions and connections (Barbey et al., 2015; Bonnelle et al., 2012). However, further investigations are required to understand the underlying mechanisms.

III) Large-scale approaches: Large-scale brain connectivity analyses such as network-based or connectome-wide approaches are more sensitive to alterations that are less apparent in gross structure (e.g. white matter integrity), because large-scale approaches consider each region's integration into a larger structure rather than consider each region as an independent entity. Therefore, large-scale approaches can provide a better understanding of brain alterations and uncover the role of brain alterations at the macro level (Carter et al., 2010; Carter et al., 2012). The importance of large-scale alterations in comparison with local alterations is more significant in mTBI than severe and moderate TBI because there is usually no significant structural damage in mTBI, indicating that this may account for a greater portion of the problem in mTBI than in moderate or severe TBI. Mapping the topography of the brain connectivity alterations at a large scale after mTBI can improve neuropsychologists' understanding of mTBI sequelae.

IV) Heterogeneity: mTBI is a heterogeneous disorder because there are: 1) different mechanisms of injury (e.g. vehicular collision vs. sports) which result in different scenarios of biomechanical loading (strain and stress); 2) different injury pathologies (e.g. neuronal injury vs. axonal injury vs. vascular injury); and 3) different subjects with different pre-existing conditions and demographic characteristics (age, gender, and education level) (Eierud et al., 2014). Because of the heterogeneous characteristic of mTBI and the close relationship between the alterations of structural and functional connectivity, neither dMRI nor rsfMRI alone is capable of characterizing the multifaceted nature of mTBI (Shenton et al., 2012).

V) Early-Stage and Late-Stage Damage and Recovery: After mTBI, the brain experiences two types of injuries: 1- early-stage or primary injuries that occur at the time of impact and as a result of the physical forces applied to the brain; and 2- late-stage or secondary injuries that initiate at the moment of injury and continue over time. Secondary injuries include hematomas, cerebral edema, increased intracranial pressure, ischemia, and various injury cascades (McAllister et al., 2001). Different types of injuries could result in different alterations in brain connectivity or functions, which complicates

investigation of brain injury. That being said, the expected outcome of most mTBI patients is eventually recovery. However, in some cases, persistent disabling sequelae caused by the initial injury can last after a period of apparent recovery. It is statistically difficult and challenging to predict an individual's full recovery process.

1.6. Current Gaps in the Field

To date, alterations in the brain's structural and functional connectivity after mTBI are still unclear, considering the high level of complexity due to several factors such as the time between injury and scan, individual subject specific features, different mechanisms of injury, and heterogeneity (Eierud et al., 2014; Ilvesmaki et al., 2014; Sharp and Jenkins, 2015). The significant lack of investigations of large-scale connectivity analysis and the recovery process further hinder our understanding of brain injury. At the same time, despite current findings, there is still a significant need for studying the relationship between the neurocognitive symptoms of an mTBI patient and their neuroimaging findings. Evaluating this relationship can lead to the development of proper diagnostic tools that are sensitive enough to accurately diagnose the brain injury and specific enough to identify the disrupted brain connections. The **goal** of my PhD dissertation is to bridge this gap by identifying the brain alterations after mTBI using large-scale structural and functional connectivity and by calculating the relationship between neuroimaging findings and neurocognitive symptoms.

CHAPTER 2. RESEARCH DESIGN

As explained in the previous chapter, the level of complexity in mTBI is high, and investigating brain connections at a large scale can help us to better understand the brain's alterations after mTBI. Furthermore, to improve clinical translation of neuroimaging findings, we need to study the relationship between these findings and mTBI patients' neurocognitive symptoms. Evaluation of the relationships between an mTBI patient's neurocognitive symptoms and brain connectivity alterations can lead to the development of better approaches to accurately diagnose and treat the brain injury.

2.1. Project Aims

Central Hypothesis: mTBI results in both structural and functional connectivity alterations at a large scale.

2.1.1. Specific Aim 1

To investigate brain structural and functional connectivity changes in mTBI patients.

Hypothesis: mTBI causes detectable alterations of brain connectivity, especially at a large scale.

Various studies have reported brain structural and functional connectivity alterations after mTBI (Iraji et al., 2015; Kou and Iraji, 2014; Mayer et al., 2011; Messe et al., 2011; Niogi and Mukherjee, 2010; Stevens et al., 2012; Tang et al., 2011); however, connectivity changes after mTBI are still unclear. This study is designed to investigate brain structural and functional connectivity at the large-scale macro level.

2.1.2. Specific Aim 2

To investigate the relationship between brain connectivity and clinical neurocognitive symptoms in mTBI patients.

Hypothesis: Neuroimaging findings in large-scale brain network connectivity predict mTBI patients' neurocognitive symptoms.

The ultimate goal of neuroimaging studies on mTBI is to identify diagnostic tools or biomarkers sensitive enough to accurately diagnose brain injury and specific enough to identify the disrupted brain functions. Achieving this goal helps physicians to prescribe proper rehabilitation plans that address

specific brain domains for speedier recoveries. Evaluating the statistical inference between neuroimaging data at the acute stage and neuropsychological data at a later stage can be one major step towards using neuroimaging data as a diagnostic tool to identify alterations in brain function at the early stage.

2.1.3. Specific Aim 3

To develop a novel approach for the analysis of brain functional connectivity to overcome the current limitations of rsfMRI analysis in the time domain.

Hypothesis: The connectivity domain analysis is superior to conventional time domain analysis in several aspects, including 1) enabling model-based analysis; 2) decreasing the influence of the group data on the brain networks of individual subjects; 3) reducing the susceptibility of analysis techniques to the choice of different parameters; and 4) being more suitable for cross-center data analysis.

2.2. Participant Population Demographics

This project focuses on the development of novel approaches to the analysis of both structural and functional brain connectivity in existing mTBI populations, supported by previous projects funded by the Department of Defense (DoD), International Society for Magnetic Resonance in Medicine, and Wayne State University, all mTBI patients' data were collected at Wayne State University (WSU) in Detroit. Healthy control participants and patients with a history of prior brain injury, neurological, neuropsychological or psychiatric disorder, or concurrent substance abuse were excluded. MRI exclusion criteria included metal and/or electronic implants, claustrophobia, pregnant or trying to become pregnant, and subjects weighing more than 300 pounds (136kg; machine's capacity limit).

Patients' eligibility was determined based on the GCS score. Only patients with a lowest-recorded GCS of 13-15 were considered. For a GCS of 15, there must be least one of the following: a) loss of consciousness less than 30 minutes, b) post-traumatic amnesia less than 24 hours, or c) an alteration in mental status (i.e., disoriented, dazed or confused).

Data from 40 mTBI patients was acquired at acute stage (within 24 hrs after injury). Among them 35 patients returned for data acquisition at follow-up (within 4-6 weeks after injury). Data was collected from a cohort of 58 healthy subjects. Among them, 36 subjects had data collected at the second time

point with an interval of 4-6 weeks. All structural MRI data, from both patients and healthy controls, were reviewed by our board certified neuroradiologist (CZ) to identify any abnormalities. The neuroradiologist was blinded to patients' diagnostic status.

2.3. Cognitive Assessment

In the acute setting, once a patient was conscious and medically stable, and came out of post-traumatic amnesia, if any; they were administered neurocognitive testing and surveyed about their post-concussion symptoms. A short instrument called the Standardized Assessment of Concussion (SAC) (McCrea M, 2000) was used as a brief assessment of neurocognitive function. The SAC was originally developed for field assessments of neurocognitive status following a sports concussion (McCrea M, 2003). It has been reported that the SAC is sensitive to the acute changes following concussion and requires limited training to administer (Naunheim RS, 2008). The SAC is scored 0 - 30 and assesses four cognitive domains including orientation, attention, immediate memory, and delayed recall. The SAC has demonstrated sensitivity to brain injury in the acute setting, particularly in delayed recall (Naunheim RS, 2008). The emergency room edition of the SAC also includes a PCS questionnaire where symptoms were graded from 0 to 3 (i.e., none, mild, moderate, severe). The PCS score was the sum of symptom scores for the questionnaire.

To assess the most common cognitive deficits, including in the domains of working memory (Barbey et al., 2015; Christodoulou et al., 2001; Hillary et al., 2011; Levine et al., 2002; McAllister et al., 2006; Nakamura et al., 2009; Newsome et al., 2007; Perlstein et al., 2004; Ricker et al., 2001; Sanchez-Carrion et al., 2008; Scheibel et al., 2007), attention (Hillary et al., 2011; Maruishi et al., 2007), processing speed (Hillary et al., 2011), and executive function (Barbey et al., 2015; Turner and Levine, 2008), we used standardized cognitive measures including the Brief Visuospatial Memory Test-Revised (Benedict et al., 2012) and the Hopkins Verbal Learning Test (Brandt, 1991; Gross et al., 2013) for memory and the Symbol Digit Modalities Test and the Color Trails Test (Dugbartey et al., 2000) for attention and processing speed. These measures provide efficient indices while avoiding ceiling or floor effects. A modified version of the post-concussion symptoms scale was obtained from the McGill Abbreviated Concussion Evaluation (Johnston et al., 2001). Finally, the Medical Symptom Validity Test (Armistead-

Jehle, 2010; Green et al., 2011) was administered to evaluate effort-related factors that affect cognitive test performance and outcome.

2.4. Imaging Protocol

MRI data was collected on a 3-Tesla Siemens Verio scanner with a 32-channel radiofrequency head-only coil. The structural image was collected using the MPRAGE sequence with TR (repetition time) = 1950ms, TE (echo time) = 2.26 ms, slice thickness = 1 mm, flip angle = 9°, field of view = 256 × 256 mm, matrix size = 256 × 256, and voxel size = 1 mm isotropic. dMRI data was acquired using a gradient echo EPI sequence with $b = 0/1000 \text{ s/mm}^2$ in 30 diffusion gradient directions with the following parameters: TR = 13300 ms, TE = 124 ms, pixel spacing size = 1.333 × 1.333 mm, matrix size = 192 × 192, number of slices = 60, slice thickness = 2 mm, flip angle = 90°, and number of excitations (NEX) = 2. rsfMRI data was performed using a gradient echo EPI sequence with the following imaging parameters: TR/TE = 2000/30 ms, slice gap = 0.595 mm, pixel spacing size = 3.125 × 3.125 mm, matrix size = 64 × 64, number of slices = 33, slice thickness = 3.5 mm, flip angle = 90°, 240 volumes for whole-brain coverage, NEX = 1, with an acquisition time of eight minutes. During resting state scans, subjects were instructed to keep their eyes closed, stay awake, and not focus on anything in particular. Data acquisition included more imaging protocols which were not used in this study. Pulsed arterial spin labeling (PASL) was acquired using a gradient echo EPI sequence with TR = 2830 ms, TE = 11 ms, flip angle = 90°, field of view = 384 × 384 mm, and voxel size = 4 mm isotropic. Susceptibility weighted imaging (SWI) was collected using T2* Gradient Recalled Echo (GRE) based sequence with long TE and 3D flow compensation. The sequence parameters include TR = 30 ms, TE = 20 ms, flip angle = 15°, field of view = 256 × 256 mm, voxel size = 0.5 × 1 × 2 mm³. T2 Fluid-attenuated inversion recovery (FLAIR) parameters are TR = 9000 ms, TE = 78 ms, flip angle = 150°, matrix size = 256 × 256 mm, slice thickness = 4 mm, and in-plane resolution = 1 mm.

CHAPTER 3. STRUCTURAL CONNECTIVITY (SC)

3.1. Background

Structural connectivity is defined as the anatomical connections among different parts of the brain physically characterized by a collection of myelinated nerve cells and their axonal and dendritic connections (Sporns et al., 2005; Wang et al., 2015). Different regions of the brain are structurally connected via white matter fibers, either directly or indirectly. Due to these direct or indirect structural connections, information is shared and transferred among brain regions. Therefore, despite spatial distance and absence of direct structural connection, brain regions are functionally linked with each other to constantly share information and perform various mental activities (Allen et al., 2011; Beckmann et al., 2005; Robinson et al., 2009; van den Heuvel et al., 2008b). For instance, considering that a brain network reflects the neural communication and interaction between brain regions, there should be a kind of (direct or indirect) structural connectivity between different regions of the brain network despite the spatial distance (Bullmore and Sporns, 2009; Damoiseaux and Greicius, 2009; van den Heuvel et al., 2008b). Focusing on the DMN, specific white matter tracts have been suggested to structurally interconnect the functionally linked regions of this network (Greicius et al., 2009; van den Heuvel et al., 2008b). dMRI provides us the ability to investigate the SC of the brain in vivo and non-invasively (Wang et al., 2015), and it is a powerful tool to evaluate microstructural integrity and the trajectories of white matter pathways (Figley et al., 2015). Before the advent of dMRI, identifying the SC of the brain using noninvasive in-vivo approaches was difficult, and most of our knowledge about SC of the brain was derived from lesions, invasive tracing, and brain dissections. dMRI maps the diffusion properties of water molecules in tissue (Johansen-Berg and Behrens, 2013). Because the diffusion process is influenced by the geometrical structure of the environment, dMRI can represent structural properties by mapping the diffusion properties in biological tissues (Johansen-Berg and Behrens, 2013). Therefore, since dMRI represents information about the tissue structure, it can be used to reconstruct brain structural connections. The basic principle of identifying the SC of the brain using dMRI is that water diffusion in the axon of white matter fibers is hindered in perpendicular directions and less restricted along axons. Therefore, water diffusion occurs primarily along fiber bundles, and by identifying the water diffusion, we can identify the direction of fibers

in each location. dMRI is a wonderful tool to non-invasively investigate fiber bundles and SC of the brain at different levels from micro to macro levels (Kou and Iraj, 2014). For this purpose, the information of the directions of fibers is calculated and is used to reconstruct SC using methods known as tractography. Tractography algorithms are used to identify the fiber bundles (streamline) between regions (Fornito and Bullmore, 2015; Honey et al., 2009). The accuracy of identifying fiber directions and SC depends on many parameters, especially the number of gradient directions, which varies from six to hundreds, and the analytical method used to reconstruct the orientations of fibers. It should be noted that these so-called fiber bundles are not axons, but instead they are indirect properties that render the actual SC (Fornito and Bullmore, 2015). Several connectivity indices can be used to calculate and quantify SC, including the number of fiber bundles (streamlines), average of FA or mean diffusivity (MD) over the putative fiber bundles, and probabilistic tractography measures (Bonnelle et al., 2012; Fornito and Bullmore, 2015; Hagmann et al., 2010; Honey et al., 2009; Uddin et al., 2011; van den Heuvel et al., 2008b; Wang et al., 2015). dMRI also allows us to investigate the brain's physiological conditions at the microstructural level that are invisible in conventional imaging (Iraj et al., 2011; Johansen-Berg and Behrens, 2013; Le Bihan and Johansen-Berg, 2012; Shenton et al., 2012; van Ewijk et al., 2012). For instance, brain injury or brain disease could lead to alteration in tissue diffusion properties such as the value of MD or FA.

3.2. Previous Findings on TBI

One common outcome of brain injury is DAI, which causes damage all over the brain, commonly in long-distance white matter tracts that connect spatially distant regions of the brain (Bonnelle et al., 2012; Sharp et al., 2014). dMRI has been reported to detect microstructural damage in major white matter tracts of mTBI patients (Kou and VandeVord, 2014; Kou et al., 2010; Niogi and Mukherjee, 2010; Niogi et al., 2008b). For microstructural damage, the most susceptible white matter tracts are the corpus callosum, the major tract that connects the two hemispheres; superior coronal radiate; cingulate bundle; superior and inferior longitudinal fasciculus; internal and external capsule; and accurate fasciculus (Bonnelle et al., 2011; Kou et al., 2012; Kou and VandeVord, 2014; Kou et al., 2010; Lipton et al., 2012; Narayana et al., 2015; Yuh et al., 2014).

While most studies show lower FA and higher MD in patients than in controls (Bonnelle et al., 2011; Grossman et al., 2013; Lipton et al., 2012; Narayana et al., 2015), these findings are not fully consistent across studies. For instance, Kou et al. reported both increased and decreased FA in different regions in the same patients in the acute setting (Kou et al., 2013). Some other studies found no significant differences in FA or MD (Ilvesmaki et al., 2014; Lange et al., 2012). Inconsistencies in the results could be due to several factors, such as the time between injury and scan, small sample sizes in previous studies, and heterogeneity and subject specific features of mTBI (Ilvesmaki et al., 2014; Sharp and Jenkins, 2015).

Since large-scale analysis can be more sensitive to alterations, it is important to explore the characteristics of brain connectivity at a large scale to have a better understanding of the disruptions in neural communication pathways (Bullmore and Sporns, 2009; Caeyenberghs et al., 2014).

3.3. Analytical Approach: Dense Individualized Common Connectivity Based Cortical Landmarks (DICCCOLs)

For structural analysis, we have used the DICCCOLs method (Iraji et al., 2016c; Zhu et al., 2013), which is briefly explained in this section. DICCCOLs are a set of brain landmarks with similar structural and functional connectivity across individuals obtained by identifying the consistent white matter (WM) fiber connection profile across subjects. This has been done using the tool available to download at <http://dicccol.cs.uga.edu/>. Zhu et al. previously identified 358 ROIs, known as DICCCOLs, distributed all across the brain. In addition to reproducibility and consistency, DICCCOL analysis has been shown to be powerful in identifying connectivity signatures in affected brains (Iraji et al., 2016c; Zhu et al., 2014a).

Identifying the locations of DICCCOLs on the brain of an individual can be summarized in following steps (Figure 2):

- 1) Deterministic tractography of the whole brain is performed (Figure 2.A). As a result, we can identify the WM fiber connection profile of each location of the brain.
- 2) Extraction of the transformation matrix for co-registering the brain of an individual subject to a brain template (Figure 2.B).

3) Application of the transformation matrix to transfer the individual surface and fiber bundles to the template space for prediction (Figure 2.C). As a result, the initial locations of DICCCOLs on the individual's brain is obtained.

4) Searching the local neighborhood (6 mm radius) of the initial location of each DICCCOL to find the optimized location of that DICCCOL. For this purpose, similarity between the fiber connection profile in the template and all local neighborhoods is measured. The neighborhood with the maximum similarity of the fiber connection profile with the fiber connection profile of the DICCCOL on the template is selected as the optimized location of the DICCCOL (Figure 2.D).

The same procedure is performed to identify optimized locations of all DICCCOLs on each individual's brain (Figure 2.E). DICCCOL landmarks have been shown to be highly reproducible across individuals (Zhu et al., 2014a). At the same time, according to the connective fingerprint concept, each brain's cytoarchitectonic area has a unique set of extrinsic inputs and outputs that largely determines the functions that each brain area performs (Passingham et al., 2002). The close relationships between structural connection patterns and brain functions have been extensively reported (Honey et al., 2009; Li et al., 2010a; Messe et al., 2015). Since each DICCCOL preserves consistent structural connection patterns, its functional role should be similar across subjects. The intrinsic functional role of each DICCCOL has been already extensively examined and validated (Yuan et al., 2013; Zhu et al., 2014a).

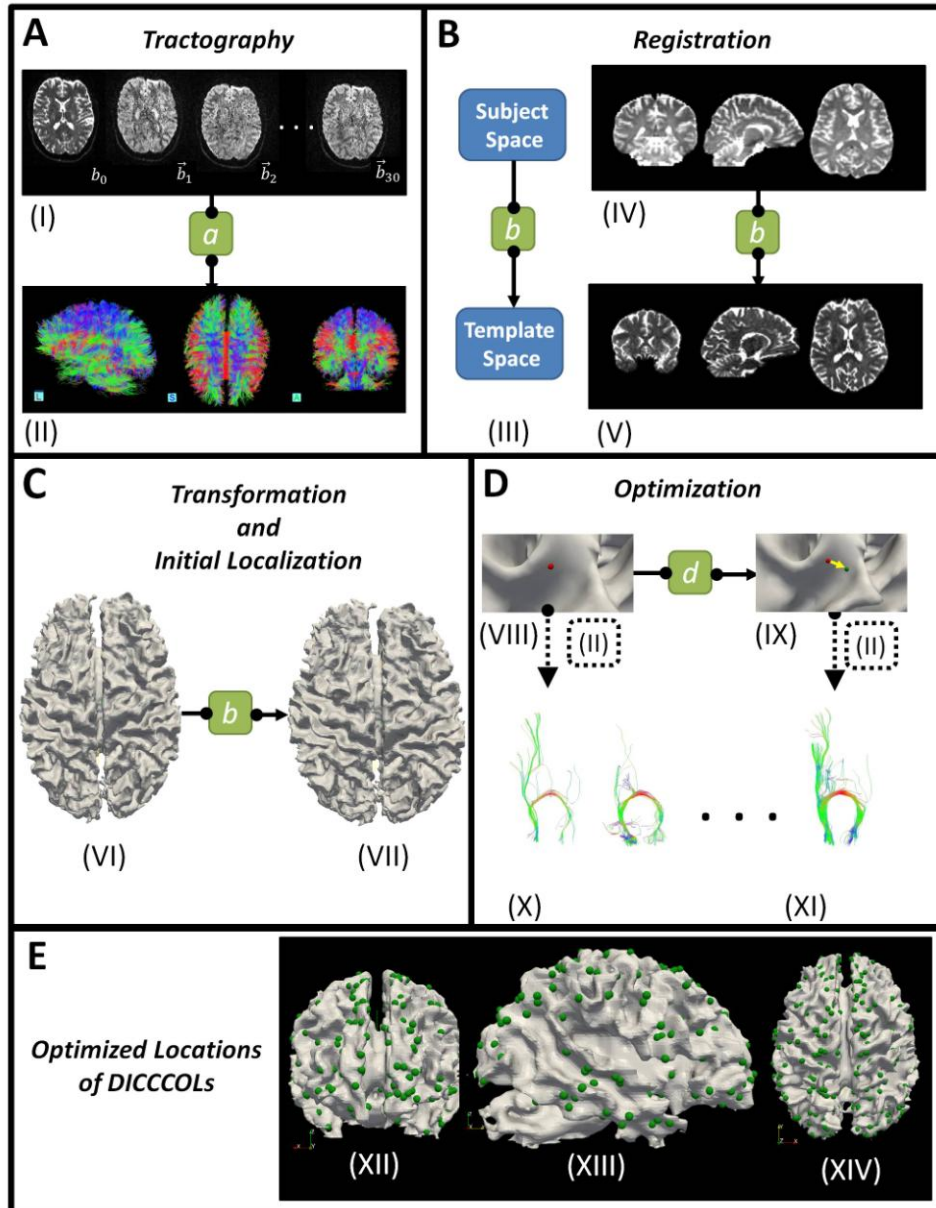


Figure 2. Pipeline for identifying the locations of DICCCOLs on the brain of an individual. Figure 2.A: Fiber tracking and tractography of the whole brain was performed via MedINRIA (<http://med.inria.fr/>). Box "a" presents the preprocessing steps (including brain extraction, motion correction, and eddy current correction) and deterministic tractography. A(I) shows diffusion data of an individual brain at b_0 and some different gradient directions, and A(II) shows the result of tractography in 3D space in the sagittal, axial, and coronal views. Figure 2.B: The transformation matrix to transfer coordinates from the subject space to the template space was obtained by registering the brain of an individual subject to the brain template. B(III) shows the schematic of this procedure in which box *b* represents the transformation matrix. B(IV) and B(V) show the coronal, axial, and sagittal views of individual and template's brains, respectively. Figure 2.C: Transformation and identification of the initial location of DICCCOLs. The transformation matrix (*b*) is applied to transfer the individual surface and fiber bundles to the template space for prediction. As a result, the initial location of DICCCOLs on the individual's brain is obtained. C(VI) is the surface of an individual in the subject space, and C(VII) is the surface of the same individual, which is transferred to the template space. The initial location of DICCCOLs on an individual's brain was obtained by overlaying the location of DICCCOLs of the template on the transformed surface of the individual. Figure 2.D: The schematic procedure of optimization in which the local neighborhood (6 mm radius) was searched in order to identify the location where the profile of connected fiber has the most similarity with the WM fiber connection profile of the DICCCOL on the template. D(VIII) shows the initial location of a DICCCOL, obtained from the previous step. Using the information of deterministic tractography (A(II)), the connected fibers at this initial location was extracted (D(X)). Next, the similarity between the connected fibers at this location and the connected WM fiber on the template was measured. The same procedure took place for all local neighborhoods, and the location with maximum similarity of the connected WM fibers was identified as the optimized location of the DICCCOL. Box *d* represents the optimization procedure. D(IX) shows the initial and optimized locations of a DICCCOL in red

and green, respectively. $D(X)$ and $D(XI)$ show the connected fibers at the initial and optimized locations of the DICCCOL, respectively. Figure 2.E represents the optimized locations of all DICCCOLs on an individual's brain. $E(XII)$, $E(XIII)$, and $E(XIV)$ show the coronal, sagittal, and axial views in 3D space, respectively.

In order to perform the optimization step (Figure 2.D), the connection profile of fiber bundling should be quantified. This has been done by measuring a fiber bundle shape descriptor index called a trace-map (Zhu et al., 2012). Briefly, the fiber bundle originating from an ROI is extracted by using the deterministic tractography algorithm (Figure 3.a). Next, the connection orientation profile for each fiber streamline is calculated (Figure 3b), and projected onto a unit sphere (Figure 3c). The result is the distribution of orientation vectors on the sphere (Figure 3d).

Next, the unit sphere is divided to 144 regions, and the number of projected points was counted for each region. The result is a vector with 144 values represented the direction profile of fiber bundle connected to the ROI. The advantage of the trace-map algorithm is that it can be used to compare overall shapes of different fiber bundles with tolerance of small variations among individuals.

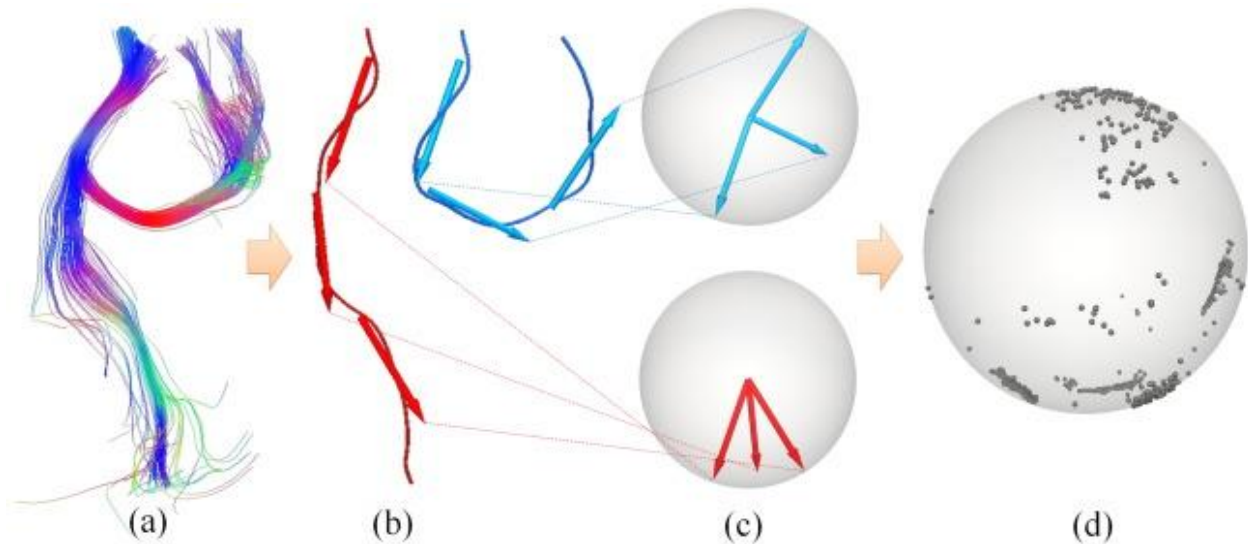


Figure 3. Illustration of trace-map calculation and DICCCOL prediction. (a)-(d): trace-map calculation. (a) The fiber bundle emanating from a selected ROI; (b) visualization of two single streamlines of the fiber bundle and calculation of the connection orientation profiles; (c) projection of directions onto unit spheres; and (d) visualization of distribution of orientation vectors on the sphere (trace-map).

3.4. Data Analysis

3.4.1. Connectome-scale Assessment of Structural and Functional Connectivity in Mild Traumatic Brain Injury at the Acute Stage - Structural Connectivity Part

Authors: Armin Iraj, Hanbo Chen, Natalie Wiseman, Tuo Zhang, Robert Welch, Brian O'Neil, Andrew Kulek, Syed Imran Ayaz, Xiao Wang, Conor Zuk, E Mark Haacke, Tianming Liu, Zhifeng Kou

Context of the Paper

This study was designed to determine the connectome-scale brain connectivity changes in mTBI at both structural and functional levels. 40 mTBI patients at the acute stage and 50 healthy controls were recruited. The DICCCOLs was applied for connectome-scale analysis of both dMRI and rsfMRI data. The DICCCOL system was designed to identify those regions with consistent structural connectivity patterns. However, since white matter structural properties can be changed due to various pathophysiological mechanisms of brain injury, the deterministic tractography step of the DICCCOL analysis could fail to correctly extract the connected fiber bundles. This failure in finding the corresponding fiber bundle, which occurs due to brain injury, is identified as a structural abnormality, and the related DICCCOLs are called discrepant DICCCOLs. Thus, by identifying those discrepant DICCCOLs whose connected fiber bundles show different patterns between healthy subjects and patients with mTBI, we can identify physically vulnerable white matter tracts. In our SC analysis, 41 out of 358 DICCCOLs were identified as structurally discrepant between patient and control groups. The major white matter tracts with the most disruptions included the corpus callosum, and superior and inferior longitudinal fasciculi.

Image Processing

Preprocessing for this study was performed using the FSL software (Jenkinson et al., 2012) (<http://www.fmrib.ox.ac.uk/fsl/>). Diffusion data preprocessing included brain extraction, motion correction, and eddy current correction. Diffusion parameters has been calculated using the FDT Toolbox, part of the FSL software. Deterministic fiber tracking was performed via MedINRIA (<http://med.inria.fr/>). The gray matter cortical surface was reconstructed based on the segmented white matter FA image (Liu et al.,

2007; Liu et al., 2008). Each DICCCOL optimized location for each subject was identified using the process explained in the previous section.

The trace-map, which represents the shape of fiber bundles connected to a DICCCOL, can be used to find the DICCCOLs that have alterations in connected fibers in the patient group. The trace-map distance parameter measured by Euclidean distance can be used to measure the similarity of SC patterns between two trace-maps (Equation 1). A lower value for the trace-map distance parameter represents greater similarity between two trace-maps.

$$D(T^1, T^2) = \frac{\sum_{i=1}^{144} (T_i^1 - T_i^2)}{144} \quad (1)$$

Where T^1 and T^2 are two trace map vectors, i is the index of a 144 dimension feature vector which describe the trace-map.

For each DICCCOL, the trace-map distance parameter was measured compared to the average trace-map vector of the healthy subject group. A two-sample t-test (p -value = 0.01) was applied to the trace-map distance parameters to compare structural connectivity characteristics between healthy subject and patient groups. The DICCCOLs that show significant differences between the two groups are considered discrepant DICCCOLs, i.e. structurally discrepant between patient and healthy control groups.

Findings

An example of dMRI-derived axonal fiber bundles connected to a randomly selected common DICCCOL for 20 patients' brains and 20 healthy subjects' brains are shown in Figure 4.A and Figure 4.B. The corresponding trace-map distances are shown in Figure 4.C and Figure 4.D, accordingly. By visual inspection, the shape patterns of fiber bundles are relatively consistent across individuals for both patients and healthy subjects. The trace-map distance similarity between patients and healthy subjects can also be observed in the trace-map distance obtained for the same common DICCCOL (Figure 4.C and Figure 4.D). On the other hand, Figure 4.E and Figure 4.F demonstrate the connected fibers to a randomly selected discrepant DICCCOL. By visual inspection, the connection pattern of this DICCCOL is still consistent in healthy subjects; however, as highlighted by the red boxes, it is obvious that the SC

profile of the selected discrepant DICCCOL varies across patients' brains. This could be caused by any source of structural abnormality in white matter connectivity which disrupted the tractography step of the DICCCOL analysis and causes it to fail to identify the proper location for this DICCCOL. Moreover, the trace-map distance for this discrepant DICCCOL has been demonstrated for the same 20 patients and 20 healthy subjects in the Figure 4.G and Figure 4.H. Results show that patients have higher trace-map distances than controls.

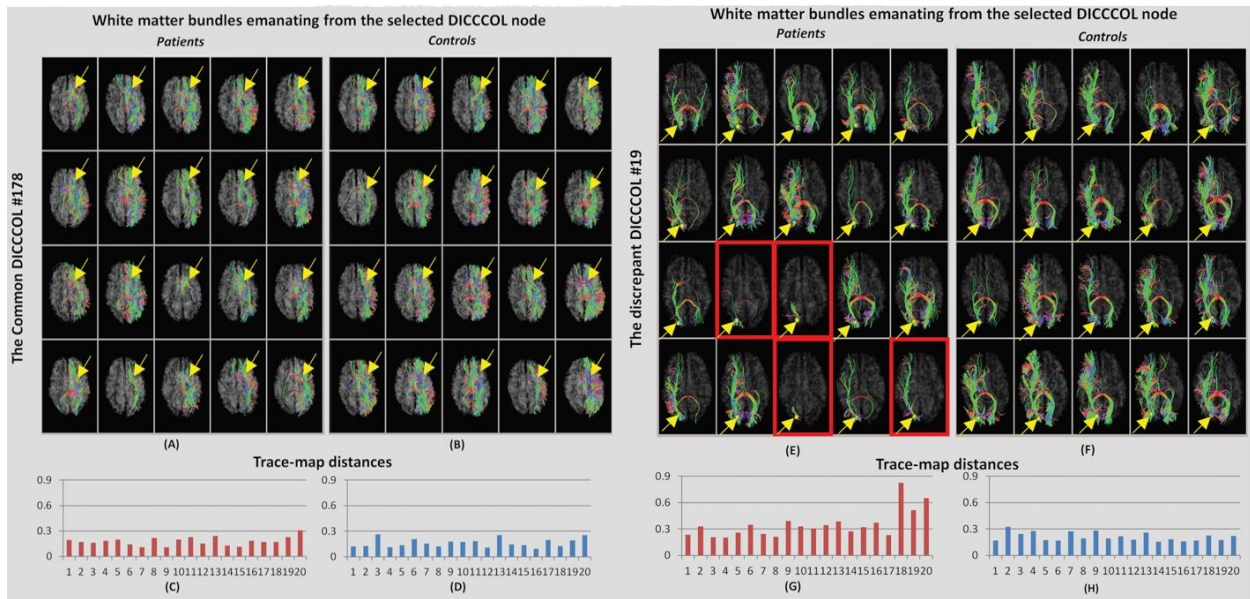


Figure 4. Joint visualization of a common DICCCOL (#178, yellow arrows) and the discrepant DICCCOL # 19 (indicated by yellow arrows). (A) and (B) show the connected DTI-derived axonal fibers (colorful lines) connected to the common DICCCOL on the cortical surface for 20 patients and 20 control subjects, respectively. Visual inspection reveals the patterns of fiber bundles are consistent across individuals for both patients and healthy subjects. Figure (C) and (D) respectively show the trace-map distance for 20 patients and 20 healthy controls selected in (A) and (B). As we can see, healthy subjects and patients have similar trace-map distance values for the common DICCCOL # 178. (E) and (F) show the connected DTI-derived axonal fibers (colorful lines) connected to the discrepant DICCCOL # 19 on the cortical surface for the same 20 patients and 20 control subjects as figures (A) and (B), respectively. Several patients have different fiber shapes (red outlines) in these randomly chosen 20 samples, which drive the group difference between patients and controls. At the same time, measuring the trace-map distances for DICCCOL #19 for same subjects shows that patients in general have a higher trace-map distance. Same scale has been used to make it visually easy to compare with the trace-map distance of discrepant DICCCOL.

In total, 41 discrepant DICCCOLs were identified among 358 DICCCOLs using statistical analysis on the trace-map distance. The distribution of the discrepant DICCCOLs in the brain is shown in Figure 5.

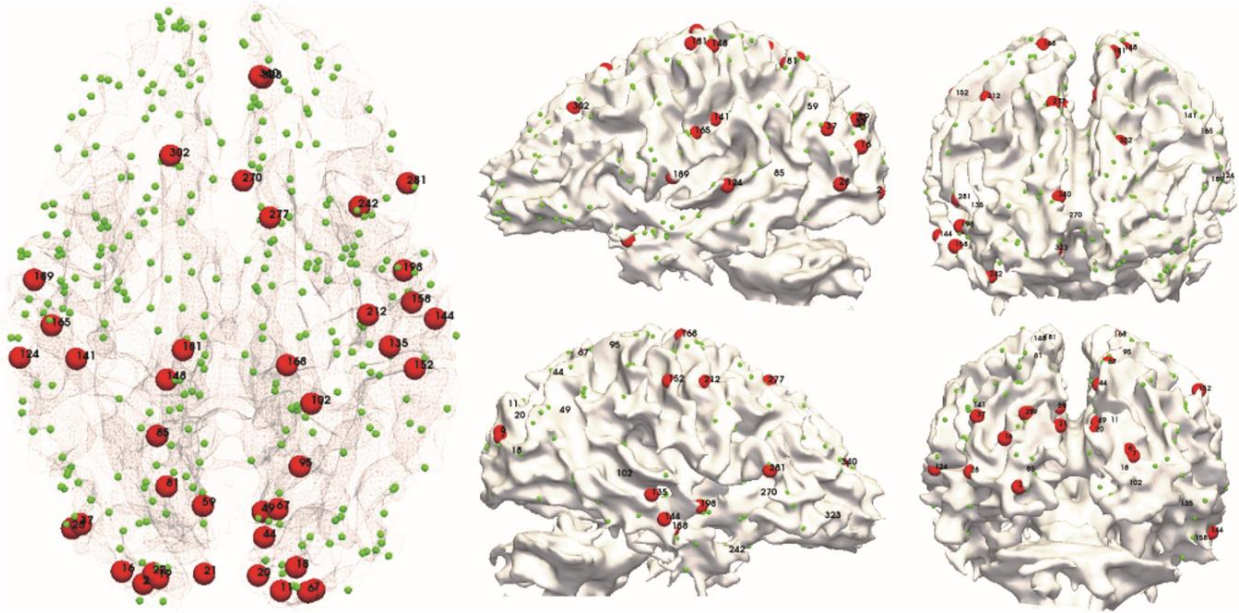


Figure 5. Visualization of location of discrepant DICCCOLs (red sphere) and the rest DICCCOLs (green sphere) on cortical surface. ID numbers are shown for discrepant DICCCOLs.

Furthermore, by using these discrepant DICCCOLs as ROIs, fiber tractography can be used to visualize the difference between a randomly chosen control and randomly chosen mTBI patient (see Figure 6). In Figure 6, the yellow spheres are the discrepant DICCCOL landmarks. Despite the negative findings on the mTBI patient's structural MRI, the patient's white matter structure shows significant differences in the white matter bundles emanating from these 41 discrepant DICCCOL landmarks.

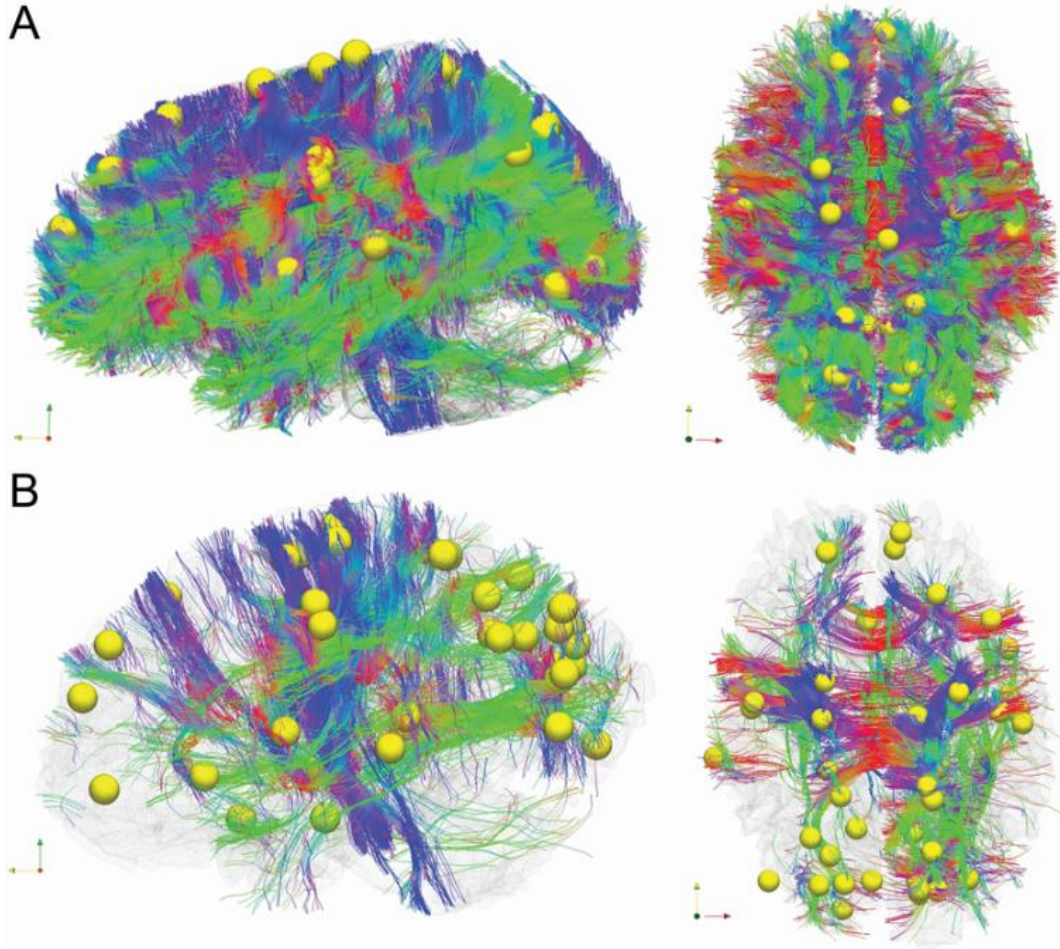


Figure 6. White matter fiber tractography of a randomly chosen control subject (A) and a randomly chosen mTBI patient (B) by using the 41 discrepant DICCCOLs (yellow spheres) as seed points. Despite the negative findings on the mTBI patient's structural MRI, the patient's white matter structure shows significant differences in the 41 discrepant networks in comparison with controls. Of particular note, the difference in the major white matter tracts between controls and patients is not because of the loss of white matter tracts in the patient; instead, it is the injury at these discrepant networks fail the fiber tractography algorithm when using the selected DICCCOL landmark as seed regions.

Our visual inspection of the connected white matter tracts of each discrepant DICCCOL also found white matter pathways that are structurally different from healthy subjects after injury, which is confirmed in a group comparison using the trace-map algorithm. Table 1 demonstrates the locations of discrepant DICCCOLs in Brodmann areas (BAs) and their connected major fibers. The superior and inferior longitudinal fasciculi, the corpus callosum, the arcuate fibers, and the cingulate bundle are the most commonly affected white matter tracts. This finding is consistent with the summary of published literature regarding the mostly easily damaged fibers (Kou and VandeVord, 2014). Importantly, the DICCCOL-based analysis offers fine-granularity dissection and measurement of such coarse-granularity fiber pathways.

Table 1. Locations of discrepant DICCCOLs and their Brodmann areas and connected major fiber tracts

DICCCOL ID	BA	CC	ILF	IFOF	SFOF	SLF	PF	AF	Cing	UF
2	18		✓	✓						
6	18	✓	✓	✓						
7	17	✓	✓	✓						
11	18	✓	✓							
16	19	✓	✓	✓						
18	17	✓	✓							
19	18	✓	✓	✓						
20	18	✓	✓							
21	18	✓	✓							
22	18	✓	✓	✓						
28	19		✓	✓						
37	39		✓	✓						
44	7	✓								
49	7	✓	✓	✓						
59	7	✓							✓	
67	7	✓	✓		✓					
81	7	✓				✓	✓			
85		✓				✓				
95	5	✓				✓	✓			
102		✓						✓		
124	42		✓							
135	22							✓		
141	3					✓				
144	36							✓		
148	3	✓					✓			
152	2				✓					
158	38		✓					✓		
165	40				✓					
168	3	✓			✓		✓			
181	4	✓			✓		✓			
189	43					✓				
198	41		✓							
212	6				✓					
242	38		✓							✓
270		✓								
277	8	✓		✓						
281	44							✓		
302	9	✓				✓	✓			
323	10	✓								
340	10	✓							✓	
Area total:		25	18	10	6	6	6	5	3	1

BA: Brodmann Area; CC: corpus callosum; ILF: inferior longitudinal fasciculus; IFOF: inferior fronto-occipital fasciculus; SFOF: superior fronto-occipital fasciculus; SLF: superior longitudinal fasciculus; PF: projection fibers; AF: arcuate fasciculus; Cing: cingulum; UF: uncinat fasciculus.

3.4.2. Validation of Results of DICCCOL Framework Analyzed Using Probabilistic Tractography

Context

In this step, we are going to compare and validate the DICCCOL prediction of structural disrupted fibers by evaluating overall FA along affected white matter bundles. Using DICCCOLs analysis we have identified the corpus callosum and inferior longitudinal fasciculus (ILF) as the most structurally disrupted white matter tracts, respectively. Since the corpus callosum is a heterogeneous structure, which connects

two hemispheres, an overall FA value for the corpus callosum is not a justifiable value to assess differences between two groups. Therefore, we performed statistical analysis on the overall FA value for ILF.

Image Processing

Preprocessing includes brain extraction, motion correction, and eddy current correction. The FDT Toolbox, part of FSL software, has been used for probabilistic tractography (Smith et al., 2004). Diffusion parameters were estimated using BEDPOSTX and tractography was performed using PROBTRACKX2 (probabilistic tracking with crossing fibers) (Behrens et al., 2007). The transformation matrix was obtained by nonlinear registration of the FA map of each subject to the default FA atlas image (FMRIB58_FA) available in FSL. The “seed,” “target,” “termination,” and “exclusion” masks were transformed to subject native space using transformation matrix information. This transformation matrix will also be used later to transform the tractography results from native subject space to the 1x1x1 MNI standard space. In tractography, a streamline (tract) starts from a voxel in the seed mask, and the fiber direction is identified at each voxel using diffusion probability density (Behrens et al., 2007). Tractography was carried out in subject native space and the white matter pathways were identified. The obtained tract density was then transferred to 1x1x1 standard space using the nonlinear transformation matrix. The registered tract density maps in the standard MNI space were then normalized by dividing by the total number of particles (de Groot et al., 2013; Diedrichsen et al., 2009). The normalized tract density was used as a weight to measure weighted averaging of FA values along pathways (Besseling et al., 2013).

Findings

Performing statistical analysis on the overall FA shows decreases in FA in the right ILF in mTBI patients (P-value = 0.036). Figure 7 shows an example of tractography in five healthy controls and five patients in the right ILF. By visual inspection, the consistency of the white matter structure seems to be disrupted among patients.

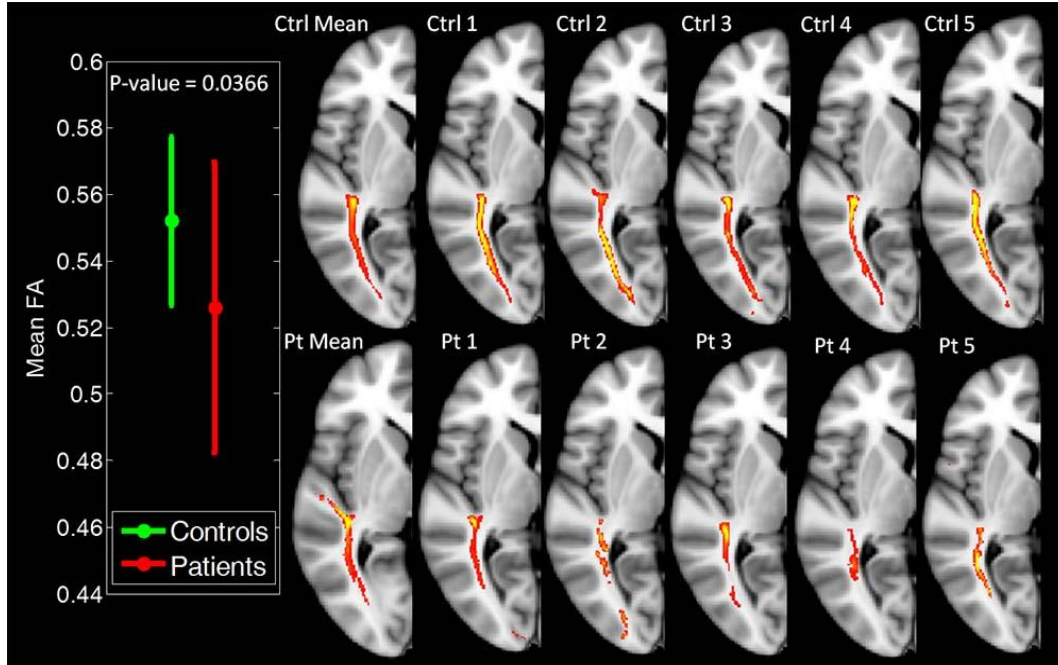


Figure 7. Validation of the DICCCOL prediction of structurally disrupted fibers by evaluating overall FA along affected white matter bundles. The right ILF shows decreased FA values in mTBI patients.

3.5. Discussion

Brain structure is very complex with considerable morphological variations across subjects. Due to the high level of complexity of cytoarchitecture and notable disagreement of the boundaries of cytoarchitectonic areas across subjects, it is difficult to identify regions with similar structural and functional connectivity across individuals (Brett et al., 2002; Zhu et al., 2011). The complex shape of the cortex makes it hard to find corresponding regions among individuals (Zhu et al., 2011). Considering the fact that a slight change in a connectivity node location can have a significant effects on results, the importance of identifying connectivity nodes as precisely as possible is clear (Zhu et al., 2011). The DICCCOL frameworks allow us to select connectivity nodes that are specific to individual brains but also are consistent and robust across the population for large-scale comparisons (Zhu et al., 2013). The DICCCOL system aims to identify the common cortical landmarks with similar structural and functional profiles across individuals using the shape of fiber tracts which emanate from cortex. While the DICCCOL frame work can potentially improve structural and functional comparisons across subjects and prevent errors caused by image registration, it still needs improvement to become a first choice approach to replace commonly-used registration approaches. For example, one limitation is that the current

framework uses diffusion tensor for tractography and extraction of fiber tracts. We can further improve the resolution of DICCCOLs via high-angular resolution diffusion imaging data. Moreover, there is a need to improve the cortical surface reconstruction. Currently, the cortical surface is reconstructed based on the segmented fractional anisotropy (FA) image of white matter (Liu et al., 2007; Liu et al., 2008). While using the FA map has some advantages, it also carries some limitations, the most of which is that cortex reconstructed from the FA map is not optimized and disregards some of the cortical characteristics such as thickness or shape. Therefore, development of a superior way to identify and obtain the cortical surface would have a substantial impact on this method. The other area that requires improvement is the optimization process. Currently, the DICCCOL framework uses the trace-map, which is obtained by dividing the space into 144 sections. However, this procedure is suboptimal, and there is an essential need to improve it.

CHAPTER 4. FUNCTIONAL CONNECTIVITY (FC)

4.1. Background

For several years, scientists assessed the function of human and animal brains using any possible opportunity, such as investigating the brain after injury, creating deliberate brain injury, and measuring various features that are associated with brain function using methods including electroencephalography (EEG) and magnetoencephalography (MEG), positron emission tomography (PET), and fMRI.

In fMRI, the BOLD signal is used as a feature to evaluate brain function. Since neurons do not have any internal energy supply, their activities require a quick restoration of energy supplies, including oxygen. In response to increased activity in neurons, local blood flow increases in order to provide more oxygen. The process of changes in blood flow and oxygenation in response to neural activity is called the hemodynamic response (Figure 8). However, there is a short delay of around two seconds during which oxygenated blood displaces deoxygenated blood. Thus, there is an initial small decrease in the ratio of oxyhaemoglobin (oHB) to deoxyhemoglobin (dHB), and shortly after there is an increase in the ratio of oHb to dHb due to the increase in blood flow (Kornak et al., 2011; Logothetis and Wandell, 2004). dHB is paramagnetic and oHB is diamagnetic; therefore, they have different properties (magnetic susceptibility) in a magnetic field. The contrast of the BOLD signal is created by this difference in susceptibility between oHB and dHB.

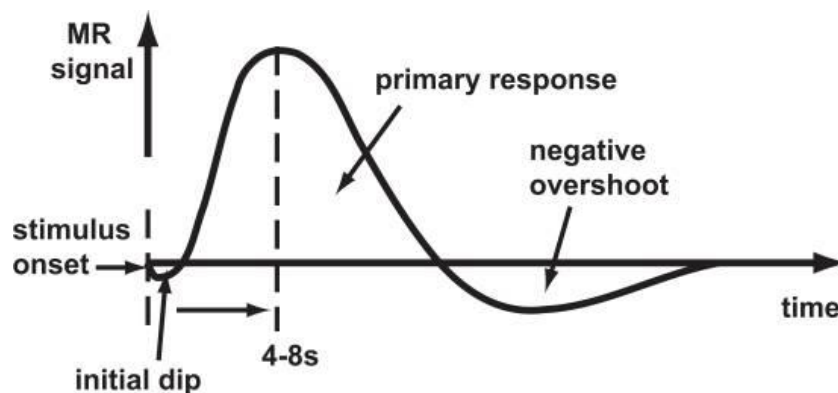


Figure 8. Schematic of the BOLD hemodynamic response morphology (Kornak et al., 2011).

While a brain region can be responsible for specific functional activities, it constantly interacts with other brain regions. The functional interaction among brain regions is defined as functional connectivity. Functional connectivity is measured by calculating the temporal dependency of neural activity (Friston et al., 1994; van den Heuvel and Hulshoff Pol, 2010; Wang et al., 2015). In fMRI, the functional connectivity can be identified by measuring temporal correlation, i.e. statistical relationships, between the BOLD signals of brain regions, thought to reflect the prior history of co-activation between brain regions (Buckner and Vincent, 2007). fMRI has provided great insights into the neural substrates that serve cognitive, emotion, sensory, and motor brain functions. Numerous studies have shown the ability of fMRI to identify the role of brain regions in different mental and physical activities of the brain and to diagnose many disorders (Chen et al., 2012; Irajy et al., 2015; Jafri et al., 2008; Johnson et al., 2012; Kou and Irajy, 2014; Mayer et al., 2011; McAllister et al., 1999; Morgan et al., 2013; Sorg et al., 2007; Tian et al., 2006; Tivarus et al., 2012; Wang et al., 2006; Zhou et al., 2007).

Task-based fMRI has been used to identify functions of specific brain regions for several years (Ogawa et al., 1992); however, brain functions are more complicated than to be understood by only investigating the brain during tasks. The brain is a highly connected system including many subunits that simultaneously work together. These subunits are sometimes defined as functional networks (Allen et al., 2011; Barbey et al., 2015; Beckmann et al., 2005; Biswal et al., 1995; Bonnelle et al., 2012; Bonnelle et al., 2011; Damoiseaux et al., 2008; Damoiseaux et al., 2006; De Luca et al., 2006; Mason et al., 2007; Seeley et al., 2007; Smith et al., 2009; Sporns, 2014; Uddin et al., 2011; van den Heuvel and Hulshoff Pol, 2010; Zuo et al., 2010). Some important functional networks include the DMN, salience network (SN), frontoparietal networks (FPNs), auditory network, motor network, primary visual network, secondary visual network, and attention network (Allen et al., 2011; Damoiseaux et al., 2006; Irajy et al., 2016a; Smith et al., 2009; van den Heuvel and Hulshoff Pol, 2010). It is impractical to investigate all of these functional networks by employing various tasks. Moreover, in many scenarios, it is not possible to perform task-based fMRI, due to subjects' health conditions, age or limited time in a medical setting to perform these tasks. Furthermore, the output of task-based fMRI is vulnerable to subjects' willingness or ability to cooperate in many cases. rsfMRI is a fMRI modality that has the ability to simultaneously investigate the functional connections between several brain regions while at rest (while not performing any specific task)

(Biswal et al., 1995; Bressler and Menon, 2010; Buckner et al., 2008; Damoiseaux et al., 2006; Greicius et al., 2003; Honey et al., 2009; Johnson et al., 2012; Lee et al., 2013; Mayer et al., 2011; Nakamura et al., 2009; van den Heuvel and Hulshoff Pol, 2010). rsfMRI provides unique insights into brain function at the macro level, which can contribute to a better understanding of the underlying pathophysiological changes in brain disorders such as Alzheimer's disease (AD), schizophrenia, attention deficit hyperactivity disorder (ADHD), and TBI (Iraji et al., 2015; Jafri et al., 2008; Johnson et al., 2012; Kou and Iraji, 2014; Mayer et al., 2011; Sorg et al., 2007; Tian et al., 2006; Wang et al., 2006; Zhou et al., 2007).

4.2. Previous Findings on TBI

Given the fact that most mTBI patients show no obvious damage using structural MRI, fMRI modalities may be a viable complementary approach for detecting injury-related abnormalities. Task-based and task-free fMRI studies have the advantage of detecting abnormalities in brain functions even in the absence of remarkable structural imaging results. Several fMRI studies have been performed on mTBI patients, and their results are promising. In task-based fMRI, mTBI patients demonstrate functional alterations in regions involved in memory (Chen et al., 2012; McAllister et al., 1999) and language (Morgan et al., 2013; Tivarus et al., 2012). rsfMRI studies have also reported several network alterations in mTBI, including in the DMN (Iraji et al., 2015; Johnson et al., 2012; Mayer et al., 2011; Zhou et al., 2012), thalamus network (Tang et al., 2011), and others (Messe et al., 2013; Sharp et al., 2014; Stevens et al., 2012). Messe et al. have done a longitudinal study (Messe et al., 2013), which showed that functional connectivity in temporal and thalamic regions was increased at the sub-acute stage in patients with post-concussion syndrome; however, it was decreased in the frontal areas at the late-stage (Messe et al., 2013). Mayer et al. have investigated dynamic functional connectivity along with static functional connectivity in mTBI patients. Although their analysis did not show group differences after multiple comparison corrections, the static and dynamic functional connectivity shows reduction trends in the DMN that align with previous studies on static functional connectivity (Mayer et al., 2015b). To date, the way that mTBI changes brain functional networks on a large-scale level, particularly at the connectome level, is still unknown; however, some unifying findings are emerging regarding brain network alteration after

brain injury (Sharp et al., 2014). The DMN and SN are two examples of these networks (Sharp et al., 2014).

4.3. Analytical Approach

As mentioned earlier, brain regions constantly communicate with each other, and the functional interactions among brain regions can be measured using the temporal dependency of neural activities (Friston et al., 1994; van den Heuvel and Hulshoff Pol, 2010; Wang et al., 2015). There are several approaches to evaluate functional connectivity. Two widely used approaches are seed-based (region-based) analysis (SBA) and independent component analysis (ICA).

4.3.1. Seed-based Analysis

SBA is categorized as a univariate analysis technique in which the temporal dependency of the time courses of the selected seed is measured against other brain regions. The temporal dependency is usually measured by calculating the temporal cross correlation; however, other mathematical indices, such as mutual information, coherence, and partial correlation have been used as well (Figure 9).

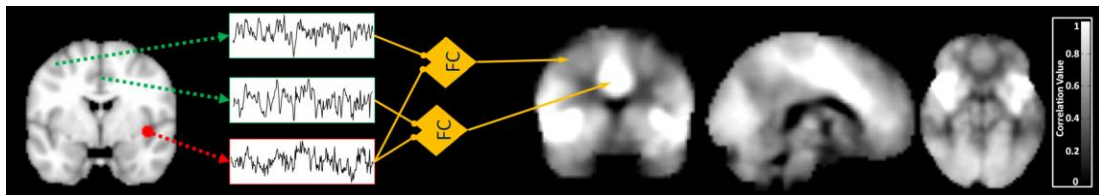


Figure 9. Functional connectivity analysis using a seed-based approach. The red circle shows an example of the desired region of interest (selected seed). The temporal dependency (for instance, the temporal correlation between the time course of the selected seed and other brain regions (two examples identifies in green) is measured. The output will be a spatial map of the brain in which a higher value represents stronger functional connectivity with the selected seed.

SBA, as implied by the name, requires a predefined seed or region of interest (ROI). A seed can be a voxel or a region obtained from an atlas. A seed can also be obtained based on previous literature or meta-analysis or extracted using a data-driven approach. This dependency and bias towards *a priori* knowledge in seed selection can be considered as a major weakness of SBA. However, because results of SBA are directly associated with the definition of functional connectivity and the result has straightforward interpretability, SBA becomes an attractive approach and probably the first choice for many users (Fox et al., 2005; Greicius et al., 2003; Margulies et al., 2007). Simply, areas with a higher

index value have stronger functional connectivity with the selected seed, so we can directly identify the functional connectivity properties of any seed region.

One major consideration of using SBA is its univariate nature which only considers the relationship between the timecourse of the seed and any other timecourse and does not consider the relationship between multiple time courses (in the ultimate case, all voxels) simultaneously. As a result, unlike multivariate analyses, SBA does not take into account information which exists across voxels. Therefore, multivariate analytical approaches such as ICA are commonly applied as a complementary approach (Iraji et al., 2015). ICA also has the benefit of removing the necessity of a priori seed selection. However, we should remember, we lose the direct interpretability with multivariate outcomes.

4.3.2. Independent Component Analysis

ICA is a multivariate data-driven approach which does not require *a priori* information to measure the sources of brain connectivity. In ICA, instead of calculating the relationship between a seed and other brain regions and identifying regions which are functionally connected to the specific seed, we assume the same type of relationship simultaneously exists between several brain regions and each brain region is involved in multiple relationships. In other words, we assume there are several sources (networks) that each have a specific temporal activity and contain several brain regions (Figure 10). To perform ICA, we apply a blind source separation (BSS) method to extract these sources and their temporal activities by assuming independency between sources and a linear mixture of their temporal activity. It should be mentioned that we are only discussing the spatial ICA which is commonly used in fMRI analysis and considering independency between spatial maps of brain networks. However, there are some fMRI studies that assume independency between temporal activities of brain networks, known as temporal ICA. Temporal ICA is more common in EEG studies. Although interpretation of ICA spatial maps is not straightforward, the spatial maps of ICA are close to known sensory, motor, behavioral, and neurocognitive systems and similar to spatial maps obtained from SBA when seeds are located in some of area of these networks. Moreover, using meta-analysis, Smith et al. obtained similar spatial maps (brain networks) from activation maps of thousands of task-based neuroimaging studies (Smith et al., 2009).

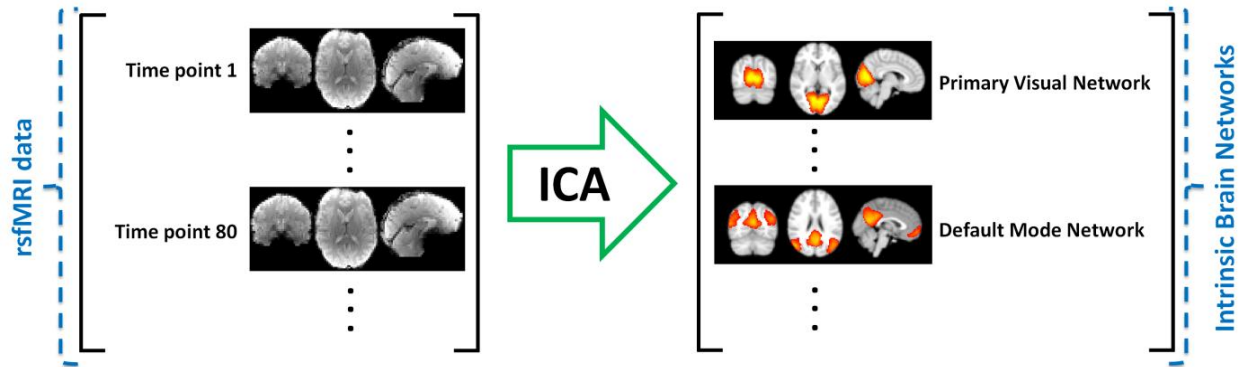


Figure 10. Functional connectivity analysis using independent component analysis (ICA). The whole collected fMRI data will be used as the input for ICA analysis, and the output will be a set of independent spatial maps including spatial maps of brain intrinsic connectivity networks (ICNs) and other spatial maps such as noises and artifacts.

4.4. Data Analysis

4.4.1. Image Preprocessing

Preprocessing for rsfMRI data was also performed using the FSL software (Jenkinson et al., 2012). For rsfMRI data, the first five volumes were excluded due to magnetization equilibrium. Brain extraction, motion correction, slice-time correction, spatial smoothing (FWHM = 6 mm), temporal prewhitening, grand mean scaling, and temporal high-pass filtering were then applied on rsfMRI data accordingly.

If an analysis needed the data of different subject to be transformed to the same space, brain registration was further performed. The rsfMRI data was registered to the Montreal Neurological Institute (MNI) standard space in following steps: 1) the rsfMRI data was registered to the structural T1 image of the same subject using linear registration using degree of freedom (DOF) = 6; 2) the result of the previous step was registered to the MNI standard space using the information of nonlinear registration of T1 image to MNI atlas with 10 mm warp. The registered data was resampled to 3 mm isotropic voxel size. Further preprocessing steps may have been done depending the applied analysis methods which will be mentioned below when we describe the analytic technique.

For the studies in which corresponding ROIs among subjects have been identified using the DICCCOL approach, rsfMRI data was directly registered to the b0 image of diffusion data using a 6 DOF affine transformation. The 6 DOF affine transformation is adequate for image registration of fMRI data of

an individual on the b0 image of the diffusion data of the same individual as reported in (Li et al., 2010b; Penny et al., 2011).

4.4.2. Resting State Functional Connectivity in Mild Traumatic Brain Injury at the Acute Stage: Independent Component and Seed Based Analyses

Authors: Armin Iraj, Randall R. Benson, Robert D. Welch, Brian J. O'Neil, John L. Woodard, Syed Imran Ayaz, Andrew Kulek, Valerie Mika, Patrick Medado, Hamid Soltanian-Zadeh, Tianming Liu, E Mark Haacke, Zhifeng Kou

Context of the Paper

In this preliminary study, a cohort of 12 mTBI patients were recruited at the acute stage. Sixteen age- and gender-matched healthy controls were also recruited for comparison. Both group-based and individual-based ICA of rsfMRI demonstrated reduced FC in both PCC and precuneus regions of the DMN in comparison with healthy controls. Further seed-based analysis (SBA) demonstrated increased FC between these regions and regions of the brain which do not belong to the DMN. SBA using the thalamus, hippocampus and amygdala regions further demonstrated increased FC between these regions and other regions of the brain, particularly in the frontal lobe, in mTBI. Our data demonstrates alterations of multiple brain networks at the resting state, particularly decreased within-DMN functional connectivity and increased FC in frontal lobe, in response to brain concussion at the acute stage.

Image Processing

In this study, which was the first study that we have done on rsfMRI data of mTBI, we performed the most commonly used methods on rsfMRI in order to evaluate the effect of mTBI on rsfMRI data and used their results to compare to and assess our findings from other analyses. We used both ICA and SBA to analyze the rsfMRI data.

Independent Component Analysis (ICA)

ICA was performed using the GIFT software package from MIALAB (<http://mialab.mrn.org/software/gift/>), and 52 components were chosen for analysis. ICA was performed at

both group and individual levels. Evaluation of the output of ICA analysis was mainly performed in the DMN and the basal ganglia network (BGN).

Group ICA: The group ICA (GICA) was performed in the healthy control and patient groups. The group difference was measured between patients and controls in major network regions of both the DMN and BGN. Furthermore, the reliability and reproducibility of the results were measured using a cross-validation method. Specifically, for each group (patient or healthy control), seven subgroups were randomly chosen with six subjects in each subgroup. GICA was performed for each subgroup, and the number of voxels in each network region associated with the related network and the voxel dependency were measured. Voxel dependency is a voxel's value in a network map (the result of ICA), indicating its likelihood of belonging to the network. In other words, it is the extent to which a voxel belongs to the network.

Individual ICA: Individual ICA was performed using two reported methods, dual regression (Beckmann et al., 2009; Calhoun et al., 2001) and back projection (Beckmann et al., 2009; Calhoun et al., 2001), as well as a new atlas-based ICA approach, proposed by us, to evaluate the alterations in mTBI patients. The new atlas-based ICA method solves some of the main confounding factors of these two common methods. The common space in the "dual regression" and "back projection" methods is created using the whole dataset of a particular study; therefore, the common spaces are different when the datasets of studies differ from each other. Consequently, intrinsic connectivity networks (ICNs) of an individual are affected by the group that the individual belongs to. On the other hand, in the temporal concatenation group ICA, we assume that there is a common space among all individuals; therefore, using the data of that study to find the common space is not ideal, especially when the number of samples is small, like in our study. Therefore, a template or atlas that indicates the common space of a big population is required. To overcome the abovementioned problem, we proposed an atlas-based ICA method.

Proposed atlas-based ICA: In the atlas-based ICA, independent components extracted from 602 subjects (Allen et al., 2011) were used as the common space and a spatially constrained ICA method (Lin

et al., 2010) was used to extract the individual components corresponding to the common space components.

In the atlas-based ICA, unlike the dual regression and back projection methods, instead of using the independent components of group ICA of our dataset as a common space for individual ICA, the independent components from a large group of healthy subjects is considered as a true common space. In this case, 1) The brain networks extracted from an individual's rsfMRI data are more reliable since independent components were extracted from an atlas which is based on a large population instead of a small group of subjects; 2) Independent components and subsequent analysis and results among various studies with different data sets only depend on individual differences rather than the whole data set in an study, because the common space is the same among all of this study. In other words, the difference between various subjects is only the result of the intrinsic variability between each pair of them. Note that, because this method uses atlas components to extract the individual components in individual subjects, it automatically solves the problem of finding corresponding ICNs across subjects. As previously explained, this method only requires the individual subject's data instead of a whole set of subjects' data.

Seed Based Analysis (SBA)

After ICA analysis, SBA was also performed by calculating the Pearson correlation value between major seed regions and the whole brain, and the correlation maps were used to compare healthy controls and patients. The seed regions were selected for the DMN, BGN, amygdala and hippocampus based on previous studies (Johnson et al., 2012; Mayer et al., 2011; Tang et al., 2011). Specifically, the PCC, precuneus, angular, anterior prefrontal cortex (BA 10), and orbitofrontal cortex (BA 11) were selected for the DMN; and the putamen, pallidum, thalamus, and caudate were selected for the BGN.

A Pearson correlation coefficient was calculated between the average of all voxels in a selected region and all brain voxels to create a correlation map for each region (Tang et al., 2011). The correlation maps were corrected using the Fisher z-transformation in order to perform FC comparisons. The FC mask was obtained by only selecting voxels that have correlation value more than 0.2 in at least one of the mean group correlation maps. For FC comparisons, a correlation mask was first applied to select voxels that are eligible for statistical analysis. Then, statistical analysis was performed using two-sample

t-tests on corrected correlation maps and were further corrected by spatial thresholding to reduce the false positives and increase reliability.

Findings

Group ICA (GICA)

Figure 11 shows a significant decrease in the number of associated voxels in the PCC and precuneus regions of the DMN in mTBI patients as compared with controls. Figure 12 further shows significantly decreased dependency of associated voxels in the same regions in mTBI patients as compared with controls. The voxel-wise two-sample t-test on cross validation group ICA identifies a cluster of 50 voxels in the PCC and a cluster of 442 voxels in the precuneus which have significantly lower voxel dependency to the DMN in patients as compared to healthy control subjects (Figure 13). To sum up, our comprehensive GICA analysis demonstrates a consistent difference in PCC and precuneus between groups, suggesting that connectivity in these regions could discriminate between patients and healthy controls. For the BGN, the cross-validation GICA did not reveal any changes in either voxel dependency or the number of voxels in the BGN.

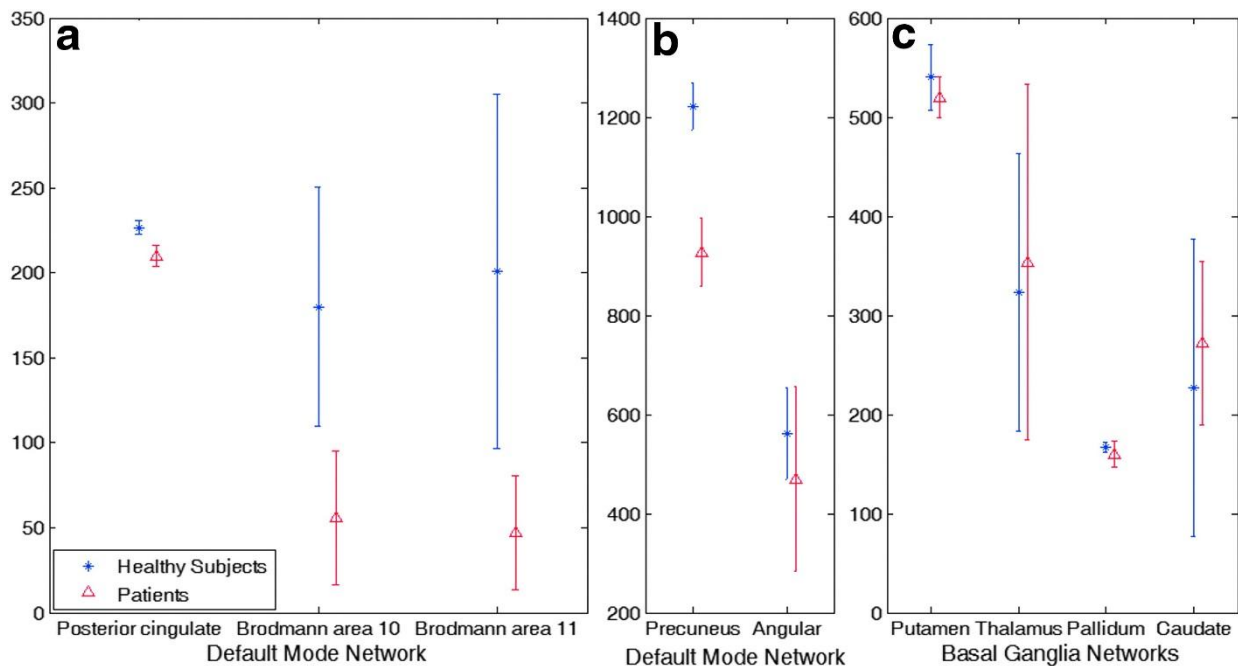


Figure 11 Cross-validation results of the group independent component analysis on number of associated voxels to the ICNs. The DMN shows a difference between the two groups in (a) the PCC, Brodmann area (BA) 10, BA 11 and (b) precuneus. (c) The basal ganglia network does not show any significant difference. Error bar is one standard deviation.

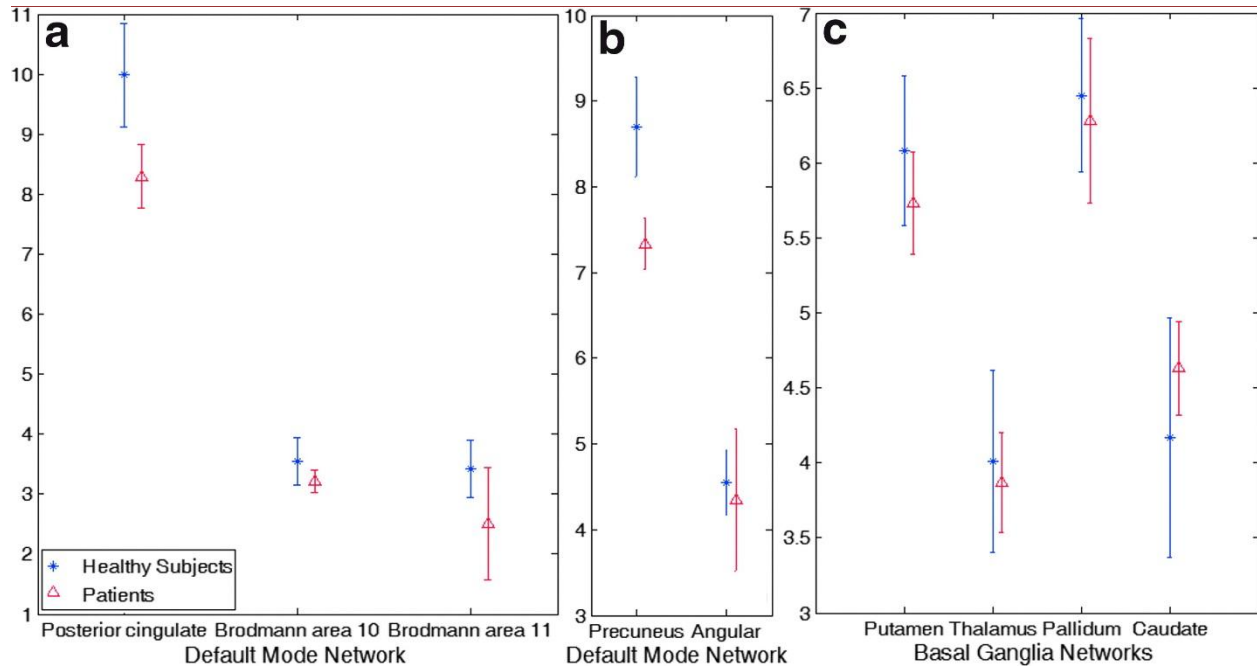


Figure 12. Cross-validation results of the group independent component analysis on voxel dependency to the ICNs. The DMN shows a difference between the two groups in the (a) PCC and (b) precuneus. (c) The basal ganglia network does not show any significant difference. Error bar is one standard deviation.

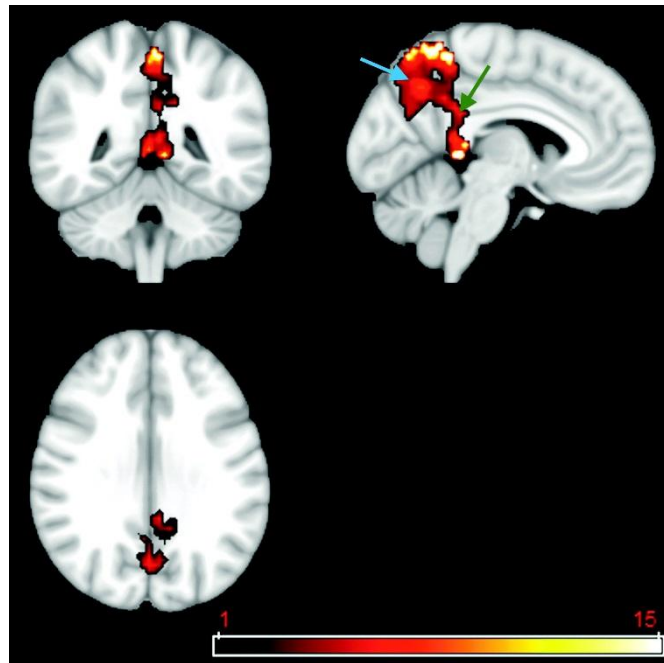


Figure 13. Two-sample t-test using a p-value of 0.001 on the DMN extracted from the cross-validation of group independent component analysis. Results identified a cluster of 50 voxels in the PCC (green arrow) and a cluster of 442 voxels in the precuneus (blue arrow) that have significantly lower voxel dependency to the DMN in patients as compared with healthy control subjects.

Individual ICA was performed to investigate alterations of the DMN and BGN in patients as compared with healthy controls. Dual regression, back projection, and the atlas-based spatially constrained ICA have all been applied. Neither dual regression nor back projection was able to

discriminate between the two groups in individual analysis. However, the atlas-based spatially constrained ICA method demonstrated an intriguing result. Consistent with GICA results, a two-sample t-test on the DMNs extracted from the atlas-based ICA method revealed a significant difference between the two groups in the PCC and surrounding areas including the precuneus. For a p-value = 0.05, the two-sample t-test map, which was corrected using the spatial thresholding, manifested a cluster of 137 voxels with reduced voxel dependency to the DMN in the patient group as compared to controls. This includes 55 voxels in the PCC (Figure 14). This suggests reduced connectivity within the DMN, which is consistent with our GICA results. The ICA results are also consistent with results of the previous ICA study (Stevens et al., 2012).



Figure 14. Two-sample t-test results demonstrate a difference in the DMN between the two groups in individual independent component analysis. Highlighted area shows the cluster is statistically significant ($p < 0.05$), which includes 55 voxel in the PCC. The warm color labels the voxels with reduced DMN dependency in patients compared with healthy controls.

Seed Based Analysis (SBA)

The within-group analysis on healthy controls did not reveal any significant difference; however, the between-group analysis using the same parameters as that of within-group analysis demonstrated several alterations in patients as compared to healthy controls, including in connectivity maps generated using the PCC, thalamus, amygdala, and hippocampus as seed regions.

PCC Connectivity Map: Figure 15 demonstrates the result of two-sample t-test comparisons of the PCC connectivity map (i.e. using the PCC as a seed region) between patients and controls. For p-value < 0.05 , it shows significantly higher FC between the PCC and several regions of the frontal lobe in patients compared to controls, including the dorsolateral prefrontal cortex (BA 9) and adjoining voxels in BA 8 and the anterior cingulate cortex (BA 32). For p-value < 0.01 , the two-sample t-test map showed two

clusters of 117 and 223 voxels, with higher FC in patients than in controls. These clusters include 77 and 87 voxels in the dorsolateral prefrontal cortex (BA 9), respectively. Along with a cluster containing 44 voxels in the dorsal anterior cingulate cortex (BA 32), these show the susceptibility of these regions' to alterations in mTBI patients. Of particular note, these regions do not belong to the DMN.

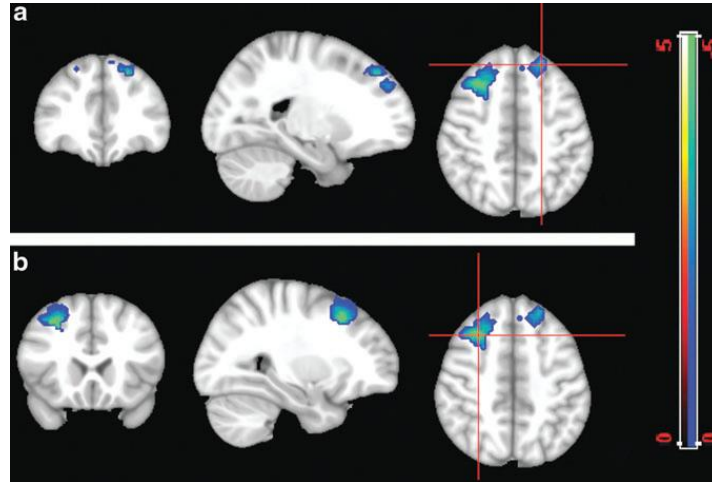


Figure 15. Two-sample t-test ($p = 0.01$) for the PCC connectivity map. The cold color labels the region that has more correlation with the posterior cingulate in the patient group than in the controls. The cross bar is located in different positions in the same FC map in images a and b. These regions do not belong to the DMN.

Precuneus Connectivity Map: Using the precuneus as a seed region, the between-group analysis (two-sample t-test) for p -value < 0.05 shows stronger FC between the precuneus and two clusters in patients as compared to healthy controls. The first cluster is in the supramarginal gyrus (BA 40) with 82 voxels; the other cluster has 85 voxels, which includes the BA 8 and the anterior cingulate cortex (BA 32) (Figure 16). Using a cut off of p -value < 0.01 did not reveal any significant difference.

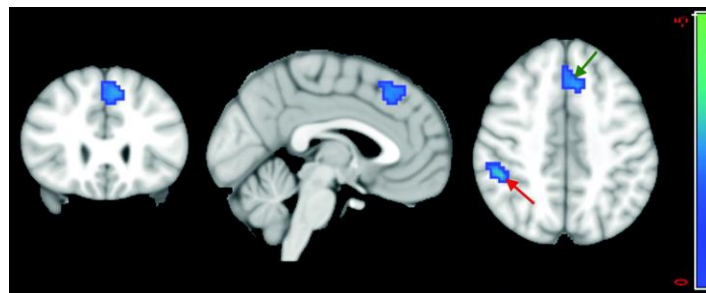


Figure 16. Two-sample t-test ($p < 0.05$) of the precuneus functional connectivity map. The between-group comparison using the precuneus as seed revealed differences in the supramarginal gyrus (red arrow) and the junction between BA 8 and the anterior cingulate cortex (BA 32) (green arrow).

Thalamus Connectivity Map: A between-group comparison (two-sample t-test) was performed using thalamus as a seed region. For p -value < 0.01 , the patient group showed significantly higher FC

with the thalamus than controls in several regions, including the anterior prefrontal cortex (BA 10) in two clusters of 83 and 123 voxels (Figure 17 (a)) and a cluster of 96 voxels in the supramarginal gyrus (BA 40) (Figure 17 (b)). This indicates an increased FC between the thalamus and other regions of the brain.

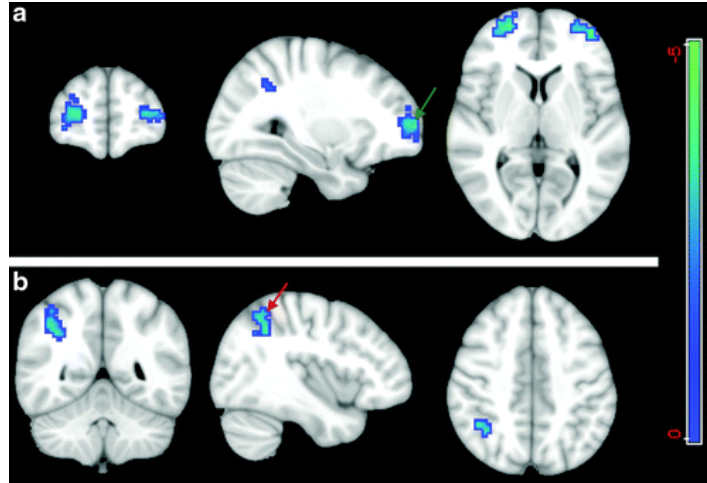


Figure 17. Two-sample t-test ($p < 0.01$) of thalamus functional connectivity map. The seed is located in the thalamus and the cold color shows the regions that have higher correlation with seed point in the patient group compared with the healthy control group. (a) Shows a statistical difference between two groups at the anterior prefrontal cortex (BA 10) (green arrow) and (b) shows the difference in the supramarginal gyrus (BA 40) (red arrow).

Amygdala Connectivity Map: By using the amygdala as a seed region, a between-group comparison (p -value < 0.01) demonstrates significantly increased FC with the left parietal superior cortex in the patient group (cluster size = 104) than control group (Figure 18). On the other hand, a one-sample t-test shows that the healthy controls have higher connectivity within the amygdala. For p -value < 0.01 , FC map of healthy controls group includes 73 and 67 voxels, while for the patient group these numbers decrease to 39 and 22 (Figure 19).

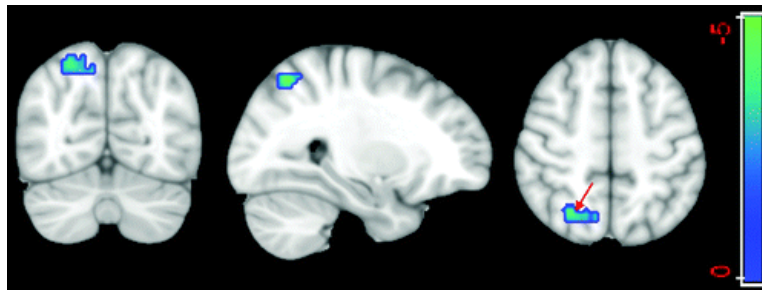


Figure 18 Two-sample t-test ($p < 0.01$) for the amygdala correlation map. The cold color labels the region (the left parietal superior cortex) that has stronger correlation with the amygdala (red arrow) in the patient group than in controls.

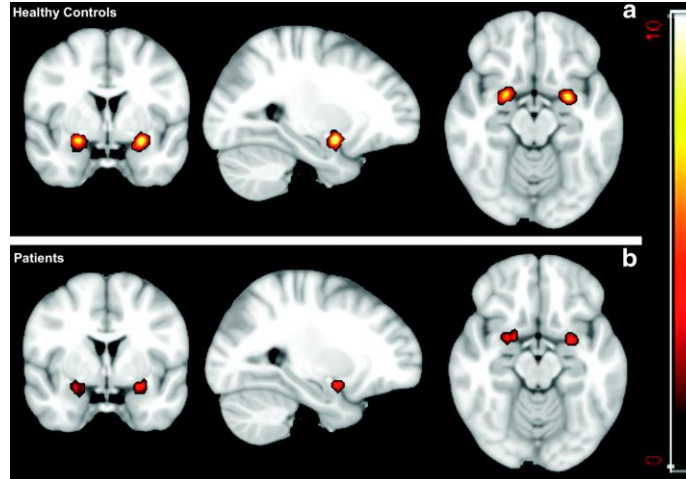


Figure 19. One-sample t-test of the amygdala map ($p < 0.01$). (a) the FC map for the healthy control group and (b) the FC map of the patient group. The higher signal intensity on (a) shows higher intrinsic FC in the amygdala in the healthy group than in patients.

Hippocampal Connectivity Map: A between-group analysis for the FC map with the hippocampus as the seed region demonstrates significant alterations in the FC of mTBI patients. For p -value < 0.01 , three clusters (cluster sizes of 135, 61, and 52 voxels) are significantly different between two groups. Figure 20 demonstrates increased FC in the fusiform gyrus and the precuneus (BA 7) and decreased FC in the inferior frontal gyrus in the patient group as compared with controls.

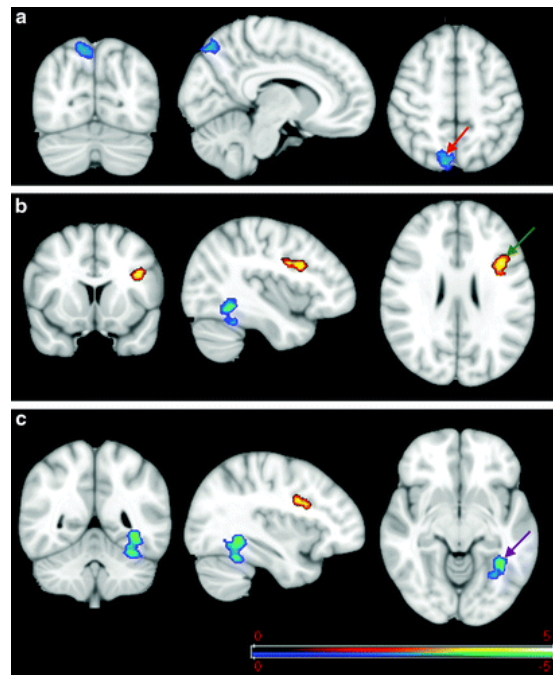


Figure 20. Two-sample t-test ($p < 0.01$) for the hippocampus FC map. The cold color labels the regions with more correlation with the hippocampus in the patient group compared with controls while the warm color labels the region with more correlation in the controls than in the patient group. The FC map was sectioned through (a) the precuneus association cortex (BA 7), red arrow; (b) the inferior frontal gyrus, green arrow; and (c) the fusiform gyrus, purple arrow.

4.4.3. Connectome-scale Assessment of Structural and Functional Connectivity in Mild Traumatic Brain Injury at the Acute Stage - Functional Connectivity Part

Authors: Armin Iraj, Hanbo Chen, Natalie Wiseman, Tuo Zhang, Robert Welch, Brian O'Neil, Andrew Kulek, Syed Imran Ayaz, Xiao Wang, Conor Zuk, E Mark Haacke, Tianming Liu, Zhifeng Kou

Context of the Paper

As mentioned before, this study was designed to determine the connectome-scale brain connectivity changes in mTBI at both structural and functional levels, and the DICCCOL approach was applied to identify the corresponding connectivity nodes among subjects. FC analysis identified 60 connectomic signatures that differentiate patients from controls with 93.75% sensitivity and 100% specificity. Analysis of functional domains showed decreased intra-network connectivity within the emotion network and among emotion-cognition interactions, and increased interactions among action-emotion and action-cognition as well as within perception networks.

Image Processing

To analyze functional connectivity using the DICCCOL framework, the time series allocated to each DICCCOL is derived from the average of the rsfMRI time courses of the gray matter area in the neighborhood of that DICCCOL. FC between each pair of DICCCOLs is obtained by measuring temporal Pearson correlation between the time series allocated to each DICCCOL. The output is a symmetric affinity matrix that represents functional connectivity of the brain at a connectomic level (Figure 21).

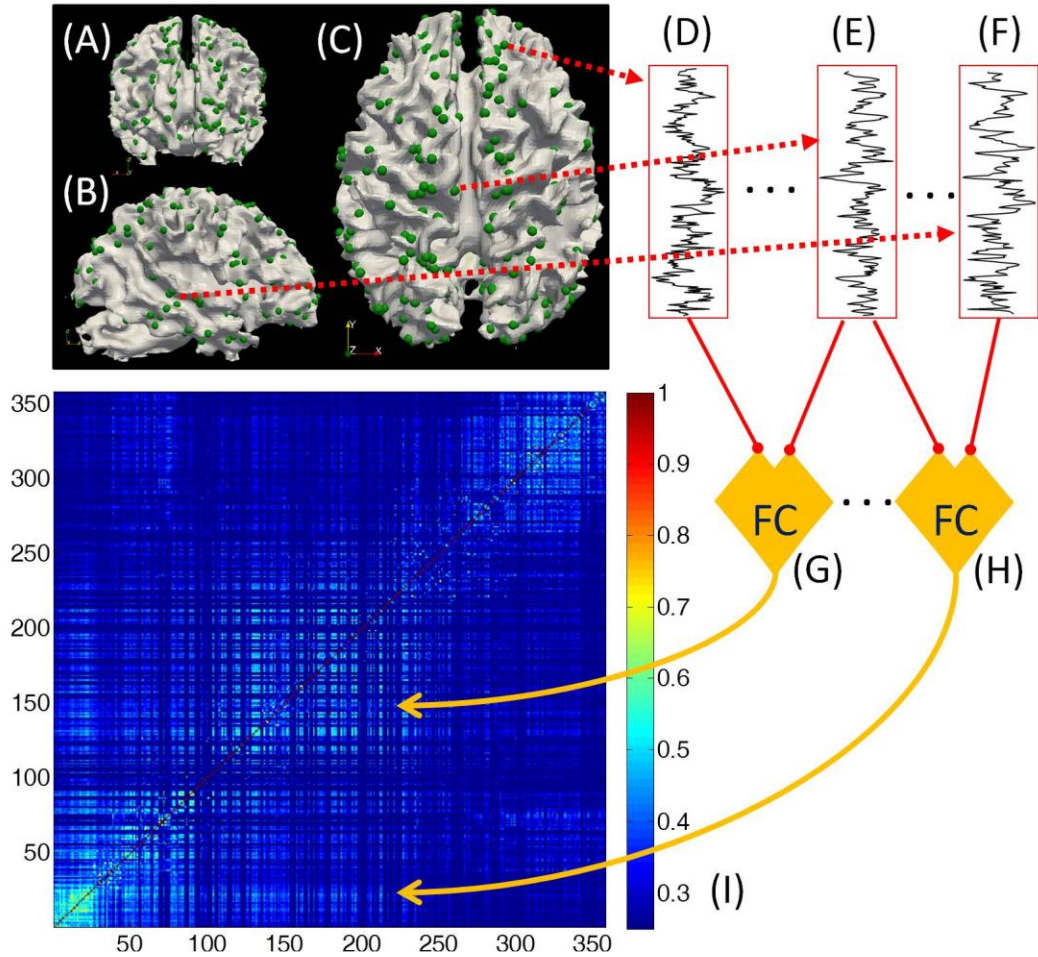


Figure 21. FC was measured across the brain using the DICCCOL framework. Figure 21.A, B, and C show the optimized locations of DICCCOLs across the brain in the coronal, sagittal and axial views, respectively. Figure 21.D, E, and F represent the time series allocated to three DICCCOLs obtained from the rsfMRI data of the gray matter of the neighborhood of each DICCCOL. The Pearson correlation was calculated between time series of each DICCCOL pairs in order to obtain the FC of the brain at large scale. Figure 21.G and H show two examples of FC measurement, and Figure 21.I is a symmetric affinity matrix, which represents FC at a connectomic level.

In this study, the time series of the closest gray matter voxel has been assigned to the DICCCOL for functional analysis. Preliminary studies have demonstrated that this is an effective method for prediction of functional nodes (Zhang et al., 2012; Zhu et al., 2014a). In order to find the most discriminate FC pairs, which will be referred to as features, we have applied a two-step feature selection procedure. First, a two sample t-test (p -value = 0.01) was performed to exclude those features that could not reveal a statistically significant difference between the mTBI patient group and the healthy subject group (remove the true negative). In the second step, the correlation-based feature selection (CFS) was used to find the most distinctive features by minimizing the degree of redundancy among features (Zhu et

al., 2011). The selected FC pairs are the most distinctive and discriminative characteristic features to distinguish between healthy subjects and patients in our dataset.

In order to assess the ability of these FC pairs to differentiate between two groups, supervised and unsupervised learning procedures were used. Specifically, a supervised learning procedure was performed using a support vector machine (SVM) classifier with 10-fold cross-validation to measure the specificity and sensitivity of the selected functional connectivity pairs. At the same time, in order to measure the similarity within each group and dissimilarity between two groups, we used an unsupervised learning method. In other words, we are interested in seeing how well the data of each group belongs to the same category. XMeans clustering was used to evaluate this similarity (Pelleg and Moore, 2000).

Findings

For this analysis, FC between each pair of common DICCCOLs was calculated to evaluate common functional alterations among mTBI patients. A symmetric 317x317 matrix of FC pairs was created using the 317 common DICCCOLs for each individual. Feature reduction was performed using two-sample t-tests to exclude those features that could not reveal a statistically significant difference between two groups (p -value = 0.01). As a result, 385 out of the 50086 features survived. To further control the false positives in these 385 features, in the second step, the CFS was utilized to select features (i.e. connectomic signatures) while minimizing the degree of redundancy among FC pairs. CFS selected 60 out of 385 FC pairs as the most distinctive and discriminative features of our data to differentiate patients from healthy control subjects. After controlling for the effect of age with an analysis of covariance (ANCOVA), 58 out these 60 connections were still significantly different between the two groups (p -value < 0.05). These were labeled as connectomic signatures for further analysis. The sensitivity, the probability of classifying a real patient correctly (a true positive), and the specificity, the probability of classifying a healthy subject correctly (a true negative), were calculated using a SVM classifier with 10 fold cross-validation. Classification gives 97.56% classification accuracy with 100% specificity and 93.75% sensitivity.

XMeans clustering was used to evaluate the similarity between subjects in each group and the dissimilarity between subjects from different groups. Only one patient among 32 patients was incorrectly

clustered in the healthy control group; however, 5 healthy subjects among 50 healthy control subjects were incorrectly clustered in the patients' cluster (incorrectly clustered instances = 7.32%). The clustering result demonstrates that connectomic signatures identified are truly different between groups. Together, they are a decent discriminant marker to categorize mTBI patients for this dataset.

4.4.4. Compensation Through Functional Hyperconnectivity: A Longitudinal Connectome Assessment of Mild Traumatic Brain Injury

Authors: Armin Iraj, Hanbo Chen, Natalie Wiseman, E Mark Haacke, Tianming Liu, Zhifeng Kou

Context of the Paper

Longitudinal connectome-wide analysis was performed using the DICCCOL approach. We applied 2x2 design ANOVA analysis using the NBS method. No statistically significant difference was found in the interaction or time effects. However, we found that 258 pairs of DICCCOLs showed group differences in which mTBI patients have higher FC than healthy controls. Categorization of altered FC (connectomic signatures) using multi-view group-wise cluster analysis, a novel clustering algorithm, identified that the two general patterns of functional hyperconnectivity among mTBI patients are (I) between the PCC and the association areas of the brain and (II) between the occipital and the frontal lobes of the brain. Our results demonstrate that brain concussion renders connectome-scale brain network connectivity changes and the brain tends to hyper-activate to compensate the physiological disturbances.

Image Processing

The time series allocated to each DICCCOL was derived from the gray matter area in the 5 mm neighborhood of that DICCCOL, and a symmetric affinity matrix with 64261 unique features was obtained to represent FC of the brain at a connectomic level (Figure 21). Network-based statistical was applied to identify the affected functional connectivity pairs. Next, a multi-view group-wise clustering (Chen et al., 2013) approach was applied to extract the patterns of alterations.

Network-Based Statistical (NBS) Analysis

NBS is a validated method which was originally developed for connectomic studies to perform nonparametric statistical analysis on large-scale connectivity analyses (Zalesky et al., 2010). While the false discovery rate (FDR) is sensitive enough to detect an independent isolated connected pair regardless of its affiliation (or conjunction) with other connected pairs, NBS improves our power to detect a nexus that includes multiple affiliated connected pairs (Zalesky et al., 2010). In other words, NBS, while controlling the family-wise error rate (FWER), implements rejection of a null hypothesis at the network level. NBS, intuitively, includes the following steps:

- a. Performing a statistical test on each connected pair independently. NBS, like other common neuroimaging software packages, uses the GLM as the statistical test. The output of this step is a set of connected pairs that are the potential candidates to be connectomic signatures (connected pairs which are statistically different between two groups).
- b. Identifying any possible connectivity structure from connected pairs which were selected at the previous step.
- c. Calculating a FWER-corrected p-value for a connectivity structure with size of K using permutation testing. Specifically, for each permutation, connectivity structures were identified and the maximal component size was obtained. Then, the p-value for any observed connectivity structure with size of K can be calculated based on the possibility of having maximal connectivity structure size $> K$ in M permutation.

NBS parameters, including the uncorrected threshold value, were chosen as follows according to previous published literature (Finn et al., 2014; Harrington et al., 2015; Korgaonkar et al., 2014; Krienen et al., 2014). Threshold = 3.5, permutation = 5000, component size = extent, and p-value = 0.05.

For the statistical longitudinal analysis, a mixed 2x2 design ANOVA was used to identify connectomic signatures. Independent variables were group (controls vs. patients) and time (acute vs. follow-up). If the interaction effect was not significant, we investigated the group and time effects. Otherwise, we investigated each simple effect. In other words, if the interaction effect was significant, we used a two-sample unpaired t-test to compare two groups and a two-sample paired t-test to investigate each group over time.

Findings

No statistically significant difference was found in the interaction effect (p -value = 0.05). The time effect did not show any significant difference (p -value = 0.05), either. However, we identified a group effect on 258 FC pairs that were significantly affected in mTBI patients (Figure 22). All of these affected FC pairs (i.e. connectomic signatures) showed increased FC in the patient group.

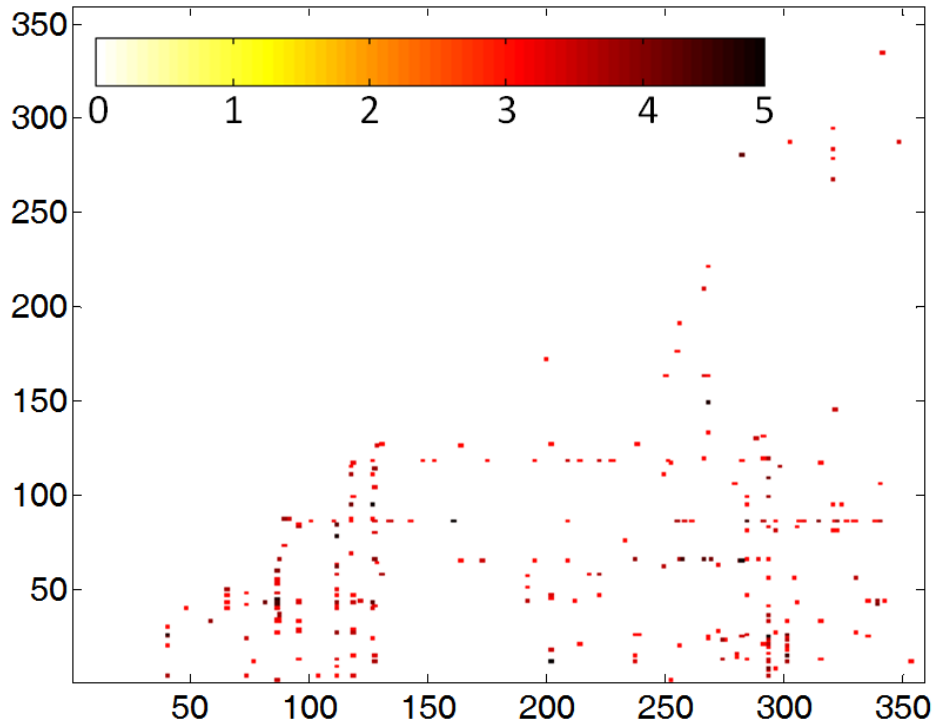


Figure 22. T-values from the longitudinal statistical analysis using a mixed design ANOVA and NBS on the 258 FC pairs which are significantly stronger in the patient group. Since the FC matrix is symmetric, only the lower half was used for the statistical analysis.

Multi-view Group-wise Clustering Approach

One aim of this study was to discover possible existing patterns among the connectomic signatures after mTBI. For this purpose, we first categorized DICCCOLs to similar clusters based on their rsfMRI time series similarity using a multi-view group-wise clustering approach. Using the multi-view group-wise clustering approach on all data (a combination of two time points and two groups), we have identified eight FC clusters (Figure 23). The estimated clusters are similar to the result of our previous work obtained in young healthy subjects (Chen et al., 2013). After identifying the corresponding cluster for each DICCCOL, the connectomic signatures were categorized based on the DICCCOLs' clustering

information. Results demonstrated that cluster #1, specifically the PCC portion of it, is the most involved cluster in FC alterations after mTBI (Figure 24). Interestingly, among all 258 connectomic signatures, 253 (98%) are involved in between-clusters interactions (Figure 24). Further investigation reveals two general patterns among the affected interactions: (I) an increase in FC between the PCC (from cluster #1) and the association areas of the brain such as the associative visual cortex, supplementary motor cortex, and the somatosensory association cortex (from clusters #4, 5, and 8), see Figure 25(a)-(c); and (II) functional hyperconnectivity between the occipital lobe of the brain from cluster #3 and the frontal lobe area from cluster #8 (Figure 25(d)).

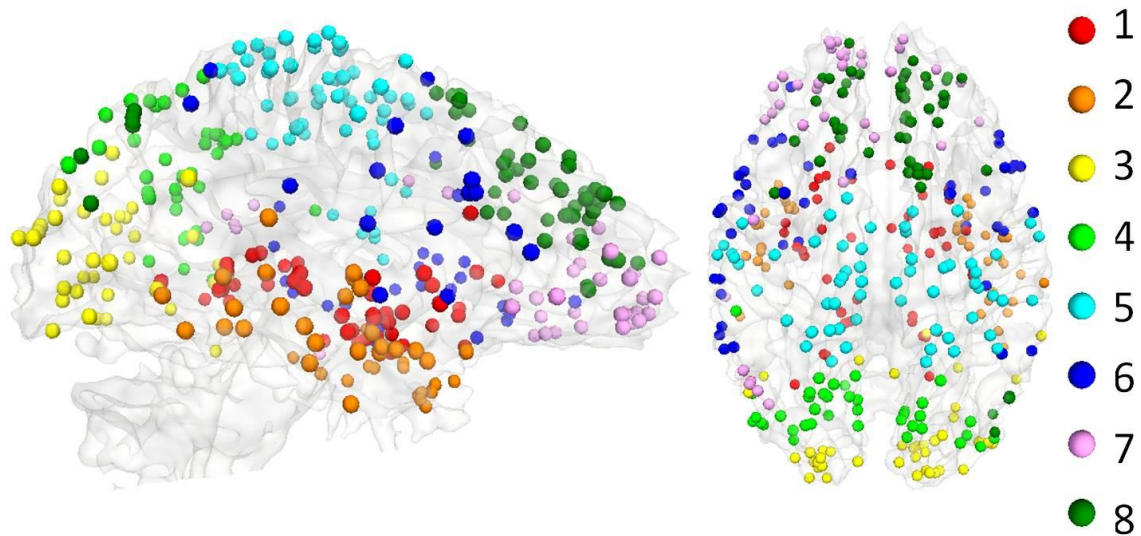


Figure 23. Eight FC clusters as results of using a multi-view group-wise clustering. Eight functional clusters were identified in different colored bubbles.

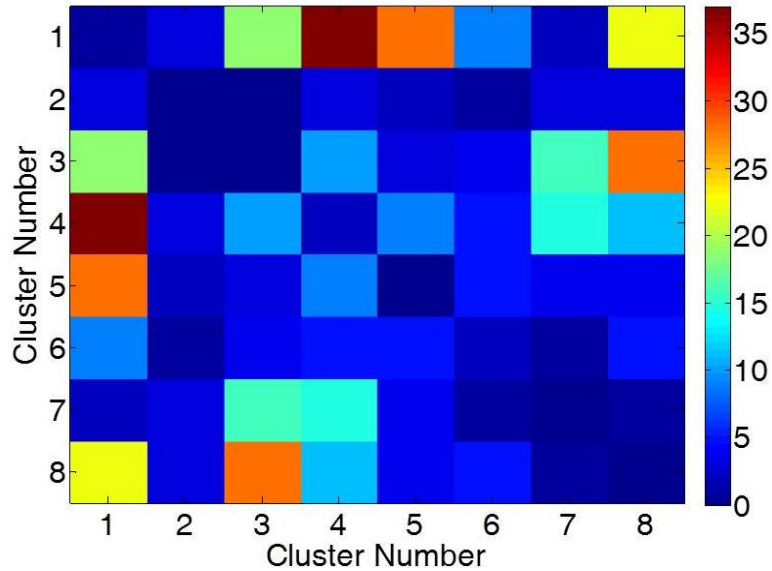


Figure 24. Categorizing the disturbed functional connectivity, which has been obtained using longitudinal statistical analysis by a mixed design ANOVA and NBS, into eight functional connectivity clusters that have been obtained using the multi-view group-wise clustering method. Results show that some clusters (especially cluster #1) are more involved in FC alteration after mTBI. The color-bar indicates number of involved connectomic signatures.

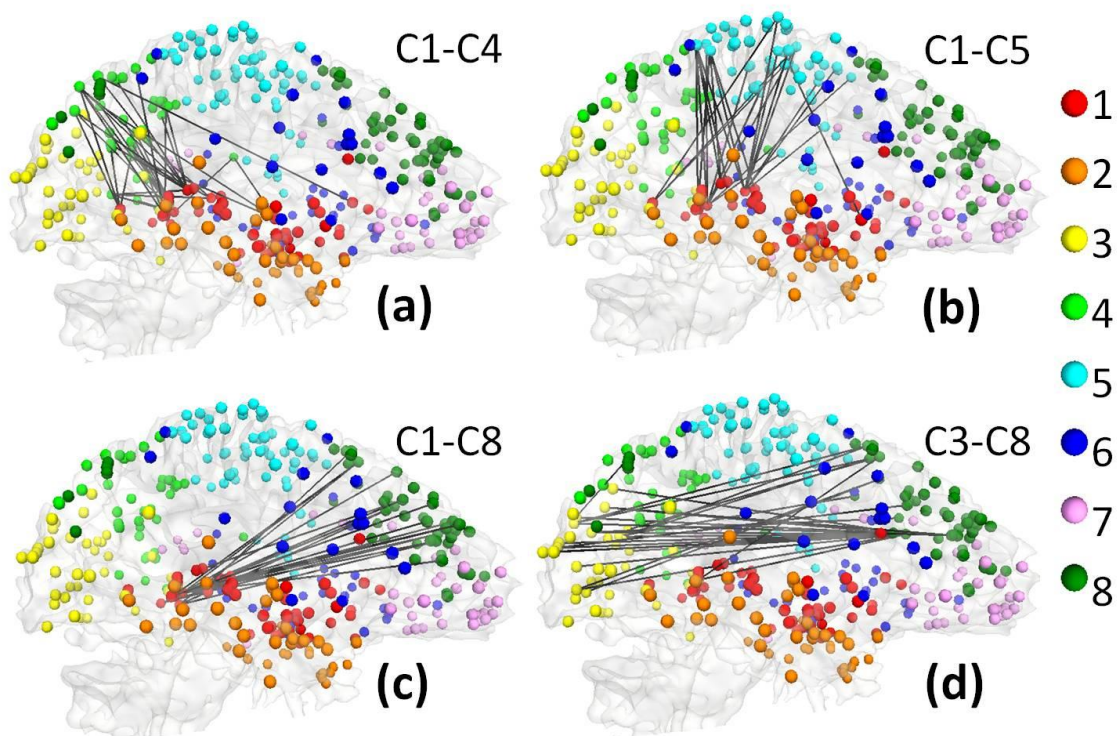


Figure 25. Categorization of affected functional connectivity using the multi-view cluster-wise cluster method. (a)-(c) shows the connectomic signatures involve in the interaction between cluster #1 (C1) and clusters #4 (C4), 5 (C5), and 8 (C8), respectively. These interactions represented in important role of the PCC as the central hub of the brain and its interactions with association brain areas as compensatory affect after brain injury. (d) reveals the interaction between the occipital lobe, cluster #3 (C3), and the frontal lobe, cluster #8 (C8).

4.5. Discussion

The summary of our extensive investigation suggests a general hyper-connectivity among brain regions, with the exception of reduced within-DMN connectivity. The DMN demonstrates rapid deactivation during attention-demanding tasks and shows an anti-correlation with brain mental activities (Bonnelle et al., 2012; Bonnelle et al., 2011; Seeley et al., 2007); in other words, the within-DMN connectivity decreases as brain activity increases. Thus, both findings suggest that the brain may be trying to recruit more sources to compensate for its functional impairments after injury. Moreover, using the DICCCOL method to finely identify connectivity nodes to investigate large-scale brain functional connectivity is one advantage of our FC analysis. Because of intrinsic relationship between gray matter and white matter, previous studies suggested that using the white matter profile can be a superior approach for identification of the connectivity nodes across individuals for functional connectivity analysis (Zhu et al., 2013; Zhu et al., 2014b). Despite our reliable findings, there are a lot of unknown facts that need to be discovered. One of the important aims of a functional connectivity study could be to investigate the interactions between regions involved in the DMN, salience network, and frontoparietal networks. These networks have been repeatedly reported to be disrupted after brain injury, so it is crucial to study their functional connectivity after mTBI. Furthermore, there is a wide range of large-scale approaches that need to be investigated to evaluate their sensitivity and accuracy in detecting robust findings. For instance, graph analysis is a commonly-used approach to study brain connectivity at large scale because it provides a wide range of ways to evaluate brain connections using different metrics (Fornito et al., 2013; Rubinov and Sporns, 2010; Wang et al., 2010). Moreover, while graph-based approaches allow us to investigate brain connectivity among different connectivity nodes, they can also provide rich, complete information about brain connections at a global level (Fornito et al., 2013; Wang et al., 2010) and to investigate the interaction between connectivity nodes in hierarchical structures (Wang et al., 2010). Another example is holistic atlases of functional networks and interactions (HAFNIs) (Lv et al., 2015a; Lv et al., 2015b). Lv et al. have used dictionary learning and sparse coding to identify a set of functional networks defined as HAFNIs (Lv et al., 2015a; Lv et al., 2015b), which can be reproduced across individuals and have highly spatially overlapping patterns (Lv et al., 2015a). One robust approach

that has been recently developed is the connectivity domain analysis method, which will be explained later in this dissertation.

CHAPTER 5. RELATIONSHIP BETWEEN NEUROPSYCHOLOGICAL DATA AND NEUROIMAGING DATA

5.1. Background

mTBI patients can experience a constellation of symptoms and impairment in neuropsychological functions after injury. The reported symptoms can occur either due to the direct effect of injury or for a number of other reasons, including a patient's emotional alterations such as pain, stress, anxiety or sadness. These symptoms are collectively known as post concussive syndrome (PCS). In some cases, these PCS symptoms develop into long-term complications, which can significantly impact a patient's quality of life. While neurocognitive testing offers us the opportunity to characterize problems with memory, attention, and other commonly affected domains, we still have difficulty in predicting the symptoms that patients may develop down the line.

5.2. Previous Findings

Following mTBI, the most affected neurocognitive domains have been found to be working memory (Barbey et al., 2015; Christodoulou et al., 2001; Hillary et al., 2011; Irajii et al., 2016b; Levine et al., 2002; McAllister et al., 2006; Nakamura et al., 2009; Newsome et al., 2007; Perlstein et al., 2004; Ricker et al., 2001; Sanchez-Carrion et al., 2008; Scheibel et al., 2007), attention (Hillary et al., 2011; Irajii et al., 2016b; Maruishi et al., 2007; Sharp et al., 2014), processing speed (Hillary et al., 2011; Losoi et al., 2015), executive function (Barbey et al., 2015; Irajii et al., 2016b; Turner and Levine, 2008), and awareness (Mayer et al., 2015a; Sharp and Jenkins, 2015; Sharp et al., 2014).

While deficits in neurocognitive domains have been frequently reported, studies have also shown the relation between disrupted structural connectivity and impairments in cognitive, emotion, and executive control in mTBI (Baek et al., 2013; Bazarian et al., 2007; Caeyenberghs et al., 2014; Grossman et al., 2013; Jorge et al., 2012; Niogi et al., 2008a; Treble et al., 2013; Wu et al., 2010). Lipton et al. suggest that executive function deficits can be predicted by dMRI data (Lipton et al., 2009). Yuh et al. shows that regions of reduced FA were statistically significant predictors of unfavorable three- and six-month GOS-E outcomes (Yuh et al., 2014). Grossman et al. show significant associations between MD and mean kurtosis (MK) of several regions, such as the thalamus, corpus callosum, and external capsule,

and various neuropsychological z score results including Digit Span Test, Symbol Digit Modality Test, and California Learning Verbal Test Total Recall (Grossman et al., 2013). Kou et al. found negative correlations between the total volume of regions with FA increases and patients' SAC scores (Kou et al., 2013).

5.3. Analytical Approach

In general, there are two different approaches to identify the impaired cognitive domains and their relationships with neuroimaging findings. In the first approach, we can use previous functional imaging studies and meta-analyses to identify the corresponding cognitive domains or functional roles of each region of the brain. As the result, we can indirectly conclude that the corresponding neurocognitive domains of those regions that are altered after injury are impaired. In the second approach, we perform neurocognitive tests and identify which cognitive domains are impaired based on neurocognitive assessments. Next, we can evaluate the relationship between neurocognitive and neuroimaging findings. This relationship can be useful especially if there is a significant relationship between neuroimaging results at the acute stage and neurocognitive findings at follow up because we can use neuroimaging data to predict patients' outcomes.

5.3.1. Meta-analysis to Predict Affected Neurocognitive Domain

In the last two decades, there has been a rapid growth of medical research and their findings. Therefore, we must combine these studies to integrate the common findings to make reliable and precise conclusions. This can save resources by preventing performing unnecessary studies and helping to design better studies. One common simple solution is review articles in which authors review several selected studies and make their interpretation of the findings of the selected articles. However, we can follow more systematic approaches and integrate a number of individual studies by performing analysis on the analyses of individual studies, which is defined as meta-analysis (Glass, 1976).

In meta-analysis, the processes of article selection, findings combination, and results interpretation follow certain statistical roles and analytic principles to make quantitative conclusions more trustworthy. In general, meta-analysis goals include, but are not limited to, increasing the statistical power and reliability of findings by summarizing and integrating results from a number of independently-

performed studies, overcoming the limitation of small sample sizes of individual studies to detect the statistical findings which require larger sample sizes, analyzing differences among the result of studies, and generating new hypotheses (Walker et al., 2008).

Although meta-analysis is a powerful tool, following the rules and conditions are critical and small violations of the principles can produce misleading results. For instance, the result of a meta-analysis depends on the selected studies; therefore, any bias in the process of finding and choosing the related studies can leads to incorrect conclusions.

In the neuroimaging field, BrainMap (<http://www.nitrc.org/projects/brainmap/>) (Laird et al., 2009) is a meta-analysis project with an accessible database of published neuroimaging literature that allows us to identify the function of a specific brain region and compare our study results with reported literature. Use of this database can significantly enhance the reliability of neuroimaging studies and identify affected neurocognitive function from neuroimaging findings. BrainMap includes the coordinate and the associated metadata of brain regions which are identified across a collection of studies (Laird et al., 2009). In a previous work, the possible functional roles for each DICCCOL were identified using meta-analysis (Yuan et al., 2013).

Briefly, the locations of DICCCOLs from the templates were registered to the MNI atlas, then a neighborhood with a radius of 3 mm around each DICCCOL was selected in order to assign a Brodmann area and determine a related functional role using the BrainMap software. 110 fMRI publications and their reported activation regions in the BrainMap database were examined to identify related functional roles for each DICCCOL (Yuan et al., 2013). Therefore, all selected DICCCOLs were categorized in five general classes (behavioral domains), based on the published fMRI data set in the Brain Map Database, and cognitive impairments were measured using these five categories: "action," "perception," "cognition," "interoception," and "emotion".

The strength of FC between two DICCCOLs can represent the strength of FC between their functional roles. For instance, if DICCCOL A was identified as cognition, and DICCCOL B was identified as action then we can interpret that the strength of FC between DICCCOLs A and B is related to the strength of FC between cognition and action. Therefore, if the FC between two categories of DICCCOLs

changes, we can conclude that the interaction between their functional roles (behavioral domains) has been affected. For example, if the majority of the strengths of FC between DICCCOLs belonging to cognition with DICCCOLs belong to action is changed due to a specific health condition, we can conclude that the interaction between cognition and action has been affected.

Two general conditions characterize the type of FC between each pair of DICCCOLs:

1. Each DICCCOL is assigned to only one behavioral domain. In this case, the correlation value between two DICCCOLs indicates the connectivity between two functional roles. For example, if DICCCOL A and DICCCOL B were respectively labeled as action and cognition functions, the correlation value between DICCCOL A and DICCCOL B associates to an action-cognition interaction.
2. One or both DICCCOLs are assigned to two or more behavioral domains. In this situation, the FC between the DICCCOL pair is associated to each pair of behavioral domains. For instance, if DICCCOL A was identified as action, and DICCCOL B was identified as action and cognition, the correlation value between DICCCOL A and DICCCOL B associates to both action-action and action-cognition interactions.

The interaction between DICCCOLs can also be divided in two categories:

1. Intra-domain interactions in which the same behavioral domain is assigned to interactive DICCCOLs, like a perception-perception interaction.
2. Inter-domain interactions in which two different behavioral domains interact with each other, like perception-action.

5.3.2. Statistical Inference between Neurocognitive and Neuroimaging Data (Prediction Analysis)

Using our acute stage neuroimaging data and one-month follow up neuropsychological assessments, we evaluated if the neuroimaging data gathered at the acute stage can predict neurocognitive complications at follow up using linear regression approach. However, this analysis is complicated in our data by two factors: 1) a small number of subjects for whom we have all of the

necessary data because human studies on mTBI are generally limited in recruitment and retention, and 2) a large number of comparisons to make because both the neuroimaging and neuropsychological data have a large number of variables.

Neuropsychological Variables

In common practice, several neuropsychology measures are collected to assess an individual's neurocognitive complications because people may do poorly on a single test for a variety of reasons unrelated to injury or do well on a test that may have low sensitivity to their particular underlying pathology. Thus, collecting various neuropsychological measures instead of one increases our chances of correctly identifying those participants with deficits and helps to make sure that we are not relying only on one piece of possible faulty data. The downside of using multiple measures is that it decreases the power of statistical analysis due to the increasing number of statistical inferences.

Calculating a composite score from collected measures is one solution to this limitation. Therefore, to overcome this barrier of a large number of neuropsychological assessments in our analysis, we calculated two composite neurocognitive scores for the most affected neurocognitive domains: a memory composite score and an attention/processing speed composite score. Briefly, they were calculated from standardized tests that include estimates of premorbid intellectual ability, verbal and visual attention, learning, memory, visuospatial functioning, and executive functioning. Composite scores were derived from individual tests by converting raw scores to z-scores and then calculating the mean z-score within each cognitive domain. The memory composite score was calculated as the mean of z-scores of four indices: Hopkins Verbal Learning Test Total Recall, Hopkins Verbal Learning Test Delayed Recall, Brief Visuospatial Memory Test Total Recall, and Brief Visuospatial Memory Test Delayed Recall. The attention/processing speed composite score was calculated as the mean of z-scores of three indices: Colored Trails Test Trial 1, Colored Trails Test Trial 2, and the Symbol Digit Modality Test. We also obtained the total neuropsychological composite calculated as the mean z-score across both domains and all seven neuropsychology indices.

Neuroimaging Variables

There are too many neuroimaging variables as a result of using a large-scale analytical approach and the DICCCOL method. Therefore, evaluating the statistical correlation between all of the neuroimaging variables and the neuropsychological composite scores and performing multiple comparison corrections would be incredibly strict and eliminate any possible true correlations. At the same time, excluding neuroimaging variables without any valid justification could potentially lead to losing possible meaningful correlations between neuropsychological outcomes and neuroimaging variables. As we will demonstrate later in this chapter, the number of mTBI subjects with both neuroimaging variables and neurocognitive variables is small and barely enough for evaluation of the correlation between neuroimaging variables and neurocognitive variables; therefore, we performed an exploratory analysis in which we defined rationales for selecting opportune neuroimaging variables and explored their correlation with neurocognitive composite scores. Based on the output of these analyses, we can potentially define a hypothesis for selecting proper neuroimaging variables. Since we are interested in predicting patient outcomes using the neuroimaging data acquired at the acute stage, we chose the sixty connectomic signatures which are the most distinctive and discriminative features at the acute stage. Next, to further cut down the number of selected neuroimaging features, we have used the knowledge of a clinical neuropsychologist and the BrainMap dataset to identify the connectomic signatures related to each neuropsychological composite score. First, the clinical neuropsychologist identified the behavioral domains of the BrainMap data which corresponded to each neuropsychological composite score. Next, we identified the connectomic signatures involved with the selected behavioral domains according to the BrainMap data. As the result, we were able to identify the connectomic signatures associated with each composite score. Among sixty connectomic signatures, 38, 18, and 41 signatures are associated with the attention/processing speed composite score, the memory composite, and the total neuropsychological composite, respectively.

Regression Analysis

Linear regression is a good way to measure the relationship between independent and dependent variables while also including potential confounders. Therefore, we used linear regression

analysis to measure the relationship between neuroimaging and neurocognitive variables. In regression analysis, the number of covariates we choose is important. Too few covariates would tend to produce biases towards incorrectly finding an association between dependent and independent variables when none exists, and too many covariates leads to overspecified models which are not generalizable to other datasets. On the one hand, we do not want to include too many covariates; however, on the other hand, we should include enough covariates to avoid misattributing results for the main parameters.

For the interpretation of neurocognitive tests and investigation of the ability of neuroimaging variables to predict neuropsychological outcome, we must carefully accommodate any covariates, which could otherwise lead to misattributing any correlations to the variables of interest (namely injury). Therefore, we need to select the covariates which should be included in the regression analysis to account for variables which are not associated with the injury outcome but contribute to the dependent variable. In general, there are two ways to select the covariates for a desired model. We can select the covariates objectively from a statistical point of view, or we can choose them subjectively based on previous findings and our understanding of the possible role of covariates in our variables of interest. In an objective approach, covariates will mainly be chosen based on the p-value associated with each covariate in the linear regression, and the number of covariates is limited by the sample size (which is small, in our case) before overfitting occurs. In general, we should have at least 10-15 observations per predictor variable in a linear regression (Babyak, 2004). Therefore, in objective analyses, we evaluate whether or not these potentially important covariates should be included in our analysis based on their p-values. In a subjective approach, according to previous studies, both neuroimaging and neurocognitive variables are affected by both gender and age, but compared to age, the gender effect is small (Allen et al., 2011). Moreover, race differences on neuropsychology tests are confounded by others factors that often come along with race, such as poor access to quality education, and/or unequal learning opportunities, or lower socioeconomic status (Silverberg et al., 2013). Therefore, neurocognitive tests, as well as brain development, is affected by these factors. To address this, the Reading (word recognition) subtest of the Wide Range Achievement Test-4 Wide Range Achievement Test 4 (WRAT4) was given to all participants (Wilkinson and Robertson, 2006). Word recognition performance tests such as the WRAT can be used as a test of premorbid functioning to adjust the model for the level of education and race of

among participants and are particularly insensitive to mTBI (Silverberg et al., 2013). So, this variable is also a good candidate to be assessed as another covariate in our regression analysis.

5.4. Data Analysis

5.4.1. Meta-analysis

Acute Stage Study

Results show that most of possible network interactions have been affected. Among them, the intra-emotion network interactions have been altered the most, with a significant decrease in the connectivity inside this network (by more than 27%). The emotion-cognition interaction also shows decreased connectivity (by 4.8%). On the other hand, intra-perception, action-perception, action-emotion, and action-cognition interactions reveal increased functional connectivity, by 22.97%, 18.62%, 14.02%, and 12.11%, respectively. These results can explain a strong disruption in emotion in patients during the acute stage (Figure 26).

For further functional analysis, the roles of individual DICCCOLs were evaluated more specifically. In this step, the functional roles of DICCCOLs have been categorized in 53 classes using Meta-analysis (Yuan et al., 2013). Among all functional roles emotion, action/execution, and cognition/attention are involved more in connectomic signatures than others, with 25, 23, and 23 DICCCOLs each, respectively (Figure 27).

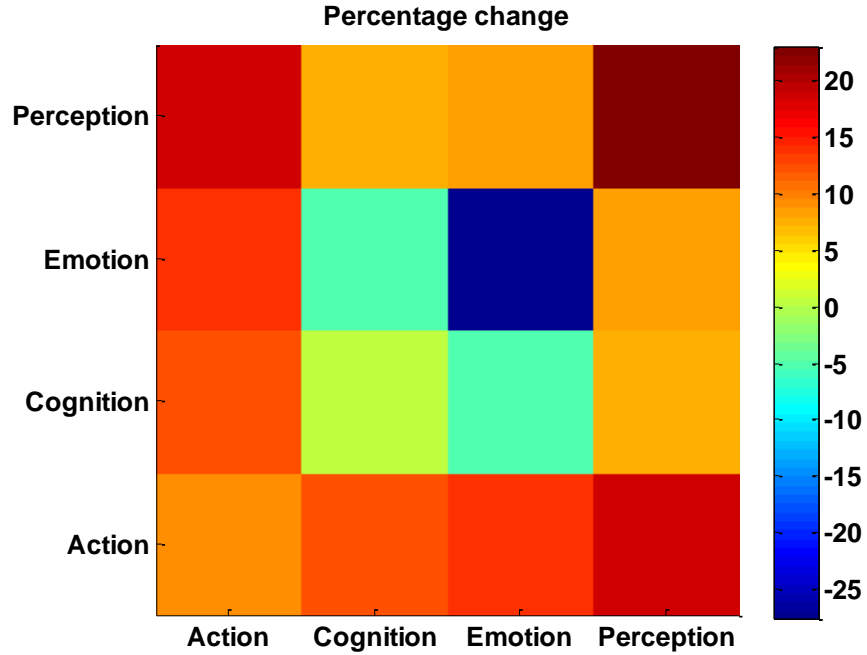


Figure 26. Changes in behavioral domain interactions at the acute state. Negative values indicate decreases in interaction in patient group. Color-bar indicates the percent change

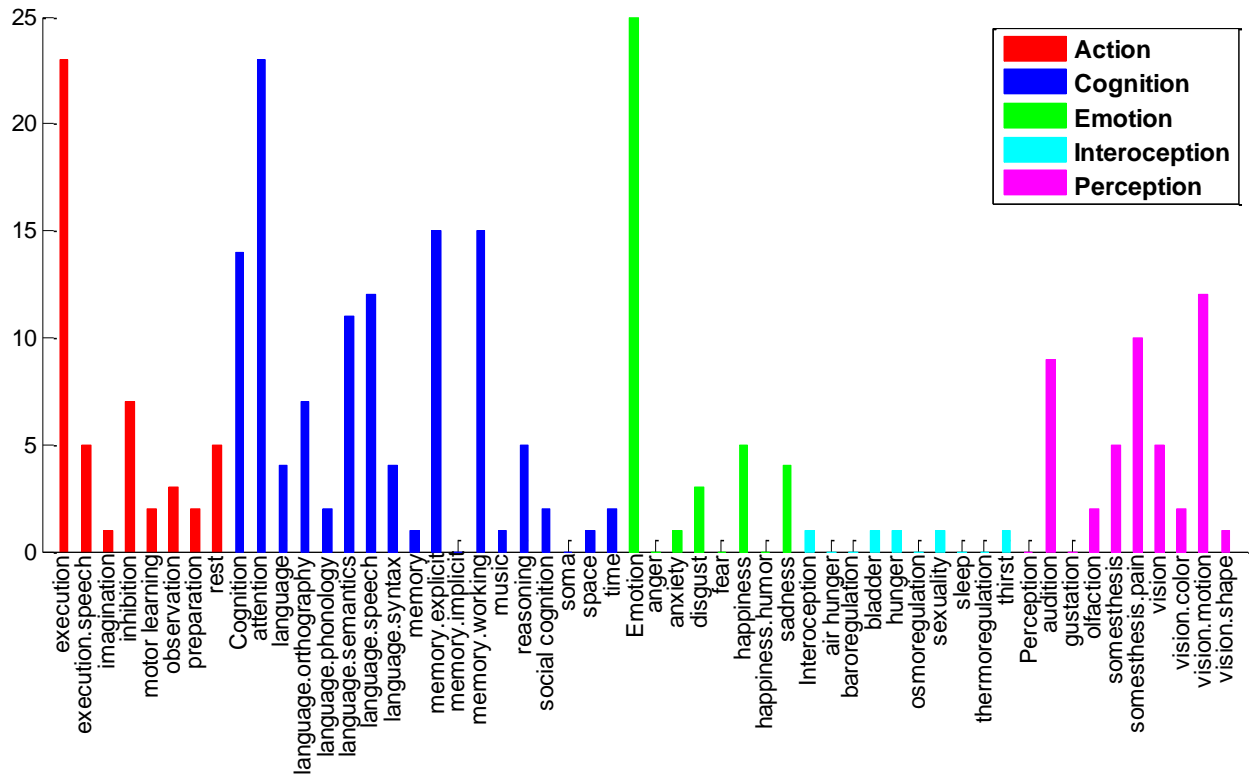


Figure 27. Functional roles of connectomic signatures. The affected DICCOCOLs were divided in 5 categories with 53 sub-categories using meta-analysis. Meta-analysis reveals that the emotion, cognition/attention, and action/execution categories are involved in more connectomic signatures than others, with 25, 23, and 23 DICCOCOLs each, respectively. The vertical axis is number of the affected DICCOCOLs associated with each functional role

Longitudinal Study

While emotion, action/execution, and cognition/attention show maximum disruption at the acute stage, in order to have a better understanding of changes in brain function after mTBI, a meta-analysis was performed on the result of the longitudinal study. We expected that the disruptions involved the emotion domain recover over time. We categorized the affected FC into the five major brain behavioral domains (action, perception, cognition, interoception, and emotion) and observed that action and cognition are more involved in altered functional connectivity as observed in the longitudinal study, especially the interaction between action and cognition networks, which has been affected the most (Figure 28). As we expected, the emotion domain, which was significantly disturbed at the acute stage, got better over time, which can be an indication of psychogenic alteration of brain injury. Further investigation of the roles of DICCCOLs which were evaluated in greater details using 53 subcategories revealed that the interaction between execution (from the action category) and attention (from the cognition category) and between execution (from action category) and working memory (from cognition category) have been effected the most, which is constant with our findings in the acute study (Figure 28).

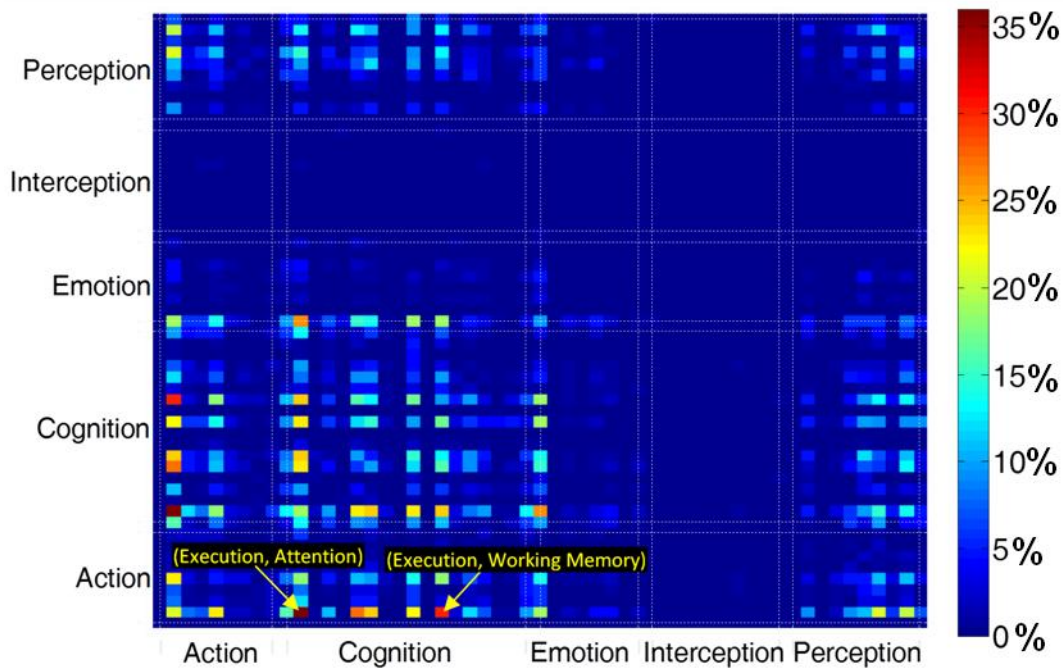


Figure 28. Categorization of altered functional connectivity in mTBI. The color-bar indicates percent change. The results show that the action and cognition networks have been disrupted the most. Further functional analysis using the 53 subcategories shows that interaction between execution (from the action category) and attention (from the cognition category) and between execution (from

the action category) and working memory (from the cognition category) have been affected the most (yellow arrow). This is consistent with published literature on attention, working memory and executive function deficit.

5.4.2. Statistical Relationship Between Neurocognitive and Neuroimaging Data

Briefly, in this step, we evaluated if our neuroimaging data at the acute stage is correlated with neurocognitive assessment results at one month. We had 32 subjects with rsfMRI data at the acute stage (first time point) and 25 subjects with complete neurocognitive evaluation at the follow up (second time point). Seventeen subjects had both rsfMRI data at acute stage and either memory composite score or attention/executive function composite score at follow up. Only sixteen subjects have both memory and attention/executive function composite scores, leaving sixteen subjects with both rsfMRI data at the acute stage and a total neurocognitive score. Table 2 shows the demographics of the mTBI patients who have neuroimaging data at the acute stage and neurocognitive data at the follow up.

Table 2. Demographic characteristics of mTBI patients with neuroimaging data at the first time point and neurocognitive data at the second time point.

		Memory composite score	Attention/Executive Function composite score	Total composite score
Age	Mean \pm SD	40.53 \pm 13.80	39.12 \pm 13.56	39.69 \pm 13.80
	Median / Range	43 / (19 ~ 63)	43 / (19 ~ 63)	43 / (19 ~ 63)
Gender	Male / Female	11/ 6	12/ 5	11/ 5
Race	African American	14	13	13
	White	2	3	2
	Others	1	1	1
Education	Mean \pm SD	12.94 \pm 2.49	13.06 \pm 2.59	12.87 \pm 2.56
	Median / Range	13.5 / (7 ~ 17)	13.5 / (7~ 17)	13 / (7 ~ 17)
WRAT	Mean \pm SD	48.82 \pm 11.83	49.53 \pm 12.62	48.37 \pm 12.07
	Median / Range	53 / (23 ~ 66)	53 / (23 ~ 68)	51.5 / (23 ~ 66)

Since the total number of subjects is very limited, from a statistical point of view, it is not recommended to include any covariates in the model despite their significant contribution (especially age and WRAT) to our outcome variables (i.e. composite neurocognitive scores) Table 3. However, I have included the results of including covariates in the model in the Appendix to demonstrate these models, which are suspected to be overfitted. Instead of including them in our main model, we used an alternative approach. We first performed the simplest regression model (NPT ~ 1 + NIM) and measured the relationship between neurocognitive variables (NPTs) and neuroimaging variables (NIMs). For those neuroimaging variables that show significant correlation with neurocognitive variables, we then measured

their relationship with age (age ~ 1 + NIM) and WRAT (WRAT ~ 1 + NIM) in order to evaluate if these parameters have an influence on the neuroimaging variables which leads to a significant relationship of the neuroimaging variables with the neurocognitive variables.

Table 3. Covariates Contributions in Neuropsychological Tests (NPTs).

	Memory composite score		Attention/Executive Function composite score		Total composite score	
	<i>P-value</i>	<i>R²</i>	<i>P-value</i>	<i>R²</i>	<i>P-value</i>	<i>R²</i>
<i>NPT~1+WRAT</i>	0.06	0.21	0.008	0.38	0.006	0.42
<i>NPT~1+age</i>	0.14	0.14	0.005	0.42	0.03	0.29
<i>NPT~1+gender</i>	0.48	0.03	0.18	0.12	0.13	0.13

The sixty connectomic signatures which showed significant differences at the acute stage were considered as the initial selected neuroimaging variables to evaluate for possible correlation with neurocognitive variables at one month. As explained earlier, we reduced the number of comparisons by combining the knowledge of a clinical neuropsychologist (JW) and BrainMap datasets.

The selected associated cognitive domains of the BrainMap dataset for neuropsychological composite scores are as follow: memory explicit for memory composite score; inhibition, motor learning, attention, and working memory for attention/processing speed composite score; and inhibition, motor learning, attention, memory, memory explicit, and working memory for the total neuropsychological composite. Identifying the corresponding connectomic signatures for those cognitive domains of the BrainMap dataset resulted in 18, 38, and 41 signatures for the memory composite score, attention/processing speed composite score, and the total neuropsychological composite score, respectively.

Total composite score: Performing the regression model (NPT ~ 1 + NIM) on 41 selected neuroimaging features revealed four connectomic signatures, numbers 15, 25, 50, and 54, which show significant correlation with the total composite score before multiple comparisons correction; however, none of them survived multiple comparison correction using false discovery rate (FDR).

Attention/processing speed composite score: Evaluation of the statistical relationship using the same regression model (NPT ~ 1 + NIM) on 38 selected neuroimaging features selected for attention/processing speed composite score revealed five connectomic signatures, numbers 10, 15, 22,

23, and 50, which showed significant correlation before but not after multiple comparisons correction using FDR.

Memory composite score: For the memory composite score, only one out of 18 connectomic signatures (number 29) showed a significant relationship using the same regression model ($NPT \sim 1 + NIM$). However, this significant relationship did not survive the multiple comparisons correction.

5.5. Discussion

Using meta-data and our neuroimaging findings together reveals that the most affected behavioral domains right after injury are emotion, execution (from the action category) and attention (from the cognition category), working memory (from cognition category), and explicit memory (from cognition category), respectively. These findings are aligned with the results of previous studies. As we expected, the disruption in the emotion domain recovers over time. Our longitudinal studies (using acute stage and one-month follow up data) revealed that the interaction between execution (from the action category) and attention (from the cognition category) and between execution (from action category) and working memory (from cognition category) have been disrupted the most.

We also evaluated the statistical relationship between large-scale functional connectivity findings at the acute stage and neurocognitive outcomes at follow-up; however, no significant correlation was observed between them. However, despite these negative findings, we cannot claim that there is no relationship between neuroimaging and neurocognitive data. There are several factors which can affect our ability to detect a statistical significant relationship, such as a complex recovery process, individual differences, sensitivity of neuropsychological tests and/or neuroimaging data, a small number of subjects, and a large number of statistical comparisons due to a large number of neuroimaging variables.

CHAPTER 6. CONNECTIVITY DOMAIN ANALYSIS

6.1. Background

There are two widely used approaches to analyze fMRI images in the time domain (i.e. analyzing the spatiotemporal information of fMRI data). The first approach includes model-based methods, such as general linear model (GLM), which show how well a certain model fits to the fMRI data (Friston et al., 1994). The second approach includes data-driven methods, such as principle component analysis (PCA) and ICA, which are based on feature extraction from fMRI data (Calhoun et al., 2003; Calhoun and Adali, 2012; van den Heuvel and Hulshoff Pol, 2010). In a model-based method, data is compared with a predefined model; therefore, model-based methods are focused on validating a prior assumption (the model) based on the data available and improving scientific understanding. However, no model is perfect, and one key aspect of a model is its robustness to incorrect assumptions, which can introduce bias to the system (Ford, 1995). Data-driven methods, on the other hand, analyze data in a more flexible manner. These methods are especially desirable when a good model does not exist or is hard to generate. Data-driven methods have the power to identify unanticipated components which can later be used in model-based approaches. Thus, data-driven methods can also be considered as model generating methods (Ford, 1995) since they can be used to obtain a model for data when there is no satisfactory model already available. However, by themselves, data-driven methods are primarily used for scientific discovery and identification of useful features from the data; they are most useful when combined within a statistical testing framework or for tasks such as prediction or classification (Calhoun and Adali, 2012; Erhardt et al., 2011).

Considering the advantages and limitations of both model-based and data-driven methods, they are complementary to each other. Therefore, in order to analyze data comprehensively and have a better understanding of brain function, it is useful to investigate data using both approaches. In the context of the model-based linear GLM and data-driven linear ICA, both approaches can be conceptualized as $X=AS$, in which the i^{th} row of the mixing matrix (A) identifies the contribution of parameters of S to create the i^{th} value of X . The main difference is that, in the data-driven method, the mixing matrix (A) needs to be estimated, whereas in the model-based method, the mixing matrix is pre-specified (Calhoun et al., 2001;

Ford, 1995). This requirement for a pre-specified design matrix makes the application of first-level model-based methods to extract brain networks challenging.

As mentioned earlier, brain network is defined as a subset of brain regions that interact with each other in a distinguishable way. Brain networks can be identified during the resting state by measuring the BOLD signal from rsfMRI data, which is related to brain activity (Buckner and Vincent, 2007). However, the fluctuations in the BOLD signal in the time domain at a specific time point are not synchronized among subjects for rsfMRI data. Therefore, the time courses of brain networks in rsfMRI are different among subjects. In other words, by considering the general form of $X=AS$, the mixing matrix (A) that represents the relationship between brain networks (S) with rsfMRI data at different time points (X) is different among subjects, which makes modeling the time-domain aspect of task-free fMRI challenging. Consequently, we cannot use the design matrix obtained from one dataset to apply a model-based method such as first-level GLM to identify underlying sources (S) in another dataset, even if matrix A is obtained from the same subjects but at a different sampling. Although some techniques such as dual regression indirectly solve this problem by relying on using the information of spatial maps obtained from the group data to indirectly perform model-based methods, those methods force the model (design matrix A) to produce similar spatial maps as the ones in the group data. Because of this, the model is related to the dataset at hand and is not reproducible for other datasets, even if they were collected on the same subjects, such as at different time points. In other words, in methods like dual regression, we do not evaluate the data from different subjects against a similar model, because instead of having a pre-specified model, we alter each subject's model to produce similar spatial maps (S) as the group data. Therefore, one consequence could be that we lose some intersubject variability. Considering this limitation of the time domain, we propose transferring the rsfMRI data from the time domain to another domain, the connectivity domain, where each value represents the same effect across homogenous subjects. It should be noted that for the sake of simplicity, for now, we only consider the brain's FC, which is usually derived from a rsfMRI experiment spanning five to 30 minutes, and the implicit assumption that the FC over this period of time is relatively static and similar among homogenous subjects. This assumption is not required for the connectivity domain analysis, and the connectivity domain analysis can also be performed to evaluate dynamic FC of the brain. Additionally, although the time courses of activity

within brain networks are different among subjects, the (static) FC of a specific region of the brain to a brain network is similar among subjects. In this situation, the mixing matrix, A , which represents the relationship between brain networks and connectivity of brain regions, should be similar among subjects, unlike in the time domain. This provides the ability to perform not only data-driven methods but also to directly perform the model-based methods in the connectivity domain. Therefore, using the connectivity domain, connectivity can be modeled among subjects and tested for differences among groups.

To construct the connectivity domain and analyze data in this domain, we need to define a set of seed networks and calculate the FC for each seed network by measuring a connectivity index. Seed networks can be constructed from any technique that identifies sets of features that are similar across subjects, so that the time courses of those features can be used to construct the connectivity domain. One simple method is to use atlas-derived anatomical locations (seed regions) across subjects as seed networks and calculate the FC for each seed region by measuring the connectivity index (for example, the correlation value) between the correspondent time series of each seed region and the whole brain. The resulting FC weights can be considered as a “basis” for our proposed domain. In the new proposed domain, (a) the connectivity of the brain can be modeled among subjects and tested for differences among groups (in other words, the relationship between the connectivity of brain regions and brain networks can be calculated and compared among different groups) and (b) with prior knowledge of the contribution of connectivity of brain regions in brain networks, we can directly calculate brain networks using model-based methods such as GLM. This can provide the opportunity to use model-based methods, like first-level GLM, without the handicap of having to estimate the mixing matrix, A , based on the combined group data (making it not a pure model-based method, but a data-informed model-based method).

Moreover, the connectivity domain can enhance the usage of data-driven analysis approaches, particularly feature-based ICA (Allen et al., 2011; Smith et al., 2009). Multiple data-driven analysis approaches have been successfully applied to rsfMRI data including clustering (Cordes et al., 2002; van den Heuvel et al., 2008a), ICA (Beckmann et al., 2005; Calhoun et al., 2001), graph analysis (Fornito et al., 2013; Rubinov and Sporns, 2010; van Wijk et al., 2010), and sparse coding (Lv et al., 2015a). ICA-based methods are one of the more widely used approaches, and their results (i.e., extracted networks)

show a high level of consistency in different conditions such as open or closed eyes; task, rest or sleep; and healthy or various mental disorders (Calhoun et al., 2008a; Calhoun et al., 2008b; Damoiseaux et al., 2006; Garrity et al., 2007; Irajy et al., 2015; Irajy et al., 2016b; Jafri et al., 2008; Sorg et al., 2007; Stevens et al., 2009; van den Heuvel and Hulshoff Pol, 2010; Whitfield-Gabrieli and Ford, 2012). ICA methods are designed to identify a set of latent spatially independent maps from rsfMRI data. A spatial map can be considered to be an underlying source (i.e. a brain network (Erhardt et al., 2011)), and the value of each voxel represents the degree to which the voxel belongs to, or is functionally connected to, that source (Calhoun and Adali, 2012; van den Heuvel and Hulshoff Pol, 2010).

Most previous ICA studies have estimated intrinsic connectivity networks (ICNs) by applying first-level ICA on the spatiotemporal information. Some new studies have also suggested the feasibility of extracting patterns of ICNs using second-level ICA analyses in which ICNs are obtained by applying ICA on extracted features, such as the amplitude of low frequency fluctuations (ALFF) map for rsfMRI, t-maps of GLM for task-based fMRI (Calhoun and Allen, 2013), the peak coordinates from meta-analysis (Smith et al., 2009), or even the outputs of the first-level ICA (Wisner et al., 2013). Since these second-level ICA analyses are applied on features extracted from the time domain, they are also considered as feature-based ICA analyses (Figure 29). While previous feature-based ICA analyses have been limited to second-level analyses, the connectivity domain enables us to perform feature-based ICA analysis as the first-level analysis (Figure 29). Furthermore, the connectivity domain has uses beyond the ICA techniques, and wide ranges of data-driven and model-based approaches can be applied in this domain (Figure 29).

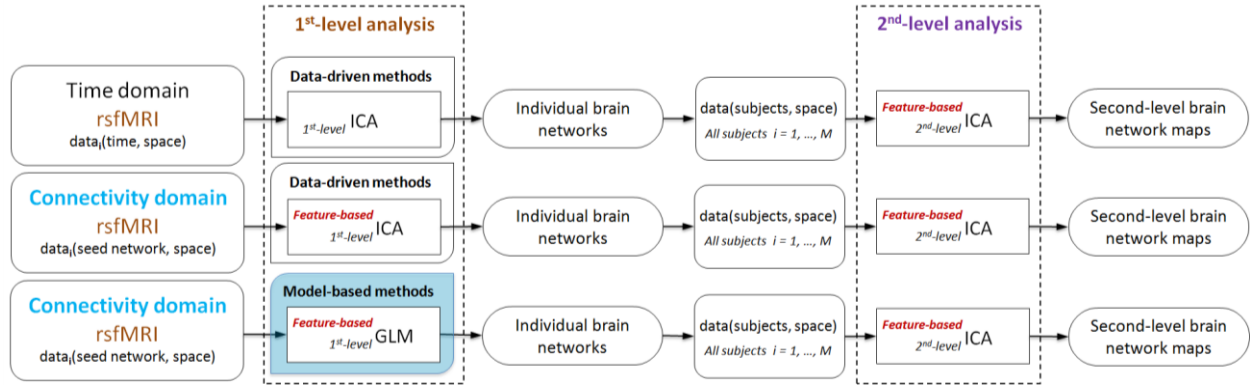


Figure 29. Schematic of analytical approaches which can be applied on rsfMRI data. The connectivity domain, similar to the time domain, allows us to perform a wide range of data-driven methods. The connectivity domain also supports implementing model-based methods such as first-level generalized linear model (GLM) on rsfMRI data (blue box). While feature-based approaches have been performed as second-level analyses, the connectivity domain provides us the opportunity to perform feature-based techniques at both first and second levels.

6.2. Analytical Approach: The Connectivity Domain

6.2.1. The Connectivity Domain: Analyzing Resting State fMRI Data Using Feature-based Data-driven and Model-based Methods

Authors: Armin Iraj, Vince D. Calhoun, Natalie Wiseman, Esmail Davoodi-Bojd, Mohammad R.N. Avanaki, E Mark Haacke, Zhifeng Kou

Context of the Paper

In this work, we first selected one example of a set of seed networks to create the connectivity domain. Then, we presented the superiority of the connectivity domain over the time domain by comparing data-driven methods applied in both domains. Lastly, we investigated the feasibility of applying model-based methods in the connectivity domain.

Image Processing

Figure 30 demonstrates a schematic of the analysis pipeline. Data collection was performed at two independent sites with different image acquisition parameters. The first site was Wayne State University, Detroit, Michigan, USA, where MRI data were collected from 17 healthy subjects (average age: 35.92 ± 8.84 ; range: 26–56) at two sessions with a 4–6 week interval in between. The second site was Henry Ford Hospital, Detroit, Michigan, USA, where MRI data were collected on a 3-Tesla GE scanner. Data was collected from 13 healthy subjects (average age: 27.25 ± 5.97 ; range: 18–39).

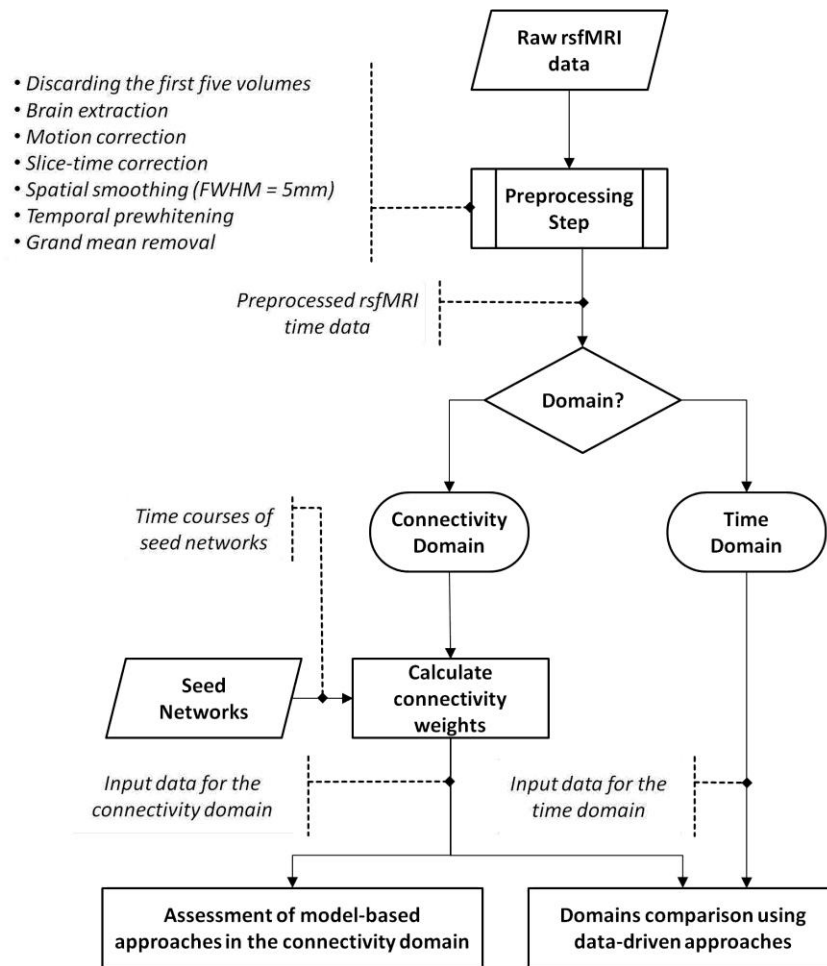


Figure 30. A schematic of the analysis pipeline. Data was preprocessed, and either kept in the time domain or transformed into the connectivity domain, which involved calculating connectivity weights using seed networks. Similar data-driven approaches were applied in both domains and compared between the two domains. Feasibility of applying model-based methods was evaluated in the connectivity domain.

Seed Network Selection

To perform data analysis in the connectivity domain, we first require an appropriate set of seed networks to calculate corresponding connectivity weights among subjects. In this study to demonstrate the feasibility of the connectivity domain, we used anatomical information to identify the seed networks. We wanted to use common, readily available atlases to define the seed networks, so we used the Harvard-Oxford cortical and subcortical atlases (Desikan et al., 2006; Frazier et al., 2005) to determine seed networks and obtained a similar set of connectivity weights across all subjects. The 145 seed regions, each 100 voxels in volume, distributed across the entire brain, were selected to calculate the connectivity weights. Figure 31.a, b, and c show some of these regions on the sagittal, coronal and axial views, respectively, on the MNI atlas. The color code of the regions is shown in Figure 31.d. The

functional connectivity (connectivity weights) of five seed networks shown in Figure 31.a and Figure 31.c in three sagittal, coronal and axial views are shown in Figure 31.e. To demonstrate the importance of selecting an appropriate set of seed networks to construct the connectivity domains, two more sets of seed networks were developed to test the sensitivity of analysis in the connectivity domain to the initial connectivity maps. The second set consisted of the same 145 seed regions from the Harvard-Oxford cortical and subcortical atlases but reduced in volume. The smaller volume was obtained by applying the Gaussian kernel with FWHM = 5mm on the previous Harvard-Oxford cortical and subcortical masks and thresholding the output at 0.55. For the third set of ROIs, 116 seed regions with a volume equal to 100 voxels were selected from the Automated Anatomical Labeling (AAL) atlas (Tzourio-Mazoyer et al., 2002).

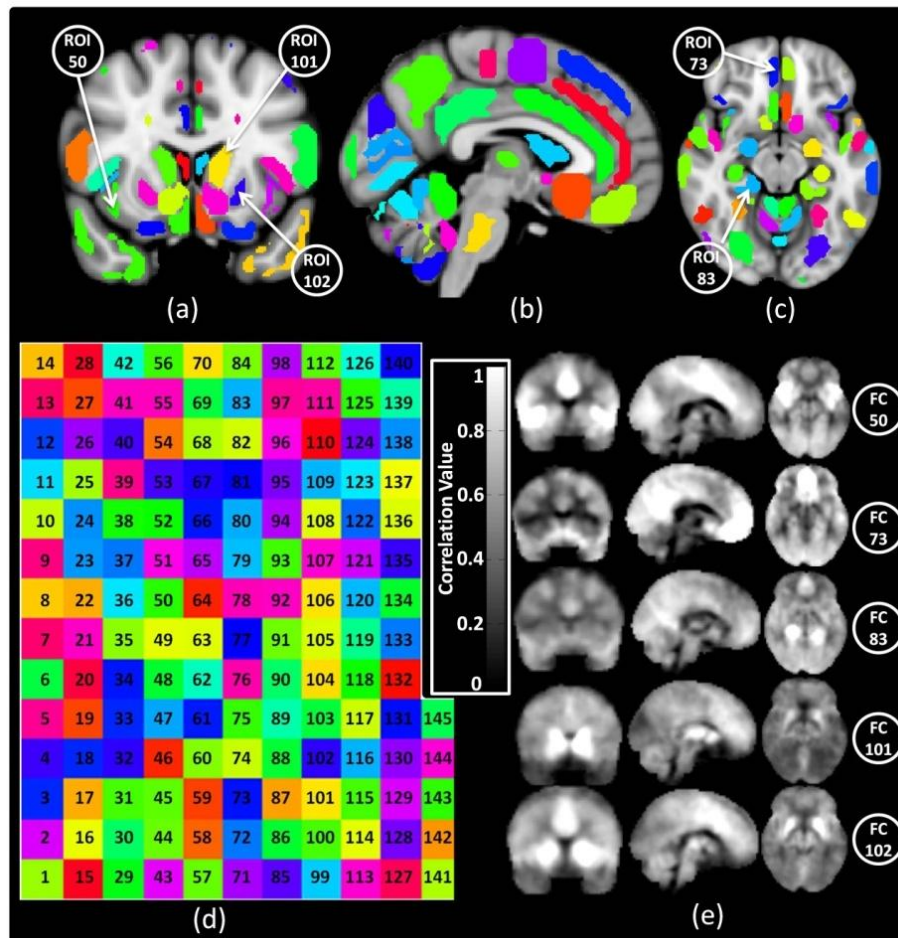


Figure 31. Functional connectivity weights calculation. Overlay of 145 ROIs on (a) coronal, (b) sagittal, and (c) axial views of MNI atlas. (d) Color code map of 145 ROIs. (e) Functional connectivity weights of ROIs 50 (right insular cortex), 75 (right subcallosal cortex), 83 (posterior division of parahippocampal gyrus), 101 (left caudate), and 102 (left putamen), respectively; the ROIs are annotated on Figure 31.a and c. For this study Harvard-Oxford cortical and subcortical structural atlases were used.

Findings

Data-driven Approaches in the Connectivity Domain vs. Time Domain

Results demonstrated that the brain intrinsic networks obtained from the time and connectivity domains using the temporal concatenation group spatial ICA followed by back-reconstruction (TC-BR), the most commonly used data-driven approach, are very similar (Figure 32). In the time domain, we identified 11 brain networks; however, one of these networks (Figure 32.²) was not identified correctly in the second session. Therefore, the time domain includes 10 brain networks that were found in both sessions. At the same time, the connectivity domain was able to identify 91% (10 out of 11) brain networks that the TC-BR method detected in the time domain. The connectivity domain also identified three extra brain networks as reported in previous studies (Allen et al., 2011; Biswal et al., 2010; Bolo et al., 2015; Laird et al., 2011; Leaver et al., 2015; Smith et al., 2009); however, these were not detected in our data when we performed the analysis in the time domain. These results indicate the ability of the connectivity domain to extract similar spatial maps as reported in previous studies analyzing data in the time domain. To evaluate test-rest reliability of the connectivity domain, we divided the data of each subject at the first session, which includes 235 volumes, into two parts with 118 and 117 volumes. Next, we converted data of each part into the connectivity domain. Therefore, for the data of each individual at the first session, two sets of data exist in each domain. Since data was collected at one session (i.e. at one time point), we expected that brain networks associated with two parts would be similar for each individual. We evaluated the spatial similarity between brain networks for each subject between the two parts in each domain for test-rest reliability. Figure 33 represents the result of our analysis for the consistent networks which were identified in Figure 32. The result of this analysis shows that the connectivity domain can produce similar and in some cases better results in comparison to the time domain. Furthermore, performing TC-BR analysis in both domains using two different sets of group data shows that the brain networks of individuals are more influenced by the group data in the time domain in comparison with the connectivity domain.

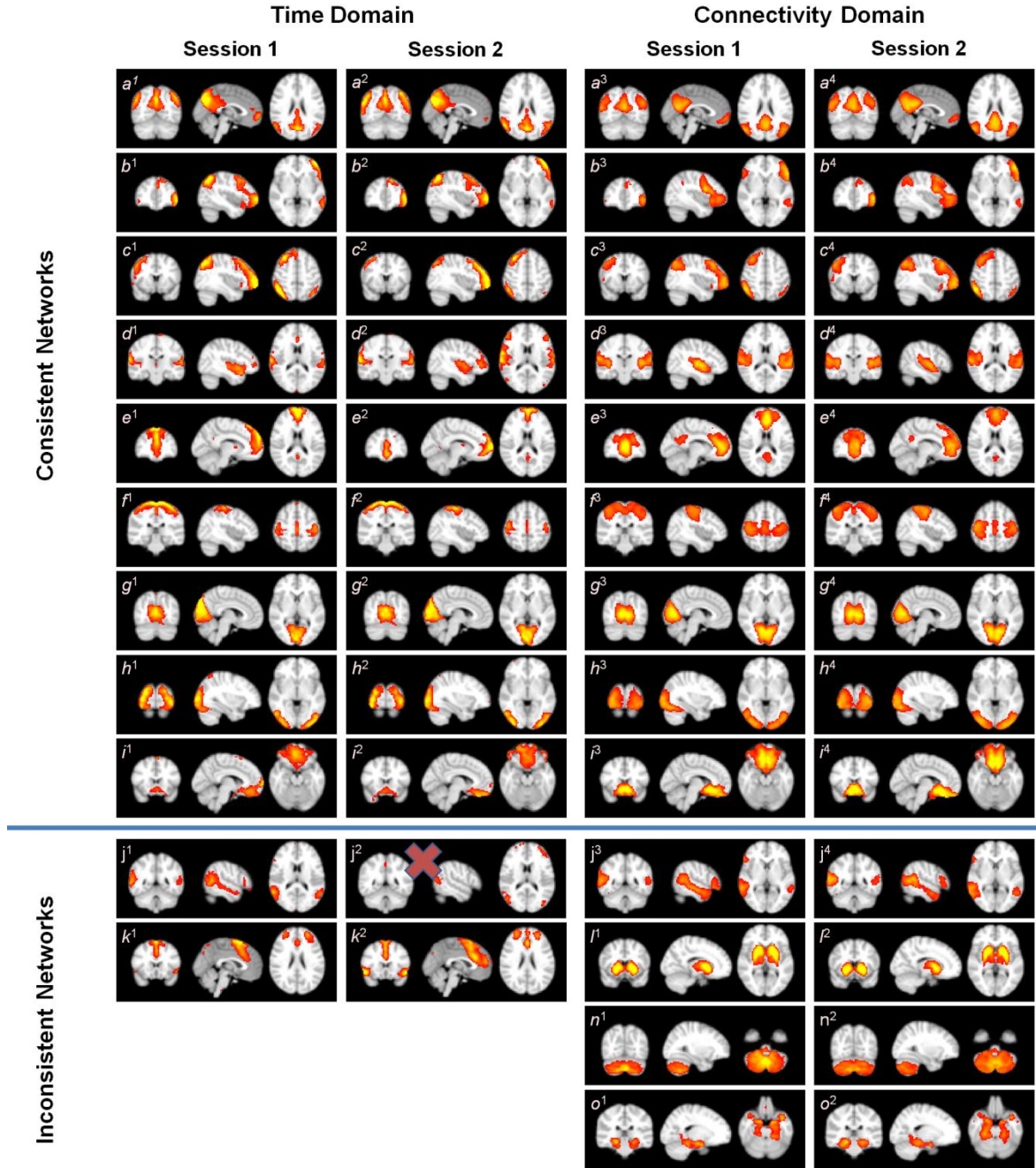


Figure 32. Spatial maps identified for both domains at both time points. The upper portion of the figure reveals nine consistent brain networks found in both domains including the DMN (a), left parietal-frontal (working memory) network (b), right parietal-frontal (working memory) network (c), auditory network (d), frontal DMN (e), motor network (f), primary visual network (g), secondary visual network (h), and subcallosal network (i). An attention network (j) seems consistent between two domains; however, it was not appropriately extracted in the second session for the time domain (j^2). The lower portion shows the spatial maps which were identified in one domain but not the other, or one time point but not the other

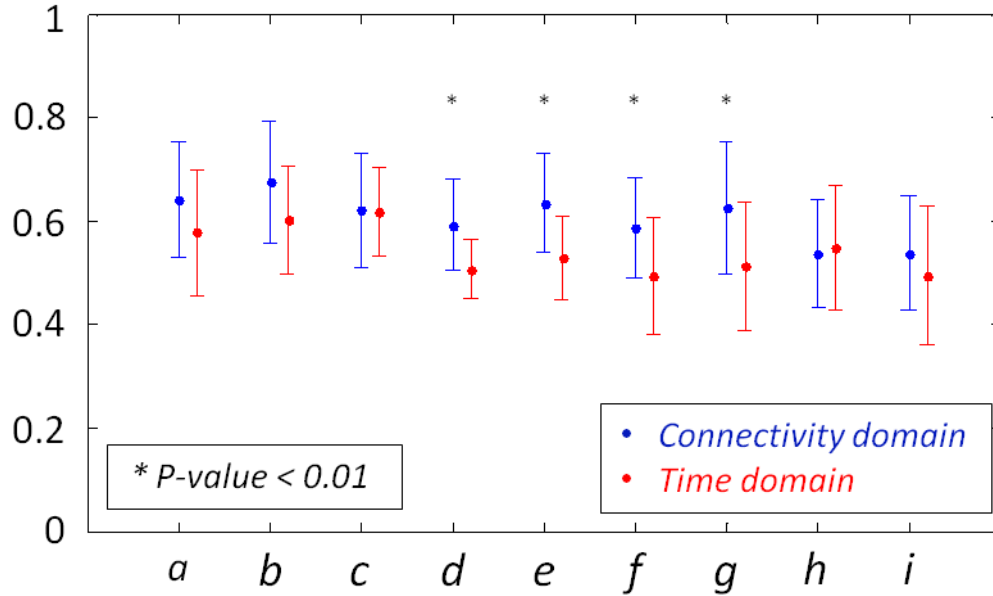


Figure 33. Spatial similarity between consistently-identified networks (Figure+++), including the DMN (a), left parietal-frontal (working memory) network (b), right parietal-frontal (working memory) network (c), auditory network (d), frontal DMN (e), motor network (f), primary visual network (g), secondary visual network (h), and subcallosal network (i) in the time (red) and connectivity (blue) domains for test-retest analysis. The spatial similarities between independent components were obtained from the TC-BR analysis using the data of the two parts of the first session. * identifies significantly higher spatial similarities in the connectivity domain as compared to the time domain.

We also investigated the impacts of variations of parameters in the TC-BR approach on the consistency of results and observed the superiority of the connectivity domain over the time domain for all investigated parameters. In brain connectivity research, one crucial step is the ability to compare and access findings across different studies. In order to have a more valid rationale to compare the results of different studies and make a valid conclusion, the findings of studies should be less susceptible to parameters which are not related to the brain connectivity information. Therefore, a superior domain is less affected by parameter variations of the applied analytical method. For this purpose, we investigated the impact of parameter variations in the TC-BR method on spatial maps of brain networks, as it is one of the most commonly used methods for investigating brain connectivity. Both the number of principal components (a preprocessing step) and the applied ICA techniques (a processing step) show that the connectivity domain is less vulnerable and therefore it is more suitable to produce robust findings. We do note that in order to make this powerful claim we should also investigate and compare the impact of the MRI scanner and other site parameters on individuals' outcomes between two domains.

Model-based Approaches in the Connectivity Domain

In addition to its strength with data-driven methods, the connectivity domain also provides the ability to use model-based methods. We found the same networks in both data-driven and model-based approaches in the connectivity domain. The ability to obtain similar brain networks using TC-BR and GLM with a high spatial similarity ($91.85 \pm 2.10\%$) supports our assumption of the similarity of the relationship between connectivity weights and brain networks among subjects. This opens a new pathway for analyzing brain function using model-based approaches. To further validate our assertion, we demonstrated the result of reconstructing the brain networks using the information, i.e. design matrix, of different studies and datasets.

Using GLM with design matrices obtained from the first and second sessions, the same brain networks were attained. Obtaining the same brain networks shows the reproducibility of model-based techniques when the design matrix from one session is utilized to analyze the data from the other session in the connectivity domain. Furthermore, high spatial similarity ($78.65 \pm 10.27\%$) between brain networks obtained using the design matrices of the two sessions shows the consistency of a design matrix over time in the connectivity domain. This could be beneficial in longitudinal studies in which one is interested in minimizing variations in healthy subjects across different time points. This could make the connectivity domain analysis more useful in investigating brain functional alterations and plasticity.

With ideal design and perfect parameter selection, we should be able to obtain ICN maps of a dataset using a design matrix obtained from a different group's data. Although this is a preliminary study without optimum design parameters such as seed choice, we observed that we could obtain similar ICNs for an independent dataset with unknown parameter information using the design matrix extracted from the first session of the WSU data (Figure 34).

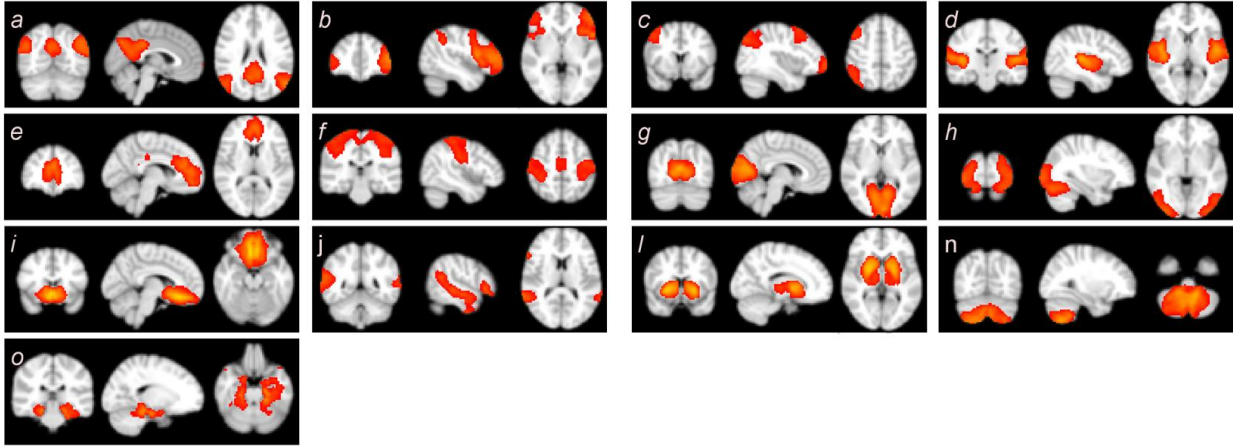


Figure 34. The ICNs identified using a GLM method from the independent dataset (i.e. Henry Ford Hospital). The design matrix that was used for this analysis is from the first session of WSU data (a different group of subjects).

We do note that the connectivity domain is affected by the choice of the set of seed regions used to build the domain. Our primary evaluations using different sizes of the same set of ROIs and different sets of ROIs reveals that the size of ROIs and more importantly the proper location of corresponding seed regions among subjects influences the results. The spatial similarity between brain networks obtained from the same set of seed networks with different sizes was $97.19 \pm 3.00\%$, and the spatial similarity between brain networks obtained from the two different sets of seed networks was $91.33 \pm 4.09\%$. This is especially important in connectomic study where identifying the fine-grained and optimized locations of seed regions is necessary. Note that, although the connectivity domain is biased towards selection of seed networks, this bias is independent to the dataset, and it would have a similar impact on all datasets. Since our aim for this study was to show the feasibility of using the connectivity domain, we reduced the sensitivity to ROI locations by choosing large ROIs and using the average time series of all voxels in each ROI to measure the functional connectivity map.

6.3. Discussion

The first step to improve the connectivity domain is to optimize the process of identifying the bases of the connectivity domain across individuals. The bases of the connectivity domain can be the time courses of seed networks. In this case, seed networks can be anatomical locations across the brain and the goal is precise, small seed regions because each location of the brain could be involved in different functions than its neighbors. Seed networks can also be made from data-driven seeds or

functional seeds. However, the bases of the connectivity domain can also directly be obtained from the temporal information of the data (for instance, using data-driven approaches such as PCA or clustering), as long as a measured connectivity index between bases and spatiotemporal information is able to represent similar characteristics across subjects.

Moreover, although we have used the Pearson correlation value as the connectivity index, the Pearson correlation is merely one index which can be used to reconstruct the connectivity domain. Thus, we have a unique opportunity to investigate the different types of connectivity and their interaction with brain networks. For instance, we can use indices which have been used for effective connectivity studies, or use other similarity indices like mutual information, coherence, or partial correlation.

In case we want to use the connectivity domain to evaluate brain functions using model-based methods, one crucial step is to estimate the true value for each array of the design matrix with a high level of accuracy. One solution is to calculate the design matrix from several datasets and perform statistical analysis. This process can also be an essential part in identification of biomarkers to discriminate between healthy subjects and patients with different disorders.

Finally, we do note that, although we implicitly considered that brain functional connectivity is constant during the resting state, the connectivity domain can also be applied to investigate non-stationary behaviors of the brain activity at rest.

Chapter 7. CONCLUSION, DISCUSSION, AND FUTURE WORK

7.1. Contribution and Conclusions

In summary, we find that mTBI causes large-scale changes in both structural and functional brain connectivity. Specifically, our work made the following contributions and led to the following findings.

1) Structural Connectivity Impairment: We carried out the first effort of investigating large-scale brain structural network connectivity after mTBI. We performed a connectome-scale assessment of structural connectivity, and our findings revealed that mTBI can cause structural abnormalities in major white matter tracts that provide structural support of brain functional networks. Our finding shows that the corpus callosum, the superior and inferior longitudinal fasciculi, the arcuate fibers, and the cingulate bundle are the most commonly affected white matter tracts. This finding is consistent with the summary of published literature regarding the white matter fibers most susceptible to injury.

2) Functional Hyperconnectivity: We performed the first resting state fMRI study for mTBI patients at the acute stage. We carried out extensive analyses of the DMN in mTBI patients and found decrease within-DMN connectivity and increased functional connectivity between DMN regions and the rest of the brain. Furthermore, we made the first effort to investigate connectome-scale brain network analysis in mTBI. In general, the connectome scale analyses show a general trend of increased functional connectivity to compensate for the effect of brain injury, and this hyper-connectivity remains persistent even one month after injury.

3) No significant Correlation between Neuroimaging and Neurocognitive: We also performed various analyses to identify the affected cognitive domains after mTBI. For the first time, we used meta-data in addition to our neuroimaging findings to identify affected behavioral domains after mTBI. We also calculated the statistical relationship between findings of our large-scale functional connectivity analysis at the acute stage and patients' neurocognitive outcomes at follow-up. This analysis did not reveal any significant correlation between the neuroimaging data and the neurocognitive data.

4) Connectivity Domain Analysis: We further developed a novel approach to analyze rsfMRI data to overcome current restrictions of analyzing rsfMRI data in the time domain. Intrinsic brain activities

are not synchronized among subjects, which leads to some limitations and challenges such as performing model-based analytical approaches. However, brain regions have similar functions and interact with each other in a similar manner across individuals. Therefore, we suggested to reconstruct the intrinsic activities of brain regions relative to intrinsic activities of other brain regions instead of relative to time. This allows us to capture the similarities of brain intrinsic activities across individuals.

This new domain in which we represent data relative to the time courses of common features across individuals instead of relative to time is called the connectivity domain. In fact, the time course of any feature which shows similarity across subjects can be used to calculate the connectivity domain. The connectivity domain have the following important characteristics: 1) It enables us to use model-based analysis techniques; 2) It decreases the influence of the group data on the brain networks of each individual subject as compared to the same analysis done in the time domain; 3) It reduces the susceptibility of analysis techniques to parameters that are not related to brain connectivity information; and 4) It is more suitable for analyzing data across different populations and studies.

7.2. Discussion

One major goal of this study was to identify the functional connectivity alterations at a large scale so we can further investigate them to uncover underpinning of mTBI patients' NP symptoms and predict patients' outcome using neuroimaging data. For this purpose, we evaluate the relationship between neuroimaging results at the acute stage and neurocognitive findings at follow up, and we did not observe a statistically significant relationship between them. However, it should be noted that our analysis still cannot exclude the potential relationship between the neuroimaging and neurocognitive variables; we should be careful not to interpret the absence of evidence of a relationship as evidence of the absence of a relationship. There are several factors which reduced our statistical power to detect a significant correlation, including a small number of subjects and a large number of statistical comparisons due to a large number of variables from both the neuroimaging and neuropsychological data. There are also some other factors which could lead to a failure to observe a significant correlation between the neuroimaging and neuropsychological data, such as complex recovery processes, individual differences, and inadequate sensitivity of neuropsychological tests and/or neuroimaging data.

7.3. Future Work

To date, alterations in the brain's structural and functional connectivity after mTBI are still unclear, considering the high level of heterogeneity due to several factors. One factor is individual subject-specific features including different pre-existing conditions and demographic characteristics (age, gender, and education level). Moreover, there are different mechanisms of injury (e.g. vehicular collision vs. sports) which result in different scenarios of biomechanical loading (strain and stress) (Eierud et al., 2014; Ilvesmaki et al., 2014; Sharp and Jenkins, 2015). This high level of heterogeneity results in a large amount of complexity and different injury pathologies (e.g. neuronal injury vs. axonal injury vs. vascular injury). One solution to overcome this high level of heterogeneity is to perform large population-based prospective studies. The necessity of a large sample size in studies becomes more obvious when we apply a large-scale analysis. Large-scale analyses involve a greater number of comparisons, which reduces the statistical power. Another solution to acquire a large data sample is to perform cross-center studies and combine the data of several centers. For cross-center studies, we can utilize the connectivity domain analysis to reduce the influence of factors related to centers' variability.

We do note that, while using larger sample size could help to address high level of heterogeneity, performing analysis at the individual level (e.g. a personalized connectome) is necessary to accurately identify personalized alterations. In general, alterations of brain connectivity can be divided in two categories: common variability features and individual (uncommon) variability features. The former includes the common alterations of brain functions among a group of individuals with a similar disorder, and the latter is personalized and may be related to the mechanism and location of the injury of each individual. While group-level analyses, i.e., comparing a group of mTBI patients with a group of normal controls, are helpful to identify the common connectivity alterations, they could provide a distorted view of overall brain connectivity alterations after mTBI because they obscure the individual differences that characterize brain injuries. Therefore, although neuroimaging studies of mTBI mainly focus on group analyses, the heterogeneity in mTBI demands individual analysis approaches to identify personalized alterations. Individual-level studies and personalized connectome research can lead to the development

of useful diagnostic tools that are sensitive enough to accurately diagnose brain injury and specific enough to identify the disrupted brain connections (Eierud et al., 2014).

One important issue that could play a significant role in not observing significant correlation between neuroimaging and neurocognitive data is the timeline of the recovery process and the time between injury and data collection. In mild TBI, the most affected neurons experience reversible injury and/or plasticity. Therefore, the compensation mechanisms and functional connectivity alterations vary over time and depend on the individual subject-specific features. Increasing the number of time points of data collection (e.g. another data acquisition at the chronic stage) could assist us to identify the stage of recovery and significantly improve our ability to evaluate the relationship between neuroimaging and neurocognitive data. Collecting data at several time points can potentially help us to identify a similar stage of the recovery process across subjects. Performing regression analysis while incorporating the information that we can obtain through collecting data at several time points could help us to more accurately assess the correlation between neuroimaging and neurocognitive data.

Another step to improve our ability to more accurately assess the relationship between neuroimaging and neurocognitive data is to refine our neuroimaging analytical approach to pinpoint the connectivity network alterations which are the source of mTBI patients' neurocognitive symptoms. For instance, considering previous findings, one promising approach is to utilize circuit-based (network-based) approaches and investigate the interactions between and within the DMN, salience network, and frontoparietal networks. Alterations in functional connectivity among areas of these networks have been consistently reported after brain injury.

Similar to the neuroimaging data, selection of sensitive and robust neuropsychological tests can assist us to more precisely evaluate the relationship between neuroimaging and neurocognitive data. While we calculated the composite scores from the results available from neuropsychological tests to have robust and accurate neurocognitive data for correlation analysis, various types of neuropsychological tests exist which could improve the accuracy and quality of calculated neurocognitive variables. Therefore, a future study is needed to select the best neuropsychological tests which better assist with evaluation of the relationship between neuroimaging and neurocognitive data

We also note that there is a close relationship between structural and functional connectivity which makes combining dMRI and rsfMRI an important avenue in neuroimaging field. A wide range of studies tries to simultaneously take an advantage of these two modalities, which can be categorized into two general categories; data integration and data fusion. Data integration itself can be divided in two groups. In the first group, data from different modalities are analyzed through separate pipelines, and the results are integrated (i.e. combined) at decision and interpretation levels. The second group of data integration approaches utilizes information from one modality to improve the overall result of other modalities. Unlike data integration approaches, in which the analysis step of each modality is performed separately and is blind to other modalities, in data fusion, the data from different modalities are combined in processing and analyzing steps and prior to post-processing (i.e. the decision and interpretation levels). In other words, analytical techniques incorporate the information of different modalities which allows us to also obtain the information that exist across modalities. On the other hand, due to the close relationship between the alterations of structural and functional connectivity, combining the structural and functional connectivity analyses together could allow us to characterize the interplay between structural and functional connectivities after brain injury. Therefore, a combined structural and functional analysis could have the potential to ameliorate the clinical management of mTBI patients in the future, which should be investigated in future studies with a large number of subjects.

For the technical goal of this project, the connectivity domain, the first step is to identify the optimized corresponding seed networks across individuals. Further studies are required to evaluate and compare the different approaches in identifying seed networks. We do note that the brain activity at rest has non-stationary behavior and that understanding network dynamics is important to provide rich characteristics of the brain (Calhoun et al., 2014; Calhoun et al., 2013). Although we implicitly considered that brain functional behavior is constant during the resting state in this study, the connectivity domain also offers a new option to investigate the dynamic characteristics of the brain. For example, one simple way is to use a sliding window approach and calculate the connectivity weights for each interval. As a result, we can evaluate alterations in brain networks and changes in contributions of regions to them over time. Moreover, since using the connectivity domain can reduce the effect of non-functional fluctuations exist in rsfMRI time courses, optimization of the approach that is used to calculate the connectivity

weights can improve the connectivity domain analysis and the evaluation of brain network connectivity. For instance, one future work could be to evaluate various mathematical indices. We can also include different covariates in the process of measuring connectivity weights to eliminate the influence on analysis. Finally, one of the advantages of the connectivity domain is its superiority in cross-centers studies. Thus, tuning the connectivity domain analysis to be most effective is in a high priority.

APPENDIX: STATISTICAL INFERENCE BETWEEN NEUROCOGNITIVE AND NEUROIMAGING VARIABLES USING COVARIATES

While for our study, it is not recommended to include any covariates in the model due to the very limited number of subjects (16 subjects with both neuroimaging and neurocognitive data), we performed an exploratory analysis including different covariates in the model. The covariates of interest are age, gender, and the reading (word recognition) subtest of the Wide Range Achievement Test (WRAT). It should be mentioned that WRAT variable accounts for several premorbid factors including education and race (Silverberg et al., 2013). We evaluated the relationship between neurocognitive and neuroimaging data using eight models including: (NPT~1+NIM), (NPT~1 + NIM + WRAT), (NPT~1 + NIM + Age), (NPT~1 + NIM + Gender), (NPT~1 + NIM + Age+ WRAT), (NPT~1 + NIM + Age+ Gender), (NPT~1 + NIM + WRAT+ Gender), and (NPT~1 + NIM + Age + WRAT+ Gender). We evaluated the relationship between each of three composite scores (from the neurocognitive data) and each of sixty connectomic signatures (from the neuroimaging data) using all eight models. It should be noted that all of the findings are referred as significant or not without performing a multiple correction except where noted otherwise. Multiple comparison correction was performed using family discovery rate (FDR).

Memory composite score: For prediction of the memory composite score, gender did not show a significant contribution in any statistical inferences when it included as a covariate. WRAT and age showed a significant contribution in 13 and 4 out of sixty connectomic signatures when they were each included as the only covariate of the model, respectively. The number of statistical inferences that showed significant contribution was reduced for these both when other covariates were included in the model. As another reminder, the statistical significance in this appendix refers to statically significant before FDR correction. Neither of these covariates revealed any significant contribution in any of models after multiple comparison correction. For the different models, various connectomic signatures showed significant correlation with the memory composite score but none of the connectomic signatures survived FDR correction (Table 4). It should be noted that while our analysis does not indicate any relationship

between the memory composite score and the neuroimaging variables, both the number of subjects and number of comparisons performed significantly reduces our statistical power to detect any significant correlation. We should be careful not to interpret the absence of evidence of a relationship as evidence of the absence of a relationship.

Table 4. Summary of regression analysis for memory composite score. Regression analysis was performed between memory composite score and 60 connectomic signatures using several models. Results shows the number of analysis that each covariate show significant contribution using p-value < 0.05.

Memory composite score	Number Significant (Out of 60)				
	NIM	NIM (FDR)	WRAT	Age	Gender
NPT~1+NIM	4	0	-	-	-
NPT~1 + NIM + WRAT	5	0	13	-	-
NPT~1 + NIM + Age	3	0	-	4	-
NPT~1 + NIM + Gender	5	0	-	-	0
NPT~1 + NIM + Age+ WRAT	7	0	6	1	-
NPT~1 + NIM + Age+ Gender	4	0	-	0	0
NPT~1 + NIM + WRAT+ Gender	5	0	9	-	0
NPT~1 + NIM + Age + WRAT+ Gender	9	0	4	0	0

To further explore these findings, for each model, we identified the connectomic signatures which showed an uncorrected significant relationship with the memory composite score. We identified the corresponding DICCCOL pairs (labeled DICCCOL A and DICCCOL B) to those connectomic signatures and their involvements with the associated behavioral domain, i.e. explicit memory, selected by a clinical neuropsychologist (JW) (Table 5). Looking at the results, connectomic signatures 21 and 26 consistently showed a significant relationship regardless of which model we use (Figure 35). Moreover, looking at the BrainMap dataset, their associated DICCCOLs are involved in memory. So we can speculate that these connectomic signatures are correlated with the memory composite score but lack significance here due to our limited number of subjects and low statistical power.

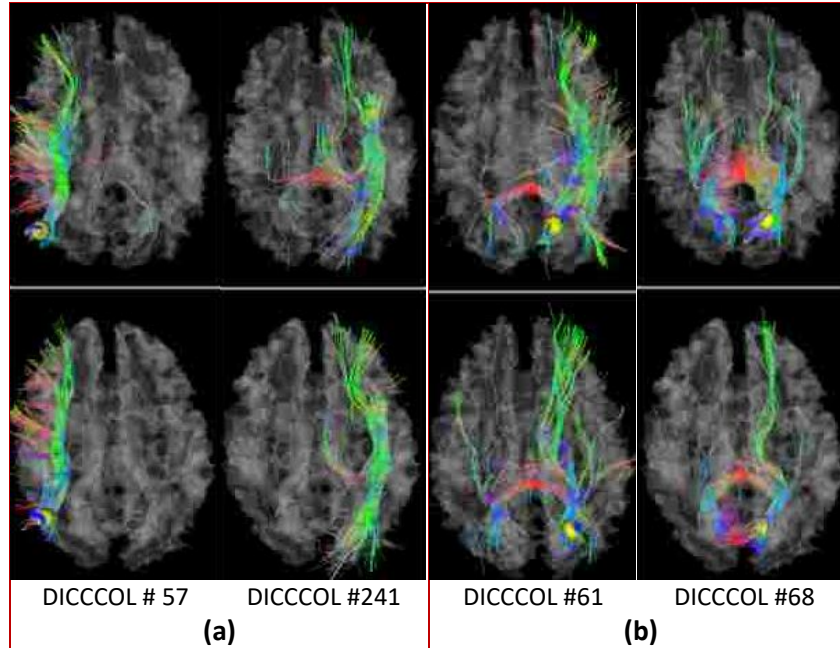


Figure 35. DICC COLs (yellow spheres) and the connected fiber bundles that are involved in the connectomic signatures 21 (a) and 26 (b). These connectomic signatures show significant correlation with the memory composite score in all the applied models

Table 5. Memory composite score. Red represents those DICC COLs that show significant relationship with both attention/executive function score and memory score. Bold shows the DICC COLs involved in more than one connectomic signature.

Connectome Signature ID	9	16	21	24	26	29	31	35	37	48	54
DICC COL A	254	174	241	68	68	244	284	169	120	197	302
DICC COL B	15	41	57	60	61	74	74	82	88	172	186
Explicit memory (cognition)		✓	✓	✓	✓			✓			
NPT~1 + NIM			x		x	x					x
NPT~1 + NIM + WRAT		x	x	x	x				x		
NPT~1 + NIM + Age			x		x	x					
NPT~1 + NIM + Gender			x		x	x				x	x
NPT~1 + NIM + Age + WRAT		x	x	x	x	x	x	x			
NPT~1 + NIM + Age + Gender			x		x	x		x			
NPT~1 + NIM + WRAT + Gender			x	x	x			x	x		
NPT~1 + NIM + Age + Gender + WART	x	x	x	x	x	x	x	x	x		

Attention/processing speed composite score: For the attention/processing speed composite score, like the memory composite score, gender showed the least contribution to the models when it added as a covariate. However, both WRAT and age show a significant contribution in most of the connectomic signatures regardless of which model was selected (Table 6). Therefore, they would be included if we had enough of subjects. Interestingly, we observe a statistically significant correlation between the attention/executive function composite score and some neuroimaging variables when age or

gender but not WRAT was included in the model. The connectomic signature #36, which is the functional connectivity between DICCCOL #82 and DICCCOL #206, showed a significant correlation with the attention/processing speed composite score for both the "NPT~1 + NIM + Gender" model and the "NPT~1 + NIM + Age + Gender" model (Figure 36). The connectomic signature #25, which is the functional connectivity between DICCCOL #60 and DICCCOL #236, showed a significant correlation with attention/processing speed composite score for the "NPT~1 + NIM + Gender" model (Figure 36). Each connectomic signatures had one DICCCOL in the left precuneus (DICCCOL #60 and DICCCOL #82), also referred to as Brodmann area 7, which is suggested to be involved in attention (Cavanna and Trimble, 2006). DICCCOL #206 is in the right precentral gyrus of the frontal lobe, also referred to as Brodmann area 4, and DICCCOL #236 is in the middle frontal gyrus of the left frontal lobe, also referred to as Brodmann area 8. We further investigated the functional roles of the DICCCOLs involved in the connectomic signatures #36 and #25 along with other connectomic signatures which showed significant correlation with the attention/processing speed composite score in any of models using meta-analysis approach (Table 7).

Table 6. Summary of regression analysis for the attention/processing speed composite score. Regression analysis was performed between attention/processing speed composite score and 60 connectomic signatures using several models. Results show the number of analysis that each covariate show significant contribution using p-value < 0.05.

Attention/Processing Speed composite score	Number of Significant contribution (Out of 60)				
	NIM	NIM (FDR)	WRAT	Age	Gender
NPT~1+NIM	8	0	-	-	-
NPT~1 + NIM + WRAT	8	0	59	-	-
NPT~1 + NIM + Age	3	1	-	60	-
NPT~1 + NIM + Gender	7	1	-	-	1
NPT~1 + NIM + Age+ WRAT	4	0	53	55	-
NPT~1 + NIM + Age+ Gender	3	1	-	52	0
NPT~1 + NIM + WRAT+ Gender	8	0	59	-	3
NPT~1 + NIM + Age + WRAT+ Gender	3	0	55	20	0

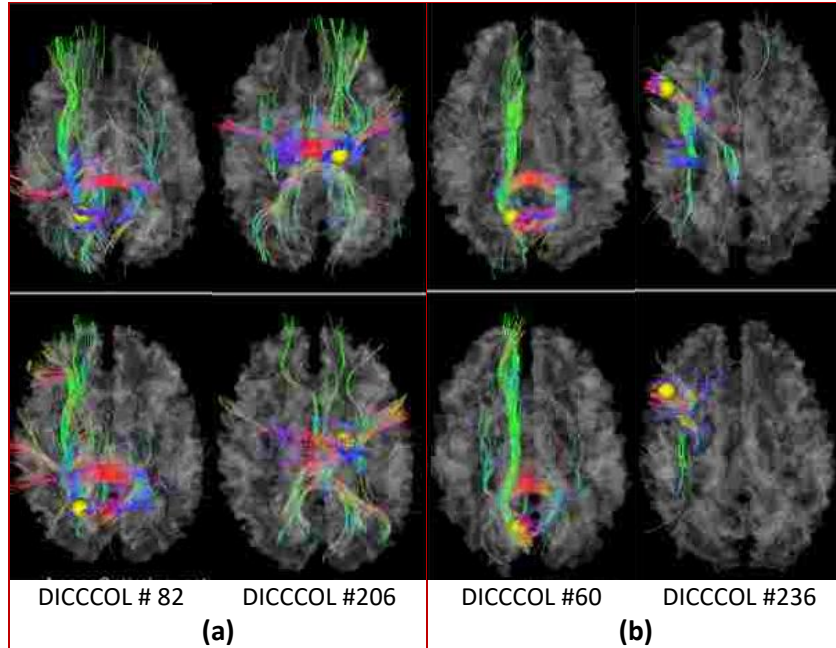


Figure 36. DICC COLs are shown in yellow sphere. DICC COLs are involved in the connectomic signatures 36 (a) and 25 (b) which show a significant correlation with the attention/processing speed composite score after FDR correction. The connected fiber bundles have also been shown.

Table 7. Attention/processing speed composite score results. Red represents those DICC COLs that show significant relationship with both attention/executive function score and memory score. Blue represents connectomic signature which shows significant correlation after FDR correction. Orange shows cognitive domains involved in both DICC COLs of a connectomic signature. Bold shows the DICC COLs involved in more than one connectomic signature.

Connectomic Signature ID	8	10	15	17	21	22	23	25	27	35	36	46	50
DICC COL A	202	272	146	71	241	259	262	236	200	169	206	236	217
DICC COL B	11	16	37	44	57	57	57	60	70	82	82	167	184
Attention (cognition)	✓		✓	✓	✓	✓	✓	✓	✓			✓	
Inhibition					✓	✓	✓	✓				✓	
Motor learning													✓
Working memory (cognition)		✓			✓	✓	✓			✓	✓	✓	✓
NPT~1 + NIM		x	x		x	x	x	x	x				x
NPT~1 + NIM + WRAT		x	x	x	x		x	x	x			x	
NPT~1 + NIM + Age		x						x			x		
NPT~1 + NIM + Gender	x		x		x	x	x	x	x				
NPT~1 + NIM + Age + WRAT		x						x	x		x		
NPT~1 + NIM + Age + Gender							x	x			x		
NPT~1 + NIM + WRAT + Gender	x		x		x		x	x	x	x		x	
NPT~1 + NIM + Age + Gender + WART								x	x		x		

It should be mentioned that while connectomic signatures #25 and #36 did not survive multiple comparison correction when both age and WRAT are included in the model, they did show significant relationship with the attention/processing speed composite score before FDR correction (Table 7).

Therefore, there is a possibility that there might be real correlations which not survive FDR correction due to the limited number of subjects.

Total composite score: Similar analysis was performed for the total composite score. As expected, WRAT has a significant contribution in almost all models when it is included. While age showed a significant contribution when it was used as the only covariate in the model, it did not contribute significantly to most of the sixty regression analyses when the model also included WRAT. Moreover, gender did not significantly contribute to most of the sixty regression analyses (Table 8). These findings, along with the results of the memory composite score and attention/processing speed composite score, suggest that WRAT should be the first covariate to be included into the model to address potential confounders and avoid misattributing results for the main parameters. The result of regression analysis reveals that there were no statistically significant correlations between the total composite score and any of the neuroimaging variables after multiple comparison correction (Table 8).

Table 8. Summary of regression analysis for the total composite score. Regression analysis was performed between the total composite score and the 60 connectomic signatures using several models. Results show the number of analyses for which each covariate showed a significant contribution using p-value < 0.05.

Total composite score	Number of Significant contribution (Out of 60)				
	NIM	NIM (FDR)	WRAT	Age	Gender
NPT~1+NIM	7	0	-	-	-
NPT~1 + NIM + WRAT	6	0	60	-	-
NPT~1 + NIM + Age	4	0	-	37	-
NPT~1 + NIM + Gender	6	0	-	-	1
NPT~1 + NIM + Age+ WRAT	4	0	58	11	-
NPT~1 + NIM + Age+ Gender	5	0	-	6	0
NPT~1 + NIM + WRAT+ Gender	7	0	59	-	10
NPT~1 + NIM + Age + WRAT+ Gender	5	0	58	2	1

Table 9. Total composite score. Orange shows cognitive domains involved in both DICCCOLs of a connectomic signature. Bold shows the DICCCOLs involved in more than one connectomic signature. Bold shows the DICCCOLs involved in more than one connectomic signature

Connectome Signature ID	9	15	17	21	25	27	29	36	37	46	48	50	54	58
DICCCOL A	254	146	71	241	236	200	244	206	120	236	197	217	302	236
DICCCOL B	15	37	44	57	60	70	74	82	88	167	172	184	186	217
Inhibition				✓	✓					✓	✓	✓		✓
Motor learning	✓													
Attention (cognition)		✓	✓	✓	✓	✓	✓		✓	✓	✓	✓	✓	✓
Working memory (cognition)				✓			✓	✓	✓	✓		✓		✓
Explicit memory (cognition)	✓	✓	✓	✓	✓		✓		✓	✓				✓
NPT~1 + NIM		x		x	x	x			x			x	x	
NPT~1 + NIM + WRAT		x	x	x		x			x	x				
NPT~1 + NIM + Age				x			x	x				x		
NPT~1 + NIM + Gender		x		x	x		x				x	x		
NPT~1 + NIM + Age + WRAT	x			x			x		x					
NPT~1 + NIM + Age + Gender				x			x	x			x			x
NPT~1 + NIM + WRAT + Gender	x	x	x	x		x			x	x				
NPT~1 + NIM + Age + Gender + WART	x	x		x			x		x					

REFERENCES

1993. Definition of mild traumatic brain injury. *The Journal of Head Trauma Rehabilitation* 8, 86-87.
- Allen, E.A., Erhardt, E.B., Damaraju, E., Gruner, W., Segall, J.M., Silva, R.F., Havlicek, M., Rachakonda, S., Fries, J., Kalyanam, R., Michael, A.M., Caprihan, A., Turner, J.A., Eichele, T., Adelsheim, S., Bryan, A.D., Bustillo, J., Clark, V.P., Feldstein Ewing, S.W., Filbey, F., Ford, C.C., Hutchison, K., Jung, R.E., Kiehl, K.A., Koditwakku, P., Komesu, Y.M., Mayer, A.R., Pearlson, G.D., Phillips, J.P., Sadek, J.R., Stevens, M., Teuscher, U., Thoma, R.J., Calhoun, V.D., 2011. A baseline for the multivariate comparison of resting-state networks. *Frontiers in systems neuroscience* 5, 2.
- Arfanakis K, Haughton VM, Carew JD, Rogers BP, Dempsey RJ, ME, M., 2002. Diffusion tensor MR imaging in diffuse axonal injury. *Am J Neuroradiol* 23, 794-802.
- Armistead-Jehle, P., 2010. Symptom validity test performance in U.S. veterans referred for evaluation of mild TBI. *Applied neuropsychology* 17, 52-59.
- Aron, A.R., Behrens, T.E., Smith, S., Frank, M.J., Poldrack, R.A., 2007. Triangulating a cognitive control network using diffusion-weighted magnetic resonance imaging (MRI) and functional MRI. *J Neurosci* 27, 3743-3752.
- Babyak, M.A., 2004. What you see may not be what you get: a brief, nontechnical introduction to overfitting in regression-type models. *Psychosomatic medicine* 66, 411-421.
- Baek, S.O., Kim, O.L., Kim, S.H., Kim, M.S., Son, S.M., Cho, Y.W., Byun, W.M., Jang, S.H., 2013. Relation between cingulum injury and cognition in chronic patients with traumatic brain injury; diffusion tensor tractography study. *NeuroRehabilitation* 33, 465-471.
- Barbey, K.A., Belli, A., Logan, A., Rubin, R., Zamroziewicz, M., Operskalski, T.J., 2015. Network topology and dynamics in traumatic brain injury. *Current Opinion in Behavioral Sciences*.
- Bazarian, J.J., Zhong, J., Blyth, B., Zhu, T., Kavcic, V., Peterson, D., 2007. Diffusion tensor imaging detects clinically important axonal damage after mild traumatic brain injury: a pilot study. *J Neurotrauma* 24, 1447-1459.

- Beckmann, C.F., DeLuca, M., Devlin, J.T., Smith, S.M., 2005. Investigations into resting-state connectivity using independent component analysis. *Philosophical Transactions of the Royal Society of London B: Biological Sciences* 360, 1001-1013.
- Beckmann, C.F., Mackay, C.E., Filippini, N., Smith, S.M., 2009. Group comparison of resting-state fMRI data using multi-subject ICA and dual regression. *NeuroImage* 47, S148.
- Beckmann, C.F., Smith, S.M., 2004. Probabilistic independent component analysis for functional magnetic resonance imaging. *IEEE transactions on medical imaging* 23, 137-152.
- Behrens, T.E.J., Berg, H.J., Jbabdi, S., Rushworth, M.F.S., Woolrich, M.W., 2007. Probabilistic diffusion tractography with multiple fibre orientations: What can we gain? *NeuroImage* 34, 144-155.
- Belanger, H.G., Vanderploeg, R.D., Curtiss, G., Warden, D.L., 2007. Recent neuroimaging techniques in mild traumatic brain injury. *The Journal of neuropsychiatry and clinical neurosciences* 19, 5-20.
- Benedict, R.H.B., Amato, M.P., Boringa, J., Brochet, B., Foley, F., Fredrikson, S., Hamalainen, P., Hartung, H., Krupp, L., Penner, I., Reder, A.T., Langdon, D., 2012. Brief International Cognitive Assessment for MS (BICAMS): international standards for validation. *BMC Neurology* 12, 55.
- Benson RR, Meda SA, Vasudevan S, Kou Z, Govindarajan KA, Hanks RA, Millis SR, Makki M, Latif Z, Coplin W, Meythaler J, EM, H., 2007. Global white matter analysis of diffusion tensor images is predictive of injury severity in TBI. *J Neurotrauma* 24, 446-459.
- Bergman, K., Bay, E., 2010. Mild traumatic brain injury/concussion: a review for ED nurses. *J Emerg Nurs* 36, 221-230.
- Besseling, R.M., Jansen, J.F., Overvliet, G.M., van der Kruijs, S.J., Ebus, S.C., de Louw, A., Hofman, P.A., Vles, J.S., Aldenkamp, A.P., Backes, W.H., 2013. Reduced Structural Connectivity between Sensorimotor and Language Areas in Rolandic Epilepsy. *PLoS one* 8, e83568.
- Biswal, B., Yetkin, F.Z., Haughton, V.M., Hyde, J.S., 1995. Functional Connectivity in the Motor Cortex of Resting Human Brain Using Echo-Planar Mri. *Magnetic Resonance in Medicine* 34, 537-541.
- Biswal, B.B., Mennes, M., Zuo, X.N., Gohel, S., Kelly, C., Smith, S.M., Beckmann, C.F., Adelstein, J.S., Buckner, R.L., Colcombe, S., Dogonowski, A.M., Ernst, M., Fair, D., Hampson, M., Hoptman, M.J.,

- Hyde, J.S., Kiviniemi, V.J., Kotter, R., Li, S.J., Lin, C.P., Lowe, M.J., Mackay, C., Madden, D.J., Madsen, K.H., Margulies, D.S., Mayberg, H.S., McMahon, K., Monk, C.S., Mostofsky, S.H., Nagel, B.J., Pekar, J.J., Peltier, S.J., Petersen, S.E., Riedl, V., Rombouts, S.A., Rypma, B., Schlaggar, B.L., Schmidt, S., Seidler, R.D., Siegle, G.J., Sorg, C., Teng, G.J., Veijola, J., Villringer, A., Walter, M., Wang, L., Weng, X.C., Whitfield-Gabrieli, S., Williamson, P., Windischberger, C., Zang, Y.F., Zhang, H.Y., Castellanos, F.X., Milham, M.P., 2010. Toward discovery science of human brain function. *Proceedings of the National Academy of Sciences of the United States of America* 107, 4734-4739.
- Blumensath, T., Jbabdi, S., Glasser, M.F., Van Essen, D.C., Ugurbil, K., Behrens, T.E., Smith, S.M., 2013. Spatially constrained hierarchical parcellation of the brain with resting-state fMRI. *NeuroImage* 76, 313-324.
- Bolo, N.R., Musen, G., Simonson, D.C., Nickerson, L.D., Flores, V.L., Siracusa, T., Hager, B., Lyoo, I.K., Renshaw, P.F., Jacobson, A.M., 2015. Functional Connectivity of Insula, Basal Ganglia, and Prefrontal Executive Control Networks during Hypoglycemia in Type 1 Diabetes. *J Neurosci* 35, 11012-11023.
- Bonnelle, V., Ham, T.E., Leech, R., Kinnunen, K.M., Mehta, M.A., Greenwood, R.J., Sharp, D.J., 2012. Salience network integrity predicts default mode network function after traumatic brain injury. *Proceedings of the National Academy of Sciences of the United States of America* 109, 4690-4695.
- Bonnelle, V., Leech, R., Kinnunen, K.M., Ham, T.E., Beckmann, C.F., De Boissezon, X., Greenwood, R.J., Sharp, D.J., 2011. Default mode network connectivity predicts sustained attention deficits after traumatic brain injury. *J Neurosci* 31, 13442-13451.
- Brandt, J., 1991. The hopkins verbal learning test: Development of a new memory test with six equivalent forms. *Clinical Neuropsychologist* 5, 125-142.
- Bressler, S.L., Menon, V., 2010. Large-scale brain networks in cognition: emerging methods and principles. *Trends in cognitive sciences* 14, 277-290.
- Brett, M., Johnsrude, I.S., Owen, A.M., 2002. The problem of functional localization in the human brain. *Nature reviews. Neuroscience* 3, 243-249.

- Bruns, J.J., Jr., Jagoda, A.S., 2009. Mild traumatic brain injury. *The Mount Sinai journal of medicine, New York* 76, 129-137.
- Buckner, R.L., Andrews-Hanna, J.R., Schacter, D.L., 2008. The brain's default network: anatomy, function, and relevance to disease. *Ann N Y Acad Sci* 1124, 1-38.
- Buckner, R.L., Vincent, J.L., 2007. Unrest at rest: default activity and spontaneous network correlations. *NeuroImage* 37, 1091-1096; discussion 1097-1099.
- Bullmore, E., Sporns, O., 2009. Complex brain networks: graph theoretical analysis of structural and functional systems. *Nature Reviews Neuroscience* 10, 186-198.
- Caeyenberghs, K., Leemans, A., Leunissen, I., Gooijers, J., Michiels, K., Sunaert, S., Swinnen, S.P., 2014. Altered structural networks and executive deficits in traumatic brain injury patients. *Brain structure & function* 219, 193-209.
- Calhoun, D.V., Adali, T., Hansen, K.L., Larsen, J., Pekar, J.J., 2003. ICA of functional MRI data: an overview.
- Calhoun, V.D., Adali, T., 2012. Multisubject independent component analysis of fMRI: a decade of intrinsic networks, default mode, and neurodiagnostic discovery. *IEEE reviews in biomedical engineering* 5, 60-73.
- Calhoun, V.D., Adali, T., Pearlson, G.D., Pekar, J.J., 2001. A method for making group inferences from functional MRI data using independent component analysis. *Human brain mapping* 14, 140-151.
- Calhoun, V.D., Allen, E., 2013. Extracting intrinsic functional networks with feature-based group independent component analysis. *Psychometrika* 78, 243-259.
- Calhoun, V.D., Kiehl, K.A., Pearlson, G.D., 2008a. Modulation of temporally coherent brain networks estimated using ICA at rest and during cognitive tasks. *Human brain mapping* 29, 828-838.
- Calhoun, V.D., Maciejewski, P.K., Pearlson, G.D., Kiehl, K.A., 2008b. Temporal lobe and "default" hemodynamic brain modes discriminate between schizophrenia and bipolar disorder. *Human brain mapping* 29, 1265-1275.

- Calhoun, V.D., Miller, R., Pearlson, G., Adali, T., 2014. The chronnectome: time-varying connectivity networks as the next frontier in fMRI data discovery. *Neuron* 84, 262-274.
- Calhoun, V.D., Yaesoubi, M., Rashid, B., Miller, R., Year Characterization of connectivity dynamics in intrinsic brain networks. In *Global Conference on Signal and Information Processing (GlobalSIP), 2013 IEEE*.
- Carter, A.R., Astafiev, S.V., Lang, C.E., Connor, L.T., Rengachary, J., Strube, M.J., Pope, D.L., Shulman, G.L., Corbetta, M., 2010. Resting interhemispheric functional magnetic resonance imaging connectivity predicts performance after stroke. *Ann Neurol* 67, 365-375.
- Carter, A.R., Shulman, G.L., Corbetta, M., 2012. Why use a connectivity-based approach to study stroke and recovery of function? *NeuroImage* 62, 2271-2280.
- Cassidy, J.D., Carroll, L., Peloso, P., Borg, J., Von Holst, H., Holm, L., Kraus, J., Coronado, V., 2004. Incidence, risk factors and prevention of mild traumatic brain injury: results of the WHO Collaborating Centre Task Force on Mild Traumatic Brain Injury. *Journal of rehabilitation medicine* 36, 28-60.
- Cavanna, A.E., Trimble, M.R., 2006. The precuneus: a review of its functional anatomy and behavioural correlates. *Brain : a journal of neurology* 129, 564-583.
- CDC, 2003. Report to Congress on Mild Traumatic brain injury in the United States: Steps to Prevent a Serious Public Health Problem. Centers for Disease Control and Prevention, National Center for Injury Prevention and Control, Atlanta (GA).
- Chen, C.J., Wu, C.H., Liao, Y.P., Hsu, H.L., Tseng, Y.C., Liu, H.L., Chiu, W.T., 2012. Working memory in patients with mild traumatic brain injury: functional MR imaging analysis. *Radiology* 264, 844-851.
- Chen, H., Li, K., Zhu, D., Jiang, X., Yuan, Y., Lv, P., Zhang, T., Guo, L., Shen, D., Liu, T., 2013. Inferring group-wise consistent multimodal brain networks via multi-view spectral clustering. *IEEE transactions on medical imaging* 32, 1576-1586.
- Christodoulou, C., DeLuca, J., Ricker, J., Madigan, N., Bly, B., Lange, G., Kalnin, A., Liu, W., Steffener, J., Diamond, B., Ni, A., 2001. Functional magnetic resonance imaging of working memory impairment after traumatic brain injury. *Journal of neurology, neurosurgery, and psychiatry* 71, 161-168.

- Cloutman, L.L., Lambon Ralph, M.A., 2012. Connectivity-based structural and functional parcellation of the human cortex using diffusion imaging and tractography. *Front Neuroanat* 6.
- Cohen, A.L., Fair, D.A., Dosenbach, N.U., Miezin, F.M., Dierker, D., Van Essen, D.C., Schlaggar, B.L., Petersen, S.E., 2008. Defining functional areas in individual human brains using resting functional connectivity MRI. *NeuroImage* 41, 45-57.
- Conturo, T.E., McKinstry, R.C., Akbudak, E., Robinson, B.H., 1996. Encoding of anisotropic diffusion with tetrahedral gradients: a general mathematical diffusion formalism and experimental results. *Magn Reson Med* 35, 399-412.
- Cordes, D., Haughton, V., Carew, J.D., Arfanakis, K., Maravilla, K., 2002. Hierarchical clustering to measure connectivity in fMRI resting-state data. *Magn Reson Imaging* 20, 305-317.
- Coronado, V.G., Xu, L., Basavaraju, S.V., McGuire, L.C., Wald, M.M., Faul, M.D., Guzman, B.R., Hemphill, J.D., 2011. Surveillance for traumatic brain injury-related deaths: United States, 1997-2007. US Department of Health and Human Services, Centers for Disease Control and Prevention Atlanta.
- Corrigan, J.D., Selassie, A.W., Orman, J.A., 2010. The epidemiology of traumatic brain injury. *J Head Trauma Rehabil* 25, 72-80.
- Damoiseaux, J.S., Beckmann, C.F., Arigita, E.J., Barkhof, F., Scheltens, P., Stam, C.J., Smith, S.M., Rombouts, S.A., 2008. Reduced resting-state brain activity in the "default network" in normal aging. *Cerebral cortex* 18, 1856-1864.
- Damoiseaux, J.S., Greicius, M.D., 2009. Greater than the sum of its parts: a review of studies combining structural connectivity and resting-state functional connectivity. *Brain structure & function* 213, 525-533.
- Damoiseaux, J.S., Rombouts, S.A., Barkhof, F., Scheltens, P., Stam, C.J., Smith, S.M., Beckmann, C.F., 2006. Consistent resting-state networks across healthy subjects. *Proceedings of the National Academy of Sciences of the United States of America* 103, 13848-13853.

- de Groot, M., Vernooij, M.W., Klein, S., Ikram, M.A., Vos, F.M., Smith, S.M., Niessen, W.J., Andersson, J.L., 2013. Improving alignment in Tract-based spatial statistics: Evaluation and optimization of image registration. *NeuroImage* 76, 400-411.
- De Luca, M., Beckmann, C.F., De Stefano, N., Matthews, P.M., Smith, S.M., 2006. fMRI resting state networks define distinct modes of long-distance interactions in the human brain. *NeuroImage* 29, 1359-1367.
- Desikan, R.S., Segonne, F., Fischl, B., Quinn, B.T., Dickerson, B.C., Blacker, D., Buckner, R.L., Dale, A.M., Maguire, R.P., Hyman, B.T., Albert, M.S., Killiany, R.J., 2006. An automated labeling system for subdividing the human cerebral cortex on MRI scans into gyral based regions of interest. *NeuroImage* 31, 968-980.
- Diedrichsen, J., Balsters, J.H., Flavell, J., Cussans, E., Ramnani, N., 2009. A probabilistic MR atlas of the human cerebellum. *NeuroImage* 46, 39-46.
- Dugbartey, A.T., Townes, B.D., Mahurin, R.K., 2000. Equivalence of the Color Trails Test and Trail Making Test in nonnative English-speakers. *Archives of clinical neuropsychology : the official journal of the National Academy of Neuropsychologists* 15, 425-431.
- Eickhoff, S.B., Stephan, K.E., Mohlberg, H., Grefkes, C., Fink, G.R., Amunts, K., Zilles, K., 2005. A new SPM toolbox for combining probabilistic cytoarchitectonic maps and functional imaging data. *NeuroImage* 25, 1325-1335.
- Eierud, C., Craddock, R.C., Fletcher, S., Aulakh, M., King-Casas, B., Kuehl, D., LaConte, S.M., 2014. Neuroimaging after mild traumatic brain injury: Review and meta-analysis. *NeuroImage. Clinical* 4, 283-294.
- Erhardt, E.B., Allen, E.A., Damaraju, E., Calhoun, V.D., 2011. On network derivation, classification, and visualization: a response to Habeck and Moeller. *Brain Connect* 1, 1-19.
- Faul, M., Xu, L., Wald, M.M., Coronado, V.G., 2010. Traumatic brain injury in the United States: emergency department visits, hospitalizations and deaths 2002–2006. Centers for Disease Control and Prevention, National Center for Injury Prevention and Control, Atlanta, GA.

- Figley, T.D., Bhullar, N., Courtney, S.M., Figley, C.R., 2015. Probabilistic atlases of default mode, executive control and salience network white matter tracts: an fMRI-guided diffusion tensor imaging and tractography study. *Frontiers in Human Neuroscience* 9, 585.
- Finn, E.S., Shen, X., Holahan, J.M., Scheinost, D., Lacadie, C., Papademetris, X., Shaywitz, S.E., Shaywitz, B.A., Constable, R.T., 2014. Disruption of functional networks in dyslexia: a whole-brain, data-driven analysis of connectivity. *Biol Psychiatry* 76, 397-404.
- Ford, I., 1995. Commentary and opinion: III. Some nonontological and functionally unconnected views on current issues in the analysis of PET datasets. *Journal of cerebral blood flow and metabolism : official journal of the International Society of Cerebral Blood Flow and Metabolism* 15, 371-377.
- Fornito, A., Bullmore, E.T., 2010. What can spontaneous fluctuations of the blood oxygenation-level-dependent signal tell us about psychiatric disorders? *Current opinion in psychiatry* 23, 239-249.
- Fornito, A., Bullmore, E.T., 2015. Connectomics: a new paradigm for understanding brain disease. *European neuropsychopharmacology : the journal of the European College of Neuropsychopharmacology* 25, 733-748.
- Fornito, A., Zalesky, A., Breakspear, M., 2013. Graph analysis of the human connectome: promise, progress, and pitfalls. *NeuroImage* 80, 426-444.
- Fornito, A., Zalesky, A., Bullmore, E.T., 2010. Network scaling effects in graph analytic studies of human resting-state FMRI data. *Frontiers in systems neuroscience* 4, 22.
- Fox, M.D., Snyder, A.Z., Vincent, J.L., Corbetta, M., Van Essen, D.C., Raichle, M.E., 2005. The human brain is intrinsically organized into dynamic, anticorrelated functional networks. *Proceedings of the National Academy of Sciences of the United States of America* 102, 9673-9678.
- Frazier, J.A., Chiu, S., Breeze, J.L., Makris, N., Lange, N., Kennedy, D.N., Herbert, M.R., Bent, E.K., Koneru, V.K., Dieterich, M.E., Hodge, S.M., Rauch, S.L., Grant, P.E., Cohen, B.M., Seidman, L.J., Caviness, V.S., Biederman, J., 2005. Structural brain magnetic resonance imaging of limbic and thalamic volumes in pediatric bipolar disorder. *The American journal of psychiatry* 162, 1256-1265.

- Friston, K.J., Holmes, A.P., Worsley, K.J., Poline, J.P., Frith, C.D., Frackowiak, R.S., 1994. Statistical parametric maps in functional imaging: a general linear approach. *Human brain mapping* 2, 189-210.
- Garrity, A.G., Pearlson, G.D., McKiernan, K., Lloyd, D., Kiehl, K.A., Calhoun, V.D., 2007. Aberrant "default mode" functional connectivity in schizophrenia. *The American journal of psychiatry* 164, 450-457.
- Glass, G.V., 1976. Primary, secondary, and meta-analysis of research. *Educational researcher* 5, 3-8.
- Glasser, M.F., Van Essen, D.C., 2011. Mapping human cortical areas in vivo based on myelin content as revealed by T1- and T2-weighted MRI. *J Neurosci* 31, 11597-11616.
- Green, P., Montijo, J., Brockhaus, R., 2011. High specificity of the Word Memory Test and Medical Symptom Validity Test in groups with severe verbal memory impairment. *Applied neuropsychology* 18, 86-94.
- Greicius, M.D., Krasnow, B., Reiss, A.L., Menon, V., 2003. Functional connectivity in the resting brain: a network analysis of the default mode hypothesis. *Proceedings of the National Academy of Sciences of the United States of America* 100, 253-258.
- Greicius, M.D., Supekar, K., Menon, V., Dougherty, R.F., 2009. Resting-state functional connectivity reflects structural connectivity in the default mode network. *Cerebral cortex* 19, 72-78.
- Gross, A.L., Rebok, G.W., Brandt, J., Tommet, D., Marsiske, M., Jones, R.N., 2013. Modeling learning and memory using verbal learning tests: results from ACTIVE. *The journals of gerontology. Series B, Psychological sciences and social sciences* 68, 153-167.
- Grossman, E.J., Jensen, J.H., Babb, J.S., Chen, Q., Tabesh, A., Fieremans, E., Xia, D., Inglese, M., Grossman, R.I., 2013. Cognitive impairment in mild traumatic brain injury: a longitudinal diffusional kurtosis and perfusion imaging study. *AJNR. American journal of neuroradiology* 34, 951-957, S951-953.
- Guskiewicz, K.M., McCrea, M., Marshall, S.W., Cantu, R.C., Randolph, C., Barr, W., Onate, J.A., Kelly, J.P., 2003. Cumulative effects associated with recurrent concussion in collegiate football players: the NCAA Concussion Study. *JAMA* 290, 2549-2555.

- Hagmann, P., Sporns, O., Madan, N., Cammoun, L., Pienaar, R., Wedeen, V.J., Meuli, R., Thiran, J., Grant, P.E., 2010. White matter maturation reshapes structural connectivity in the late developing human brain. *Proceedings of the National Academy of Sciences of the United States of America* 107, 19067-19072.
- Harrington, D.L., Rubinov, M., Durgerian, S., Mourany, L., Reece, C., Koenig, K., Bullmore, E., Long, J.D., Paulsen, J.S., Group, P.-H.i.o.t.H.S., Rao, S.M., 2015. Network topology and functional connectivity disturbances precede the onset of Huntington's disease. *Brain : a journal of neurology* 138, 2332-2346.
- Hillary, F.G., Medaglia, J.D., Gates, K., Molenaar, P.C., Slocomb, J., Peechatka, A., Good, D.C., 2011. Examining working memory task acquisition in a disrupted neural network. *Brain : a journal of neurology* 134, 1555-1570.
- Hillary, F.G., Rajtmajer, S.M., Roman, C.A., Medaglia, J.D., Slocomb-Dluzen, J.E., Calhoun, V.D., Good, D.C., Wylie, G.R., 2014. The rich get richer: brain injury elicits hyperconnectivity in core subnetworks. *PloS one* 9, e104021.
- Honey, C.J., Sporns, O., Cammoun, L., Gigandet, X., Thiran, J.P., Meuli, R., Hagmann, P., 2009. Predicting human resting-state functional connectivity from structural connectivity. *Proceedings of the National Academy of Sciences of the United States of America* 106, 2035-2040.
- Hou, R., Moss-Morris, R., Peveler, R., Mogg, K., Bradley, B.P., Belli, A., 2012. When a minor head injury results in enduring symptoms: a prospective investigation of risk factors for postconcussional syndrome after mild traumatic brain injury. *Journal of neurology, neurosurgery, and psychiatry* 83, 217-223.
- Huisman, T.A., Schwamm, L.H., Schaefer, P.W., Koroshetz, W.J., Shetty-Alva, N., Ozsunar, Y., Wu, O., Sorensen, A.G., 2004. Diffusion tensor imaging as potential biomarker of white matter injury in diffuse axonal injury. *AJNR. American journal of neuroradiology* 25, 370-376.

- Ilvesmaki, T., Luoto, T.M., Hakulinen, U., Brander, A., Ryymin, P., Eskola, H., Iverson, G.L., Ohman, J., 2014. Acute mild traumatic brain injury is not associated with white matter change on diffusion tensor imaging. *Brain : a journal of neurology* 137, 1876-1882.
- Inglese, M., Makani, S., Johnson, G., Cohen, B.A., Silver, J.A., Gonen, O., Grossman, R.I., 2005. Diffuse axonal injury in mild traumatic brain injury: a diffusion tensor imaging study. *J Neurosurg* 103, 298-303.
- Iraji, A., Benson, R.R., Welch, R.D., O'Neil, B.J., Woodard, J.L., Ayaz, S.I., Kulek, A., Mika, V., Medado, P., Soltanian-Zadeh, H., Liu, T., Haacke, E.M., Kou, Z., 2015. Resting State Functional Connectivity in Mild Traumatic Brain Injury at the Acute Stage: Independent Component and Seed-Based Analyses. *J Neurotrauma* 32, 1031-1045.
- Iraji, A., Calhoun, V.D., Wiseman, N.M., Davoodi-Bojd, E., Avanaki, M.R., Haacke, E.M., Kou, Z., 2016a. The connectivity domain: Analyzing resting state fMRI data using feature-based data-driven and model-based methods. *NeuroImage* 134, 494-507.
- Iraji, A., Chen, H., Wiseman, N., Welch, R.D., O'Neil, B.J., Haacke, E.M., Liu, T., Kou, Z., 2016b. Compensation through Functional Hyperconnectivity: A Longitudinal Connectome Assessment of Mild Traumatic Brain Injury. *Neural Plast* 2016, 4072402.
- Iraji, A., Chen, H., Wiseman, N., Zhang, T., Welch, R., O'Neil, B., Kulek, A., Ayaz, S.I., Wang, X., Zuk, C., Haacke, E.M., Liu, T., Kou, Z., 2016c. Connectome-scale assessment of structural and functional connectivity in mild traumatic brain injury at the acute stage. *NeuroImage. Clinical* 12, 100-115.
- Iraji, A., Davoodi-Bojd, E., Soltanian-Zadeh, H., Hossein-Zadeh, G.A., Jiang, Q., 2011. Diffusion kurtosis imaging discriminates patients with white matter lesions from healthy subjects. *Conference proceedings : ... Annual International Conference of the IEEE Engineering in Medicine and Biology Society. IEEE Engineering in Medicine and Biology Society. Annual Conference 2011*, 2796-2799.
- Irimia, A., Wang, B., Aylward, S.R., Prastawa, M.W., Pace, D.F., Gerig, G., Hovda, D.A., Kikinis, R., Vespa, P.M., Van Horn, J.D., 2012. Neuroimaging of structural pathology and connectomics in traumatic brain injury: Toward personalized outcome prediction. *NeuroImage. Clinical* 1, 1-17.

- Jafri, M.J., Pearlson, G.D., Stevens, M., Calhoun, V.D., 2008. A method for functional network connectivity among spatially independent resting-state components in schizophrenia. *NeuroImage* 39, 1666-1681.
- Jenkinson, M., Beckmann, C.F., Behrens, T.E., Woolrich, M.W., Smith, S.M., 2012. Fsl. *NeuroImage* 62, 782-790.
- Johansen-Berg, H., Behrens, T.E., 2013. *Diffusion MRI: from quantitative measurement to in vivo neuroanatomy*. Academic Press.
- Johnson, B., Zhang, K., Gay, M., Horovitz, S., Hallett, M., Sebastianelli, W., Slobounov, S., 2012. Alteration of brain default network in subacute phase of injury in concussed individuals: resting-state fMRI study. *NeuroImage* 59, 511-518.
- Johnston, K.M., Lassonde, M., Ptito, A., 2001. A contemporary neurosurgical approach to sport-related head injury: the McGill concussion protocol. *Journal of the American College of Surgeons* 192, 515-524.
- Jorge, R.E., Acion, L., White, T., Tordesillas-Gutierrez, D., Pierson, R., Crespo-Facorro, B., Magnotta, V.A., 2012. White matter abnormalities in veterans with mild traumatic brain injury. *The American journal of psychiatry* 169, 1284-1291.
- Kashluba, S., Paniak, C., Blake, T., Reynolds, S., Toller-Lobe, G., Nagy, J., 2004. A longitudinal, controlled study of patient complaints following treated mild traumatic brain injury. *Archives of clinical neuropsychology : the official journal of the National Academy of Neuropsychologists* 19, 805-816.
- Kay T, 1993. Neuropsychological treatment of mild traumatic brain injury. *J Head Trauma Rehab* 8, 74-85.
- Korgaonkar, M.S., Fornito, A., Williams, L.M., Grieve, S.M., 2014. Abnormal structural networks characterize major depressive disorder: a connectome analysis. *Biol Psychiatry* 76, 567-574.
- Kornak, J., Hall, D.A., Haggard, M.P., 2011. Spatially extended fMRI signal response to stimulus in non-functionally relevant regions of the human brain: preliminary results. *Open Neuroimaging J* 5, 24-32.

- Kou Z, Benson RR, Haacke EM, 2010. Susceptibility weighted imaging in traumatic brain injury, in: Gillard J, Waldman A, Barker P (Ed.), Clinical MR Neuroimaging, 2nd Edition. Cambridge University, Cambridge.
- Kou Z, Shen Y, Zakaria N, Kallakuri S, Cavanaugh JM, Yu Y, Hu J, EM, H., 2007. Correlation of Fractional Anisotropy with Histology for Diffuse Axonal Injury in a Rat Model, Joint Annual Meeting ISMRM-ESMRMB, Berlin, Germany.
- Kou, Z., Benson, R.R., Haacke, E.M., 2012. Magnetic Resonance Imaging Biomarkers of Mild Traumatic Brain Injury, in: Dambinova S, e.a. (Ed.), Biomarkers for Traumatic Brain Injury. Royal Society of Chemistry.
- Kou, Z., Gattu, R., Kobeissy, F., Welch, R.D., O'Neil, B.J., Woodard, J.L., Ayaz, S.I., Kulek, A., Kas-Shamoun, R., Mika, V., Zuk, C., Tomasello, F., Mondello, S., 2013. Combining biochemical and imaging markers to improve diagnosis and characterization of mild traumatic brain injury in the acute setting: results from a pilot study. PloS one 8, e80296.
- Kou, Z., Iraj, A., 2014. Imaging brain plasticity after trauma. Neural Regen Res 9, 693-700.
- Kou, Z., VandeVord, P.J., 2014. Traumatic white matter injury and glial activation: from basic science to clinics. Glia 62, 1831-1855.
- Kou, Z., Wu, Z., Tong, K.A., Holshouser, B., Benson, R.R., Hu, J., Haacke, E.M., 2010. The role of advanced MR imaging findings as biomarkers of traumatic brain injury. J Head Trauma Rehabil 25, 267-282.
- Krienen, F.M., Yeo, B.T., Buckner, R.L., 2014. Reconfigurable task-dependent functional coupling modes cluster around a core functional architecture. Philosophical transactions of the Royal Society of London. Series B, Biological sciences 369, 20130526.
- Laird, A.R., Eickhoff, S.B., Kurth, F., Fox, P.M., Uecker, A.M., Turner, J.A., Robinson, J.L., Lancaster, J.L., Fox, P.T., 2009. ALE Meta-Analysis Workflows Via the Brainmap Database: Progress Towards A Probabilistic Functional Brain Atlas. Frontiers in neuroinformatics 3, 23.

- Laird, A.R., Fox, P.M., Eickhoff, S.B., Turner, J.A., Ray, K.L., McKay, D.R., Glahn, D.C., Beckmann, C.F., Smith, S.M., Fox, P.T., 2011. Behavioral interpretations of intrinsic connectivity networks. *Journal of cognitive neuroscience* 23, 4022-4037.
- Lange, R.T., Iverson, G.L., Brubacher, J.R., Madler, B., Heran, M.K., 2012. Diffusion tensor imaging findings are not strongly associated with postconcussional disorder 2 months following mild traumatic brain injury. *J Head Trauma Rehabil* 27, 188-198.
- Le Bihan, D., Johansen-Berg, H., 2012. Diffusion MRI at 25: exploring brain tissue structure and function. *NeuroImage* 61, 324-341.
- Leaver, A.M., Espinoza, R., Joshi, S.H., Vasavada, M., Njau, S., Woods, R.P., Narr, K.L., 2015. Desynchronization and Plasticity of Striato-frontal Connectivity in Major Depressive Disorder. *Cerebral cortex*.
- Lee, M.H., Smyser, C.D., Shimony, J.S., 2013. Resting-state fMRI: a review of methods and clinical applications. *AJNR. American journal of neuroradiology* 34, 1866-1872.
- Levine, B., Cabeza, R., McIntosh, A.R., Black, S.E., Grady, C.L., Stuss, D.T., 2002. Functional reorganisation of memory after traumatic brain injury: a study with H(2)(15)O positron emission tomography. *Journal of neurology, neurosurgery, and psychiatry* 73, 173-181.
- Li, K., Guo, L., Faraco, C., Zhu, D., Deng, F., Zhang, T., Jiang, X., Zhang, D., Chen, H., Hu, X., Year Individualized ROI optimization via maximization of group-wise consistency of structural and functional profiles. In *Advances in Neural Information Processing Systems*.
- Li, K., Guo, L., Li, G., Nie, J., Faraco, C., Zhao, Q., Miller, L.S., Liu, T., Year Cortical surface based identification of brain networks using high spatial resolution resting state fMRI data. In *Biomedical Imaging: From Nano to Macro, 2010 IEEE International Symposium on*.
- Lin, Q.H., Liu, J., Zheng, Y.R., Liang, H., Calhoun, V.D., 2010. Semiblind spatial ICA of fMRI using spatial constraints. *Human brain mapping* 31, 1076-1088.

- Lipton, M.L., Gulko, E., Zimmerman, M.E., Friedman, B.W., Kim, M., Gellella, E., Gold, T., Shifteh, K., Ardekani, B.A., Branch, C.A., 2009. Diffusion-tensor imaging implicates prefrontal axonal injury in executive function impairment following very mild traumatic brain injury. *Radiology* 252, 816-824.
- Lipton, M.L., Kim, N., Park, Y.K., Hulkower, M.B., Gardin, T.M., Shifteh, K., Kim, M., Zimmerman, M.E., Lipton, R.B., Branch, C.A., 2012. Robust detection of traumatic axonal injury in individual mild traumatic brain injury patients: intersubject variation, change over time and bidirectional changes in anisotropy. *Brain imaging and behavior* 6, 329-342.
- Liu, T., Li, H., Wong, K., Tarokh, A., Guo, L., Wong, S.T., 2007. Brain tissue segmentation based on DTI data. *NeuroImage* 38, 114-123.
- Liu, T., Nie, J., Tarokh, A., Guo, L., Wong, S.T., 2008. Reconstruction of central cortical surface from brain MRI images: method and application. *NeuroImage* 40, 991-1002.
- Logothetis, N.K., Wandell, B.A., 2004. Interpreting the BOLD signal. *Annu. Rev. Physiol.* 66, 735-769.
- Losoi, H., Silverberg, N., Waljas, M., Turunen, S., Rosti-Otajarvi, E., Helminen, M., Luoto, T.M., Julkunen, J., Ohman, J., Iverson, G.L., 2015. Recovery from Mild Traumatic Brain Injury in Previously Healthy Adults. *J Neurotrauma*.
- Lv, J., Jiang, X., Li, X., Zhu, D., Chen, H., Zhang, T., Zhang, S., Hu, X., Han, J., Huang, H., Zhang, J., Guo, L., Liu, T., 2015a. Sparse representation of whole-brain fMRI signals for identification of functional networks. *Med Image Anal* 20, 112-134.
- Lv, J., Jiang, X., Li, X., Zhu, D., Zhang, S., Zhao, S., Chen, H., Zhang, T., Hu, X., Han, J., Ye, J., Guo, L., Liu, T., 2015b. Holistic atlases of functional networks and interactions reveal reciprocal organizational architecture of cortical function. *IEEE transactions on bio-medical engineering* 62, 1120-1131.
- Mac Donald CL, Dikranian K, Song SK, Bayly PV, Holtzman DM, DL, B., 2007. Detection of traumatic axonal injury with diffusion tensor imaging in a mouse model of traumatic brain injury. *Experimental Neurology* 205, 116–131.

- Mac Donald, C.L., Johnson, A.M., Cooper, D., Nelson, E.C., Werner, N.J., Shimony, J.S., Snyder, A.Z., Raichle, M.E., Witherow, J.R., Fang, R., Flaherty, S.F., Brody, D.L., 2011. Detection of blast-related traumatic brain injury in U.S. military personnel. *N Engl J Med* 364, 2091-2100.
- Malec, J.F., Brown, A.W., Leibson, C.L., Flaada, J.T., Mandrekar, J.N., Diehl, N.N., Perkins, P.K., 2007. The mayo classification system for traumatic brain injury severity. *J Neurotrauma* 24, 1417-1424.
- Margulies, D.S., Kelly, A.M., Uddin, L.Q., Biswal, B.B., Castellanos, F.X., Milham, M.P., 2007. Mapping the functional connectivity of anterior cingulate cortex. *NeuroImage* 37, 579-588.
- Maruishi, M., Miyatani, M., Nakao, T., Muranaka, H., 2007. Compensatory cortical activation during performance of an attention task by patients with diffuse axonal injury: a functional magnetic resonance imaging study. *Journal of neurology, neurosurgery, and psychiatry* 78, 168-173.
- Mason, M.F., Norton, M.I., Van Horn, J.D., Wegner, D.M., Grafton, S.T., Macrae, C.N., 2007. Wandering minds: the default network and stimulus-independent thought. *Science* 315, 393-395.
- Mayer, A.R., Bellgowan, P.S., Hanlon, F.M., 2015a. Functional magnetic resonance imaging of mild traumatic brain injury. *Neurosci Biobehav Rev* 49, 8-18.
- Mayer, A.R., Ling, J.M., Allen, E.A., Klimaj, S.D., Yeo, R.A., Hanlon, F.M., 2015b. Static and Dynamic Intrinsic Connectivity following Mild Traumatic Brain Injury. *J Neurotrauma* 32, 1046-1055.
- Mayer, A.R., Mannell, M.V., Ling, J., Gasparovic, C., Yeo, R.A., 2011. Functional connectivity in mild traumatic brain injury. *Human brain mapping* 32, 1825-1835.
- McAllister, T.W., Flashman, L.A., McDonald, B.C., Saykin, A.J., 2006. Mechanisms of working memory dysfunction after mild and moderate TBI: evidence from functional MRI and neurogenetics. *J Neurotrauma* 23, 1450-1467.
- McAllister, T.W., Saykin, A.J., Flashman, L.A., Sparling, M.B., Johnson, S.C., Guerin, S.J., Mamourian, A.C., Weaver, J.B., Yanofsky, N., 1999. Brain activation during working memory 1 month after mild traumatic brain injury: a functional MRI study. *Neurology* 53, 1300-1308.
- McAllister, T.W., Sparling, M.B., Flashman, L.A., Saykin, A.J., 2001. Neuroimaging findings in mild traumatic brain injury. *J Clin Exp Neuropsychol* 23, 775-791.

- McCrea M, Guskiewicz KM, Marshall SW, Barr W, Randolph C, Cantu RC, et al, 2003. Acute effects and recovery time following concussion in collegiate football players: the NCAA Concussion Study. *JAMA* 290, 2556-2563.
- McCrea M, Randolph C, Kelly JP, 2000. Standardized Assessment of Concussion (SAC): Manual for Administration, Scoring and Interpretation, 2nd ed. CNS Inc., Waukesha, WI.
- McMahon, P., Hricik, A., Yue, J.K., Puccio, A.M., Inoue, T., Lingsma, H.F., Beers, S.R., Gordon, W.A., Valadka, A.B., Manley, G.T., Okonkwo, D.O., 2014. Symptomatology and functional outcome in mild traumatic brain injury: results from the prospective TRACK-TBI study. *J Neurotrauma* 31, 26-33.
- Meda, S.A., Calhoun, V.D., Astur, R.S., Turner, B.M., Ruopp, K., Pearlson, G.D., 2009. Alcohol dose effects on brain circuits during simulated driving: an fMRI study. *Human brain mapping* 30, 1257-1270.
- Menon, V., Uddin, L.Q., 2010. Saliency, switching, attention and control: a network model of insula function. *Brain structure & function* 214, 655-667.
- Messe, A., Caplain, S., Paradot, G., Garrigue, D., Mineo, J.F., Soto Ares, G., Ducreux, D., Vignaud, F., Rozec, G., Desal, H., Pelegrini-Issac, M., Montreuil, M., Benali, H., Lehericy, S., 2011. Diffusion tensor imaging and white matter lesions at the subacute stage in mild traumatic brain injury with persistent neurobehavioral impairment. *Human brain mapping* 32, 999-1011.
- Messe, A., Caplain, S., Pelegrini-Issac, M., Blancho, S., Levy, R., Aghakhani, N., Montreuil, M., Benali, H., Lehericy, S., 2013. Specific and evolving resting-state network alterations in post-concussion syndrome following mild traumatic brain injury. *PloS one* 8, e65470.
- Messe, A., Rudrauf, D., Giron, A., Marrelec, G., 2015. Predicting functional connectivity from structural connectivity via computational models using MRI: an extensive comparison study. *NeuroImage* 111, 65-75.
- Morgan, A.T., Masterton, R., Pigdon, L., Connelly, A., Liegeois, F.J., 2013. Functional magnetic resonance imaging of chronic dysarthric speech after childhood brain injury: reliance on a left-hemisphere compensatory network. *Brain : a journal of neurology* 136, 646-657.

- Nakamura, T., Hillary, F.G., Biswal, B.B., 2009. Resting network plasticity following brain injury. *PLoS one* 4, e8220.
- Narayana, P.A., Yu, X., Hasan, K.M., Wilde, E.A., Levin, H.S., Hunter, J.V., Miller, E.R., Patel, V.K., Robertson, C.S., McCarthy, J.J., 2015. Multi-modal MRI of mild traumatic brain injury. *NeuroImage. Clinical* 7, 87-97.
- National Academy of Neuropsychology, 2002. Mild Traumatic Brain Injury-An Online Course. National Academy of Neuropsychology, Denver, Co.
- National Institutes of Health, 1999. NIH consensus development panel on rehabilitation of persons with traumatic brain injury. *Journal of the American Medical Association (JAMA)* 282, 974-983.
- Naunheim RS, Matero D, Fucetola R, 2008. Assessment of Patients with Mild Concussion in the Emergency Department. *J Head Trauma Rehabil* 23, 116-122.
- Nelson, S.M., Cohen, A.L., Power, J.D., Wig, G.S., Miezin, F.M., Wheeler, M.E., Velanova, K., Donaldson, D.I., Phillips, J.S., Schlaggar, B.L., Petersen, S.E., 2010. A parcellation scheme for human left lateral parietal cortex. *Neuron* 67, 156-170.
- Newsome, M.R., Scheibel, R.S., Steinberg, J.L., Troyanskaya, M., Sharma, R.G., Rauch, R.A., Li, X., Levin, H.S., 2007. Working memory brain activation following severe traumatic brain injury. *Cortex* 43, 95-111.
- Niogi, S.N., Mukherjee, P., 2010. Diffusion tensor imaging of mild traumatic brain injury. *J Head Trauma Rehabil* 25, 241-255.
- Niogi, S.N., Mukherjee, P., Ghajar, J., Johnson, C., Kolster, R.A., Sarkar, R., Lee, H., Meeker, M., Zimmerman, R.D., Manley, G.T., McCandliss, B.D., 2008a. Extent of microstructural white matter injury in postconcussive syndrome correlates with impaired cognitive reaction time: a 3T diffusion tensor imaging study of mild traumatic brain injury. *AJNR. American journal of neuroradiology* 29, 967-973.

- Niogi, S.N., Mukherjee, P., Ghajar, J., Johnson, C.E., Kolster, R., Lee, H., Suh, M., Zimmerman, R.D., Manley, G.T., McCandliss, B.D., 2008b. Structural dissociation of attentional control and memory in adults with and without mild traumatic brain injury. *Brain : a journal of neurology* 131, 3209-3221.
- Ogawa, S., Tank, D.W., Menon, R., Ellermann, J.M., Kim, S.G., Merkle, H., Ugurbil, K., 1992. Intrinsic signal changes accompanying sensory stimulation: functional brain mapping with magnetic resonance imaging. *Proceedings of the National Academy of Sciences of the United States of America* 89, 5951-5955.
- Passingham, R.E., Stephan, K.E., Kotter, R., 2002. The anatomical basis of functional localization in the cortex. *Nature reviews. Neuroscience* 3, 606-616.
- Paterakis K, Karantanas AH, Komnos A, Volikas Z, 2000. Outcome of patients with diffuse axonal injury: the significance and prognostic value of MRI in the acute phase. *J Trauma* 49, 1071-1075.
- Pelleg, D., Moore, W., Year X-means: Extending K-means with Efficient Estimation of the Number of Clusters. In ICML.
- Penny, D.W., Friston, J.K., Ashburner, T.J., Kiebel, J.S., Nichols, E.T., 2011. Statistical parametric mapping: the analysis of functional brain images: the analysis of functional brain images. Academic press.
- Perlstein, W.M., Cole, M.A., Demery, J.A., Seignourel, P.J., Dixit, N.K., Larson, M.J., Briggs, R.W., 2004. Parametric manipulation of working memory load in traumatic brain injury: behavioral and neural correlates. *Journal of the International Neuropsychological Society : JINS* 10, 724-741.
- Ptak T, Sheridan RL, Rhea JT, Gervasini AA, Yun JH, Curran MA, Borszuk P, Petrovick L, RA, N., 2003. Cerebral fractional anisotropy score in trauma patients: a new indicator of white matter injury after trauma. *AJR Am J Roentgenol* 181, 1401-1407.
- Rao, H., Wang, J., Giannetta, J., Korczykowski, M., Shera, D., Avants, B.B., Gee, J., Detre, J.A., Hurt, H., 2007. Altered resting cerebral blood flow in adolescents with in utero cocaine exposure revealed by perfusion functional MRI. *Pediatrics* 120, e1245-1254.

- Reichenbach JR, Venkatesan R, Schillinger DJ, Kido DK, Haacke EM, 1997. Small vessels in the human brain: MR venography with deoxyhemoglobin as an intrinsic contrast agent. *Radiology* 204, 272–277.
- Ricker, J.H., Muller, R.A., Zafonte, R.D., Black, K.M., Millis, S.R., Chugani, H., 2001. Verbal recall and recognition following traumatic brain injury: a [0-15]-water positron emission tomography study. *J Clin Exp Neuropsychol* 23, 196-206.
- Robinson, S., Basso, G., Soldati, N., Sailer, U., Jovicich, J., Bruzzone, L., Kryspin-Exner, I., Bauer, H., Moser, E., 2009. A resting state network in the motor control circuit of the basal ganglia. *BMC Neurosci* 10, 137.
- Rubinov, M., Sporns, O., 2010. Complex network measures of brain connectivity: uses and interpretations. *NeuroImage* 52, 1059-1069.
- Ruff, R., 2005. Two decades of advances in understanding of mild traumatic brain injury. *J Head Trauma Rehabil* 20, 5-18.
- Ruff, R.M., Jurica, P., 1999. In search of a unified definition for mild traumatic brain injury. *Brain injury* 13, 943-952.
- Sanchez-Carrion, R., Gomez, P.V., Junque, C., Fernandez-Espejo, D., Falcon, C., Bargallo, N., Roig-Rovira, T., Ensenat-Cantalops, A., Bernabeu, M., 2008. Frontal hypoactivation on functional magnetic resonance imaging in working memory after severe diffuse traumatic brain injury. *J Neurotrauma* 25, 479-494.
- Scheibel, R.S., Newsome, M.R., Steinberg, J.L., Pearson, D.A., Rauch, R.A., Mao, H., Troyanskaya, M., Sharma, R.G., Levin, H.S., 2007. Altered brain activation during cognitive control in patients with moderate to severe traumatic brain injury. *Neurorehabil Neural Repair* 21, 36-45.
- Seeley, W.W., Menon, V., Schatzberg, A.F., Keller, J., Glover, G.H., Kenna, H., Reiss, A.L., Greicius, M.D., 2007. Dissociable intrinsic connectivity networks for salience processing and executive control. *J Neurosci* 27, 2349-2356.
- Sharp, D.J., Jenkins, P.O., 2015. Concussion is confusing us all. *Practical Neurology* 15, 172-186.

- Sharp, D.J., Scott, G., Leech, R., 2014. Network dysfunction after traumatic brain injury. *Nature reviews. Neurology* 10, 156-166.
- Shenton, M.E., Hamoda, H.M., Schneiderman, J.S., Bouix, S., Pasternak, O., Rathi, Y., Vu, M.A., Purohit, M.P., Helmer, K., Koerte, I., Lin, A.P., Westin, C.F., Kikinis, R., Kubicki, M., Stern, R.A., Zafonte, R., 2012. A review of magnetic resonance imaging and diffusion tensor imaging findings in mild traumatic brain injury. *Brain imaging and behavior* 6, 137-192.
- Shimony JS, McKinstry RC, Akbudak E, Aronovitz JA, Snyder AZ, Lori NF, Cull TS, TE, C., 1999. Quantitative diffusion-tensor anisotropy brain MR imaging: normative human data and anatomic analysis. *Radiology* 212, 770-784.
- Shulman, R.G., Rothman, D.L., Behar, K.L., Hyder, F., 2004. Energetic basis of brain activity: implications for neuroimaging. *Trends in neurosciences* 27, 489-495.
- Silverberg, N.D., Hanks, R.A., Tompkins, S.C., 2013. Education quality, reading recognition, and racial differences in the neuropsychological outcome from traumatic brain injury. *Archives of clinical neuropsychology : the official journal of the National Academy of Neuropsychologists* 28, 485-491.
- Skudlarski, P., Jagannathan, K., Anderson, K., Stevens, M.C., Calhoun, V.D., Skudlarska, B.A., Pearlson, G., 2010. Brain connectivity is not only lower but different in schizophrenia: a combined anatomical and functional approach. *Biol Psychiatry* 68, 61-69.
- Smith, S.M., Fox, P.T., Miller, K.L., Glahn, D.C., Fox, P.M., Mackay, C.E., Filippini, N., Watkins, K.E., Toro, R., Laird, A.R., Beckmann, C.F., 2009. Correspondence of the brain's functional architecture during activation and rest. *Proceedings of the National Academy of Sciences of the United States of America* 106, 13040-13045.
- Smith, S.M., Jenkinson, M., Woolrich, M.W., Beckmann, C.F., Behrens, T.E., Johansen-Berg, H., Bannister, P.R., De Luca, M., Drobnjak, I., Flitney, D.E., 2004. Advances in functional and structural MR image analysis and implementation as FSL. *NeuroImage* 23, S208-S219.
- Smith, S.M., Miller, K.L., Salimi-Khorshidi, G., Webster, M., Beckmann, C.F., Nichols, T.E., Ramsey, J.D., Woolrich, M.W., 2011. Network modelling methods for FMRI. *NeuroImage* 54, 875-891.

- Sorg, C., Riedl, V., Muhlau, M., Calhoun, V.D., Eichele, T., Laer, L., Drzezga, A., Forstl, H., Kurz, A., Zimmer, C., Wohlschlager, A.M., 2007. Selective changes of resting-state networks in individuals at risk for Alzheimer's disease. *Proceedings of the National Academy of Sciences of the United States of America* 104, 18760-18765.
- Sporns, O., 2013. Network attributes for segregation and integration in the human brain. *Curr Opin Neurobiol* 23, 162-171.
- Sporns, O., 2014. Contributions and challenges for network models in cognitive neuroscience. *Nature neuroscience* 17, 652-660.
- Sporns, O., Tononi, G., Kotter, R., 2005. The human connectome: A structural description of the human brain. *PLoS computational biology* 1, e42.
- Stevens, M.C., Lovejoy, D., Kim, J., Oakes, H., Kureshi, I., Witt, S.T., 2012. Multiple resting state network functional connectivity abnormalities in mild traumatic brain injury. *Brain imaging and behavior* 6, 293-318.
- Stevens, M.C., Pearlson, G.D., Calhoun, V.D., 2009. Changes in the interaction of resting-state neural networks from adolescence to adulthood. *Human brain mapping* 30, 2356-2366.
- Stulemeijer, M., van der Werf, S., Borm, G.F., Vos, P.E., 2008. Early prediction of favourable recovery 6 months after mild traumatic brain injury. *Journal of neurology, neurosurgery, and psychiatry* 79, 936-942.
- Tang, L., Ge, Y., Sodickson, D.K., Miles, L., Zhou, Y., Reaume, J., Grossman, R.I., 2011. Thalamic resting-state functional networks: disruption in patients with mild traumatic brain injury. *Radiology* 260, 831-840.
- Tian, L.X., Jiang, T.Z., Wang, Y.F., Zang, Y.F., He, Y., Liang, M., Sui, M.Q., Cao, Q.J., Hu, S.Y., Peng, M., Zhuo, Y., 2006. Altered resting-state functional connectivity patterns of anterior cingulate cortex in adolescents with attention deficit hyperactivity disorder. *Neurosci Lett* 400, 39-43.
- Tivarus, M.E., Starling, S.J., Newport, E.L., Langfitt, J.T., 2012. Homotopic language reorganization in the right hemisphere after early left hemisphere injury. *Brain and language* 123, 1-10.

- Toga, A.W., Clark, K.A., Thompson, P.M., Shattuck, D.W., Van Horn, J.D., 2012. Mapping the human connectome. *Neurosurgery* 71, 1-5.
- Treble, A., Hasan, K.M., Iftikhar, A., Stuebing, K.K., Kramer, L.A., Cox, C.S., Jr., Swank, P.R., Ewing-Cobbs, L., 2013. Working memory and corpus callosum microstructural integrity after pediatric traumatic brain injury: a diffusion tensor tractography study. *J Neurotrauma* 30, 1609-1619.
- Turner, G.R., Levine, B., 2008. Augmented neural activity during executive control processing following diffuse axonal injury. *Neurology* 71, 812-818.
- Tzourio-Mazoyer, N., Landeau, B., Papathanassiou, D., Crivello, F., Etard, O., Delcroix, N., Mazoyer, B., Joliot, M., 2002. Automated anatomical labeling of activations in SPM using a macroscopic anatomical parcellation of the MNI MRI single-subject brain. *NeuroImage* 15, 273-289.
- Tzourio, N., Petit, L., Mellet, E., Orssaud, C., Crivello, F., Benali, K., Salamon, G., Mazoyer, B., 1997. Use of anatomical parcellation to catalog and study structure-function relationships in the human brain. *Human brain mapping* 5, 228-232.
- Uddin, L.Q., Supekar, K.S., Ryali, S., Menon, V., 2011. Dynamic reconfiguration of structural and functional connectivity across core neurocognitive brain networks with development. *J Neurosci* 31, 18578-18589.
- van den Heuvel, M., Mandl, R., Hulshoff Pol, H., 2008a. Normalized cut group clustering of resting-state fMRI data. *PLoS one* 3, e2001.
- van den Heuvel, M., Mandl, R., Luigjes, J., Hulshoff Pol, H., 2008b. Microstructural organization of the cingulum tract and the level of default mode functional connectivity. *J Neurosci* 28, 10844-10851.
- van den Heuvel, M.P., Hulshoff Pol, H.E., 2010. Exploring the brain network: a review on resting-state fMRI functional connectivity. *European neuropsychopharmacology : the journal of the European College of Neuropsychopharmacology* 20, 519-534.
- van den Heuvel, M.P., Sporns, O., Collin, G., Scheewe, T., Mandl, R.C., Cahn, W., Goni, J., Hulshoff Pol, H.E., Kahn, R.S., 2013. Abnormal rich club organization and functional brain dynamics in schizophrenia. *JAMA psychiatry* 70, 783-792.

- van Ewijk, H., Heslenfeld, D.J., Zwiers, M.P., Buitelaar, J.K., Oosterlaan, J., 2012. Diffusion tensor imaging in attention deficit/hyperactivity disorder: a systematic review and meta-analysis. *Neurosci Biobehav Rev* 36, 1093-1106.
- van Wijk, B.C., Stam, C.J., Daffertshofer, A., 2010. Comparing brain networks of different size and connectivity density using graph theory. *PloS one* 5, e13701.
- Vos, P.E., Alekseenko, Y., Battistin, L., Ehler, E., Gerstenbrand, F., Muresanu, D.F., Potapov, A., Stepan, C.A., Traubner, P., Vecsei, L., von Wild, K., European Federation of Neurological, S., 2012. Mild traumatic brain injury. *European journal of neurology : the official journal of the European Federation of Neurological Societies* 19, 191-198.
- Walker, E., Hernandez, A.V., Kattan, M.W., 2008. Meta-analysis: Its strengths and limitations. *Cleveland Clinic journal of medicine* 75, 431-439.
- Wang, J., Aguirre, G.K., Kimberg, D.Y., Roc, A.C., Li, L., Detre, J.A., 2003. Arterial spin labeling perfusion fMRI with very low task frequency. *Magn Reson Med* 49, 796-802.
- Wang, J., Zuo, X., He, Y., 2010. Graph-Based Network Analysis of Resting-State Functional MRI. *Frontiers in systems neuroscience* 4.
- Wang, L., Zang, Y.F., He, Y., Liang, M., Zhang, X.Q., Tian, L.X., Wu, T., Jiang, T.Z., Li, K.C., 2006. Changes in hippocampal connectivity in the early stages of Alzheimer's disease: Evidence from resting state fMRI. *NeuroImage* 31, 496-504.
- Wang, Z., Dai, Z., Gong, G., Zhou, C., He, Y., 2015. Understanding structural-functional relationships in the human brain: a large-scale network perspective. *The Neuroscientist : a review journal bringing neurobiology, neurology and psychiatry* 21, 290-305.
- Whitfield-Gabrieli, S., Ford, J.M., 2012. Default mode network activity and connectivity in psychopathology. *Annu Rev Clin Psychol* 8, 49-76.
- Wig, G.S., Schlaggar, B.L., Petersen, S.E., 2011. Concepts and principles in the analysis of brain networks. *Ann N Y Acad Sci* 1224, 126-146.

- Wilkinson, G.S., Robertson, G., 2006. Wide range achievement test (WRAT4). Psychological Assessment Resources, Lutz.
- Wisner, K.M., Atluri, G., Lim, K.O., Macdonald, A.W., 3rd, 2013. Neurometrics of intrinsic connectivity networks at rest using fMRI: retest reliability and cross-validation using a meta-level method. *NeuroImage* 76, 236-251.
- Wu, T.C., Wilde, E.A., Bigler, E.D., Yallampalli, R., McCauley, S.R., Troyanskaya, M., Chu, Z., Li, X., Hanten, G., Hunter, J.V., Levin, H.S., 2010. Evaluating the relationship between memory functioning and cingulum bundles in acute mild traumatic brain injury using diffusion tensor imaging. *J Neurotrauma* 27, 303-307.
- Yuan, Y., Jiang, X., Zhu, D., Chen, H., Li, K., Lv, P., Yu, X., Li, X., Zhang, S., Zhang, T., Hu, X., Han, J., Guo, L., Liu, T., 2013. Meta-analysis of functional roles of DICCOLs. *Neuroinformatics* 11, 47-63.
- Yuh, E.L., Cooper, S.R., Mukherjee, P., Yue, J.K., Lingsma, H.F., Gordon, W.A., Valadka, A.B., Okonkwo, D.O., Schnyer, D.M., Vassar, M.J., Maas, A.I., Manley, G.T., 2014. Diffusion tensor imaging for outcome prediction in mild traumatic brain injury: a TRACK-TBI study. *J Neurotrauma* 31, 1457-1477.
- Zalesky, A., Fornito, A., Bullmore, E.T., 2010. Network-based statistic: identifying differences in brain networks. *NeuroImage* 53, 1197-1207.
- Zhang, D., Raichle, M.E., 2010. Disease and the brain's dark energy. *Nature reviews. Neurology* 6, 15-28.
- Zhang, T., Guo, L., Li, K., Jing, C., Yin, Y., Zhu, D., Cui, G., Li, L., Liu, T., 2012. Predicting functional cortical ROIs via DTI-derived fiber shape models. *Cerebral cortex* 22, 854-864.
- Zhang, Z., Liao, W., Chen, H., Mantini, D., Ding, J.R., Xu, Q., Wang, Z., Yuan, C., Chen, G., Jiao, Q., Lu, G., 2011. Altered functional-structural coupling of large-scale brain networks in idiopathic generalized epilepsy. *Brain : a journal of neurology* 134, 2912-2928.
- Zhou, Y., Liang, M., Tian, L.X., Wang, K., Hao, Y.H., Liu, H.H., Liu, Z.N., Jiang, T.Z., 2007. Functional disintegration in paranoid schizophrenia using resting-state fMRI. *Schizophr Res* 97, 194-205.
- Zhou, Y., Milham, M.P., Lui, Y.W., Miles, L., Reaume, J., Sodickson, D.K., Grossman, R.I., Ge, Y., 2012. Default-mode network disruption in mild traumatic brain injury. *Radiology* 265, 882-892.

- Zhu, D., Li, K., Faraco, C.C., Deng, F., Zhang, D., Guo, L., Miller, L.S., Liu, T., 2012. Optimization of functional brain ROIs via maximization of consistency of structural connectivity profiles. *NeuroImage* 59, 1382-1393.
- Zhu, D., Li, K., Guo, L., Jiang, X., Zhang, T., Zhang, D., Chen, H., Deng, F., Faraco, C., Jin, C., Wee, C.Y., Yuan, Y., Lv, P., Yin, Y., Hu, X., Duan, L., Hu, X., Han, J., Wang, L., Shen, D., Miller, L.S., Li, L., Liu, T., 2013. DICCOL: dense individualized and common connectivity-based cortical landmarks. *Cerebral cortex* 23, 786-800.
- Zhu, D., Li, K., Terry, D.P., Puente, A.N., Wang, L., Shen, D., Miller, L.S., Liu, T., 2014a. Connectome-scale assessments of structural and functional connectivity in MCI. *Human brain mapping* 35, 2911-2923.
- Zhu, D., Zhang, D., Faraco, C., Li, K., Deng, F., Chen, H., Jiang, X., Guo, L., Miller, L.S., Liu, T., 2011. Discovering dense and consistent landmarks in the brain. *Information processing in medical imaging : proceedings of the ... conference* 22, 97-110.
- Zhu, D., Zhang, T., Jiang, X., Hu, X., Chen, H., Yang, N., Lv, J., Han, J., Guo, L., Liu, T., 2014b. Fusing DTI and fMRI data: a survey of methods and applications. *NeuroImage* 102 Pt 1, 184-191.
- Zoroya, G., 2007. Scientists: Brain injuries from war worse than thought. *USA Today*.
- Zuo, X.N., Kelly, C., Adelstein, J.S., Klein, D.F., Castellanos, F.X., Milham, M.P., 2010. Reliable intrinsic connectivity networks: test-retest evaluation using ICA and dual regression approach. *NeuroImage* 49, 2163-2177.

ABSTRACT**BRAIN CONNECTIVITY AFTER CONCUSSION**

by

ARMIN IRAJI**May 2017****Advisor:** Dr. Zhifeng Kou**Major:** Biomedical Engineering**Degree:** Doctor of Philosophy

Mild traumatic brain injury (mTBI) accounts for over one million emergency visits in the United States each year. While most mTBI patients have normal findings in clinical neuroimaging, alterations in brain structure and functional connectivity have frequently been reported. In this study, we investigated the large-scale brain structural and functional connectivity using diffusion MRI and resting-state fMRI data. Data from 40 mTBI patients was acquired at the acute stage (within 24 hrs after injury). 35 patients returned for data acquisition at a follow-up (4-6 weeks after injury). Data was also collected from a cohort of 58 healthy subjects, 36 of whom returned for data acquisition at the second time point, 4-6 weeks later. All data was collected at Wayne State University, Detroit, Michigan, USA. We also evaluated the relationship between functional connectivity findings at the acute stage and neurocognitive symptoms at follow up to assess the feasibility of using neuroimaging data to predict neurocognitive complications after mTBI. Moreover, we developed the connectivity domain, a new analysis method which can potentially improve reproducibility and ability to compare findings across datasets.

AUTOBIOGRAPHICAL STATEMENT

ARMIN IRAJI

EDUCATION

- 2012 - 2017 Ph.D. - Biomedical Engineering, Wayne State University, Detroit, MI
 2008 - 2011 M.Sc. - Biomedical Engineering, University of Tehran, Tehran, Iran
 2002 - 2007 B.Sc. - Biomedical Engineering, Amirkabir University of Technology, Tehran, Iran

HONORS, AWARDS AND RANKS

- 2017 Olbrot Travel Awards for Excellence in Graduate Student Research
 2016 National Neurotrauma Society Travel Grants
 2016 Drs. Anthony and Joyce Danielski Kales Endowed Scholars Award in Biomedical Engineering
 2015 Thomas C. Rumble University Graduate Fellowships Award, Wayne State University
 2015 Magna Cum Laude Merit Award, ISMRM 23rd Annual Meeting & Exhibition, Canada
 2015 Drs. Anthony and Joyce Danielski Kales Endowed Scholars Award in Biomedical Engineering
 2015 The Garrett T. Heberlein Excellence in Teaching Award
 2015 Outstanding Teaching Assistant Award, Wayne State University
 2013 Educational Stipend Award, ISMRM 21st Annual Meeting & Exhibition, USA

JOURNAL PUBLICATIONS

- Iraji, A.**, et al., Connectome-scale Assessment of Structural and Functional Connectivity in Mild Traumatic Brain Injury at the Acute Stage. *NeuroImage: Clinical*, 2016.
Iraji, A., et al., The Connectivity Domain: Analyzing Resting State fMRI Data Using Feature-based Data-driven and Model-based Methods. *Neuroimage*, 2016.
Iraji, A., et al., Compensation through Functional Hyperconnectivity: A Longitudinal Connectome Assessment of Mild Traumatic Brain Injury. *Journal of Neural Plasticity*, 2016.
Iraji, A., et al., Resting State Functional Connectivity in Mild Traumatic Brain Injury at the Acute Stage: Independent Component and Seed-Based Analyses. *Journal of Neurotrauma*, 2015.
 Kou, Z. and **Iraji, A.**, Imaging Brain Plasticity after Trauma. *Neural Regeneration Research*, 2014.

SELECTED CONFERENCE PAPERS AND ABSTRACTS

- Iraji, A.**, et al., Connectivity Domain Analysis of the Default Mode Network in Mild Traumatic Brain Injury at The Acute Stage. *Oral presentation* at International Society for Magnetic Resonance in Medicine (ISMRM), 2016.
 Lv, J.*, **Iraji, A.***, and et al., Group-wise sparse representation of brain states reveal network abnormalities in mild traumatic brain injury. *IEEE International Symposium on Biomedical Imaging (ISBI)*, 2016. *Co-first authors.
Iraji, A., et al., Transferring from Time Space to Connectivity Space: Extracting Brain Networks. *Human Brain Mapping (OHBM)*, 2015.
 Chen, H*, **Iraji, A.***, and et al., Longitudinal Analysis of Brain Recovery after Mild Traumatic Brain Injury Based on Groupwise Consistent Brain Network Clusters. *MICCAI*, 2015. *Co-first authors.
Iraji, A., et al., Connectome-scale Assessment of Structural and Functional Connectivity in Mild Traumatic Brain Injury. *ISMRM*, 2015.
Iraji, A., et al., et al., Longitudinal Analysis of Structural and Functional Connectivity of the Thalamus and Anterior Cingulate Cortex in Mild Traumatic Brain Injury. *ISMRM*, 2015.
Iraji, A., et al., Seemingly Inconsistency between Damaged White Matter Structure and Increased Functional Connectivity in Cingulum: Initial Response of Brain Plasticity to Trauma. *ISMRM*, 2014.
Iraji, A., et al., Functional Connectivity in Posterior Cingulate Cortex Alters in Brain Concussion Patients at the Acute Stage. *ISMRM*, 2013.